Analytical, Numerical and Experimental Study of Self-Loosening of Bolted Joints

by

Rashique Iftekhar ROUSSEAU

MANUSCRIPT-BASED THESIS PRESENTED TO ÉCOLE DE TECHNOLOGIE SUPÉRIEURE IN PARTIAL FULFILLMENT FOR THE DEGREE OF DOCTOR OF PHILOSOPHY
PH.D.

MONTREAL, DECEMBER 18, 2024

ÉCOLE DE TECHNOLOGIE SUPÉRIEURE
UNIVERSITÉ DU QUÉBEC

BOARD OF EXAMINERS

THIS THESIS HAS BEEN EVALUATED

BY THE FOLLOWING BOARD OF EXAMINERS

Mr. Abdel-Hakim Bouzid, Thesis Supervisor
Department of Mechanical Engineering at École de technologie supérieure

Mr. Omar Chaallal, President of the Board of Examiners
Department of Construction Engineering at École de technologie supérieure

Mr. Anh Dung Ngô, Member of the jury
Department of Mechanical Engineering at École de technologie supérieure

Mr. Massimiliano De Agostinis, External Evaluator
Department of Industrial Engineering at University of Bologna

THIS THESIS WAS PRENSENTED AND DEFENDED

IN THE PRESENCE OF A BOARD OF EXAMINERS AND PUBLIC

DECEMBER 18, 2024

AT ÉCOLE DE TECHNOLOGIE SUPÉRIEURE

DEDICATION

To my loving wife

Sabrina Shajeen Alam

For your unwavering love and care,
For being the cornerstone of my strength and resilience,
For always reminding me to *"never lose hope."*

I am forever grateful to you for everything you have done.

ACKNOWLEDGMENT

First and foremost, I would like to express my sincere gratitude to my supervisor, Prof. Abdel-Hakim Bouzid, for his tremendous support throughout my doctoral journey. I am truly honored to have had the opportunity to work and learn under his guidance. His vast knowledge and experience in the field have been a constant source of inspiration, motivating me in both my research and daily life. This achievement would not have been possible without his invaluable mentorship from the very beginning of this path.

I extend my sincere thanks to all the university technicians for their invaluable assistance in my research project. I am especially grateful to Mr. Surge Plamondon and Mr. Michel Drouin, who have been exceptionally kind to offer their advice and unwavering support in troubleshooting and solving problems during my experiments.

I would also like to express my heartfelt gratitude to my friends and colleagues, particularly Zijian Zhao and Abdelouahab Mohammed-Taifour, for their constant motivation and help during difficult times.

My deepest gratitude goes to my in-laws for always being by my side. I am especially thankful to my father-in-law for his continuous inspiration in my academic and research pursuits, to my mother-in-law for keeping me in her heartfelt prayers, and to my sisters-in-law and their families for their kindness and support.

I am profoundly grateful to my dearest mother for her unconditional love, care, and belief in every decision I have made, despite the numerous health challenges she has faced. I also extend my appreciation to my sister for being exceptionally protective of me since childhood, guiding me on what to do and what not to do, and to my brother-in-law for his encouragement and support whenever I needed it. A very special mention goes to my father, my role model, Dr. Md. Abdul Gafur, whose wise advice and timely guidance during the crucial moments of

my life have been instrumental to my achievements. Thank you for being my hero and the inspiration behind all my successes.

Lastly, words cannot fully express my gratitude to my wonderful wife, Sabrina, to whom I owe an immense debt of gratitude. Thank you for being my pillar of strength. I am equally thankful to our wonderful sons, Sahir and Safir, for bringing joy and light into my life.

ÉTUDE ANALYTIQUE, NUMERIQUE ET EXPERIMENTALE DE L'AUTO-DESSERRAGE DES ASSEMBLAGES BOULONNÉS

Rashique Iftekhar ROUSSEAU

RÉSUMÉ

La demande à grande échelle des assemblages boulonnés dans diverses applications d'ingénierie est incontestable en raison de leur bonne fiabilité fonctionnelle associée à une conception structurelle simplifiée. La question de l'auto-desserrage présente un problème important qui peut conduire à des situations catastrophiques dans les applications respectives, même si ceux-ci offrent une bonne rigidité aux connexions conjointes. Plusieurs facteurs sont responsables de l'auto-desserrage. Par exemple, les vibrations axiales peuvent contribuer au problème qui ne persiste que pendant un certain nombre de cycles. Les vibrations de torsion peuvent également déclencher le desserrage des articulations. Cependant, la cause la plus importante de son apparition est le chargement cyclique transversal. Le système boulon-écrou subit une rotation dans le sens du desserrage en raison d'une petite force transversale supplémentaire causant un glissement entre les filets et/ou sous la tête du boulon conduisant à un mouvement rotatif. En raison de la charge transversale cyclique, une réduction de la force de serrage est susceptible de se produire, suivie d'une rotation relative entre le boulon et l'écrou dans la dernière étape de chaque demi-cycle. En plus de ceux-ci, il existe d'autres facteurs responsables et la compréhension globale du mécanisme d'auto-desserrage reste un domaine nécessitant des recherches plus approfondies.

Par conséquent, cette étude vise à identifier les principaux mécanismes à l'origine du phénomène d'auto-desserrage dans les assemblages boulonnés et à explorer comment divers facteurs contribuent à son apparition. Pour atteindre cet objectif, le projet implique une enquête analytique pour comprendre le comportement de l'auto-desserrage, couplée à une analyse numérique par éléments finis (FEM) et à une validation expérimentale des résultats à l'aide d'un banc d'essai en laboratoire.

Une approche numérique basée sur la modélisation axisymétrique par éléments finis (EF) est développée pour évaluer efficacement la rigidité des composants d'un assemblage boulonné,

et en particulier la rigidité des éléments serrés et la rigidité des boulons dont les modèles existants ne sont pas fiables. Dans ce travail, dans le but d'améliorer les modèles analytiques, une large gamme de boulons de M6 à M36 ainsi que diverses longueurs de serrage des joints sont couverts dans l'analyse afin de développer une relation unique de rigidité des éléments serrés en fonction de la tête de boulon et de l'écrou et de leur largeur de contact. Suite à la validation avec différents cas de chargement, la nouvelle méthode montre la surestimation de la rigidité des éléments serrés des méthodes numériques et analytiques bien connues de la littérature.

Étant donné que la friction au sein de diverses interfaces de contact d'un assemblage boulonné contribue de manière significative à l'apparition d'un auto-desserrage, la recherche a étudié la contribution de divers couples, à savoir les couples de pas, de friction du boulon ou de l'écrou et les couples de friction du filetage, ainsi que leurs variations pendant le serrage, au repos et au desserrage. Une approche analytique est élaborée pour évaluer ces trois couples, la rotation relative entre le boulon et l'écrou, la relation entre le coefficient de frottement et le facteur d'écrou et la rigidité de l'assemblage. Un bon accord a été trouvé avec une étude expérimentale antérieure sur les cycles de chargement de serrage et de desserrage. Un modèle FE numérique tridimensionnel (3D) est développé à partir d'un joint boulonné fileté hexagonal M12 × 1.75 pour simuler les cycles de chargement de serrage et de desserrage ; ce qui valide également le modèle analytique.

Le projet a également mené des tests expérimentaux sur un banc d'essai déjà développé, qui reproduit le phénomène d'auto-desserrage dans un assemblage boulonné sous chargement transversal cyclique. Il comprenait des tests avec des boulons hexagonaux M12 × 1,75 et des éléments serrés de différentes épaisseurs et matériaux soumis à plusieurs conditions de serrage. Comme la rigidité et le frottement de surface sont des facteurs cruciaux influençant le desserrage des joints montrés dans des enquêtes antérieures, et que les deux paramètres dépendent des types de matériaux, une comparaison entre les tests menés avec des éléments serrés en acier et en polyéthylène haute densité (PEHD) a été effectuée. Une compréhension globale du desserrage de l'étape 2 (desserrage par rotation relative entre le boulon et l’écrou) est obtenue puisque chaque test se termine par une perte totale de précharge, dévoilant une gamme de modèles de phénomènes de desserrage pour une analyse comparative.

Mots clés : Auto-desserrage, assemblage boulonné, rigidité, frottement superficiel, propriété des matériaux, analyse par éléments finis, modélisation analytique

ANALYTICAL, NUMERICAL AND EXPERIMENTAL STUDY OF SELF-LOOSENING OF BOLTED JOINTS

Rashique Iftekhar ROUSSEAU

ABSTRACT

The large-scale demand for bolted joints across diverse engineering applications is indisputable because of their proven functional reliability coupled with simplified structural design. The issue of self-loosening presents a significant problem that potentially leads to catastrophic outcomes in the respective applications even though they offer a good rigidity to the joined connections. There are several factors responsible for self-loosening to occur. For instance, axial vibration can contribute to the problem that is persistent to only a certain number of cycles. Torsional vibration can also trigger the loosening of joints. However, the most significant cause of its occurrence is the transverse cyclic loading. Bolts experience rotation in the loosening direction due to a cyclic transverse force that produce slip between threads and/or under bolt heads leading to a relative rotation. Because of the cyclic transverse loading, a reduction of the clamping force is likely to occur followed by a relative rotation between the bolt and nut in the last stage of each half a cycle. In addition to these, there are other factors responsible, and a comprehensive understanding of the self-loosening mechanism remains an area in need of further investigation.

Hence, this study aims to identify the principal mechanisms behind the self-loosening phenomenon in bolted joints and to explore how various factors contribute to its occurrence. To achieve this goal, the project involves an analytical investigation to comprehend the behavior of self-loosening, coupled with numerical analysis through Finite Element Modeling (FEM) analysis, and experimental validation of the results using a laboratory test rig.

A numerical axisymmetric finite element (FE) modeling-based approach is developed to effectively evaluate accurately the stiffness of bolted joint components and particularly the stiffness of the clamped members and the bolt stiffness as current models are oversimplified. In this work, for the purpose of improving the analytical models, a wide range of bolts from M6 to M36 along with various joint grip lengths are covered in the analysis to develop a unique relationship of the stiffness of clamped members based on the bolt head or nut bearing contact.

By performing validation with various load cases, the new method reveals that several well-known numerical and analytical methods from the literature overestimate the stiffness of clamped members.

Since friction within various contact interfaces of a bolted joint significantly contributes to the occurrence of self-loosening, the study investigated the contribution of the various torques involved in a bolt, namely pitch, bolt and nut bearing friction and thread friction torques, and their variations during the tightening process, at rest after tightening is achieved and then during the untightening process. An analytical approach is elaborated to evaluate the three different torques, relative angular rotation between bolt and nut, interrelationship among the coefficient of friction and the nut factor, and stiffness of joint. This shows good agreement with the data from an earlier experimental study (Eccles, 2014) on tightening and untightening loading cycles. A three-dimensional (3D) numerical FE model is developed of a M12×1.75 hex threaded bolted joint to simulate the tightening and untightening loading cycles, which validates the analytical model as well.

The project also conducted experimental tests on a test rig already developed, which replicates the self-loosening phenomenon in a bolted joint under cyclic transverse loading. It included tests with M12×1.75 hex bolt and clamped members of different sizes and materials for different tightening conditions. As the stiffness and surface friction in a bolted joint are crucial factors influencing its loosening shown in earlier investigations, and both parameters depend on the types of material, a comparison is demonstrated between the tests conducted with steel and High-Density Polyethylene (HDPE) clamped members. A comprehensive understanding of the stage-II loosening (loosening by relative rotation between bolt and nut) is attained as every test end with a total preload drop, unveiling the effect of clamped member stiffness on the self-loosening phenomena patterns for comparative analysis.

Keywords: Self-loosening, bolted joint, stiffness, surface friction, material property, finite element analysis, analytical modeling

TABLE OF CONTENTS

Page

LIST OF TABLES

Page

LIST OF FIGURES

Page

LIST OF ABREVIATIONS

ASME	American Society of Mechanical Engineering
FEM	Finite Element Method
HDPE	High-Density Polyethylene
UDA	Uniform Displacement Analysis
UPA	Uniform Pressure Analysis
VDI	The Association of German Engineers (In German)
LVDT	Linear Variable Differential Transformer
RVDT	Rotary Variable Differential Transformer
BS	British Standard

INTRODUCTION

There are various types of joints that are designed to endure the loads and restrict the components' movement in the structures while transferring the loads between them. These joints include welded joints, adhesive bonded joints and mechanically fastened joints. Among all of them, bolted joints are the most common assemblies utilized across various industries such as aerospace, automotive, nuclear, oil and gas, manufacturing, and more. They are indisputably the most favored among non-permanent clamping methods as they are strong enough to sustain loads. Their quick assembly and disassembly times, coupled with low manufacturing and maintenance costs, have rendered them the most prevalent type of joint. A typical bolted joint consists of a bolt, a nut and one or multiple parts clamped together by the relative rotation between bolt and nut, where the bolt experiences tension along its axis due to the tightening (Figure 0.1). This tensile force is known as preload that elongates the bolt in its axial direction. The goal of achieving adequate preload in tensile joints is to securely hold the clamped parts together with sufficient force to prevent them from separating. The force exerted between the clamped members is known as clamping force and is regarded as the pivotal factor in managing tensile joints. It is important to choose the right amount of preload to achieve sufficient clamping force for having a securely tightened bolted joint in the structural elements. Too high preload may result in an over-tightened joint, which may cause material yielding of the components and lead to material failure at the end. Also, too low preload may leave the joint under-tightened that may not be strong enough to resist external forces during operations.

The most frequent issue with threaded fasteners is the self-loosening that arises from the gradual loss of preload after the joint is tightened. This issue occurs in two distinct stages as shown in Figure 0.2 - the first involves a loss of preload without any relative movement between the engaged threads, known as non-rotational loosening, and the second involves loosening due to the relative rotation between the bolt and the nut under external transverse cyclic loading, which is referred to as "self-loosening" or rotational loosening (Jiang et al., 2004). Stage-I, or non-rotational loosening, involves partial plastic deformation of the joint contact interfaces due to the high localized stresses generated during tightening, commonly referred to as embedding. This results in the loss of clamping load of approximately 1 to 5%

of the total due to embedding, which depends on the surface roughness, number of contact surfaces, joint stiffness, and the applied bearing stress. Stage-II, also known as rotational loosening or self-loosening, occurs because of the relative rotation between the bolt and the nut as soon as there are relative movements among the engaged threads and between the bearing surfaces of the bolt or nut and their adjacent clamped members due to the transverse dynamic loading. Typically, self-loosening becomes more apparent under the dynamic transverse loading compared to the axial loading, as the latter generates significantly fewer radial movements (Junker, 1969). The applied transverse loading induces relative movements between clamped members by negating the frictional resistance primarily generated by the bolt preload between the engaged parts of the assembly. These relative movements initially take place between the bearing contact interfaces and the engaged thread flanks because of small displacements. With the gradual increase of displacements, the bolt starts bending once it surpasses the thread clearance. Once slippage occurs between the bolthead or nut bearing surface and the corresponding clamped member, the bolthead or nut and the threads slides relative to each other. Therefore, loosening of joints by the relative movement in threads causes rotation of bolt and nut because an internal off-torque is generated from the preload acting on the thread helix angle.

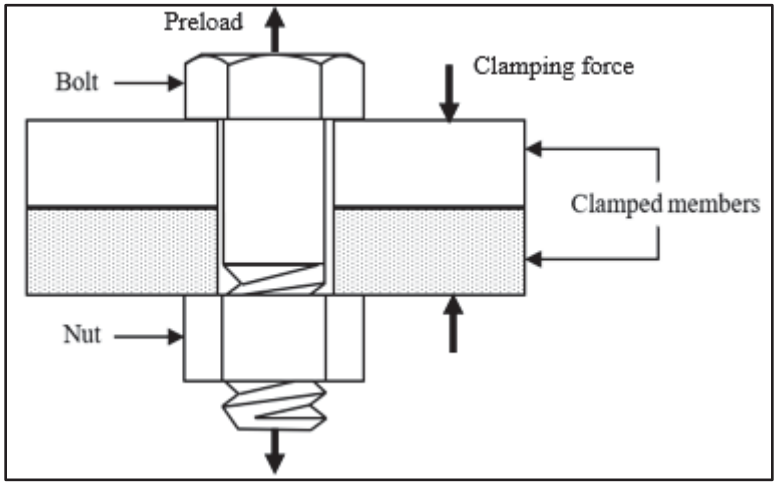

Figure 0.1 Schematic of a typical bolted joint

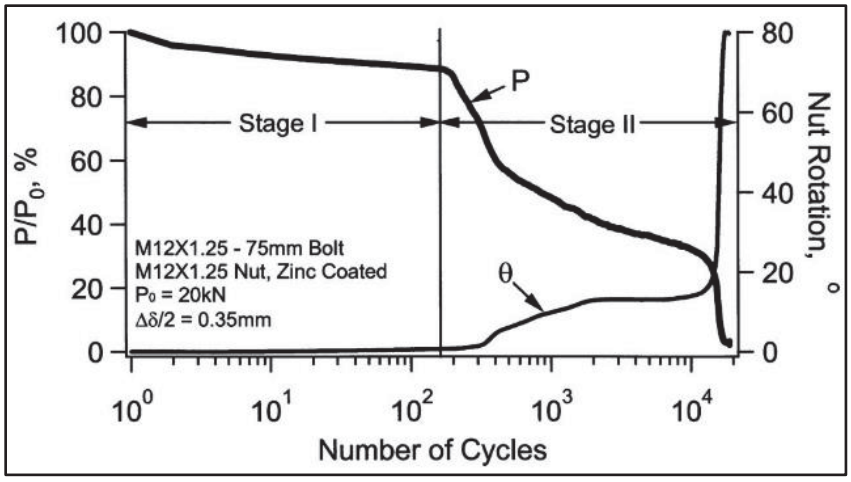

Figure 0.2 Stage-I (non-rotational) and stage-II (rotational) loosening
Taken from Jiang, Zhang & Lee (2003)

The challenges posed by self-loosening make bolted joints critical for the safe operation of various equipment in practical applications, including manufacturing, transportation, and power generation industries. Failure to promptly retighten loosened bolted joints can result in severe equipment damage in various applications, such as liquid or gas leakage, bolt breakage, and catastrophic accidents in plants, potentially halting the entire system. This can lead to significant economic losses. Therefore, ensuring proper safety measures is essential, which involves identifying the key reasons behind self-loosening of bolted joints through extensive investigation of the responsible parameters.

Problem definition

Extensive research has been conducted to understand the complex behavior of self-loosening of bolted joints and the underlying causes of its occurrence from various perspectives using analytical, numerical, and experimental approaches. All these efforts aimed to investigate joint loosening by focusing on various parameters, such as the initial preload, surface conditions and friction coefficients, size and dimensions joint components, types and amounts of applied loading, hole and thread clearance, materials, and joint stiffness. This research is going to address the following challenges:

1. As the stiffness of the components in a bolted joint is a crucial factor affecting the loosening phenomenon, a new methodology for accurately evaluating stiffness, particularly for the clamped members of a bolted joint and the bolts will be developed.
2. Measuring the different friction torques resulting from the input torque applied to the joint after initial tightening and their variations during the processes of tightening and untightening is highly challenging. Therefore, a well-defined tightening-untightening simulation methodology is needed to obtain the various torques involved in the two processes. An analytical model will be used to validate the simulation.
3. Parameters such as stiffness and surface friction in a bolted joint are sensitive to self-loosening. Therefore, a comparison demonstrating the thickness and materials effects of the clamped components is necessary.

To address the above-mentioned challenges, the current project has chosen the following objectives:

1. Develop a finite element-based numerical methodology to accurately evaluate the stiffness of a bolted joint, with particular focus on the stiffness of the clamped members and the bolt and validate the results.
2. Investigate the tightening and loosening processes of a bolted joint to quantitatively measure the different torque components, including pitch torque, bearing friction torque, and thread friction torque.
3. Analyze the self-loosening of a bolted joint to explore how various factors, including material properties and the thickness of clamped members, affect its behavior.

Thesis framework

This doctoral thesis is systematically structured into five chapters to provide a comprehensive understanding of the research topic and guide the reader through its progression.

Chapter 1 introduces a thorough review of the relevant literature on the investigation of loosening of bolted joints through analytical, numerical and experimental approaches.

Chapter 2 offers a detailed overview of the experimental test rig's development, including its components, connected devices, and operating principles.

Chapter 3 presents a finite element methodology for evaluating the stiffness of a bolted joint, with particular emphasis on the clamped member and bolt. A validation method including two different loading cases is performed to verify the developed relationship of the stiffness of bolt and clamped members. This chapter is a copy of the article entitled “On the re-evaluation of the clamped members stiffness of bolted joints” that was published in the *Transactions of the Canadian Society for Mechanical Engineering* journal.

Chapter 4 outlines a methodology developed for the quantitative measurement of pitch, bearing friction and thread friction torques resulting from the external input torque in the tightening and untightening processes. Three-dimensional finite element modeling analysis is performed along with the development of an analytical model and both compared with an existing experimental test result from literature. This chapter replicates the article titled “The Tightening and untightening modeling and simulation of bolted joints”, published in the *Machines* journal.

Chapter 5 explores the effects of various parameters, such as material and thickness of the clamed members, on self-loosening of a bolted joint by conducting an experimental study. Steel and High-Density Polyethylene (HDPE) were chosen as the materials for the clamped members in the tests, where the self-loosening behavior was observed for varying grip lengths. This chapter is based on the article titled “Effect of clamped member material and thickness on bolt self-loosening” that was submitted to the *Materials* journal.

Finally, the thesis summarizes the key findings and contributions in the conclusion chapter along with future recommendations of the research on self-loosening of bolted joints.

CHAPTER 1

LITERATURE REVIEW

1.1 Introduction

A lot of research has been carried out on bolted joints, their design and development, factors affecting their loosening and the mechanism behind the occurrence of loosening. A review of the main bolted joint loosening mechanisms, will be conducted, emphasising the most important available investigations based on the three main aspects, i.e., analytical approaches, numerical finite element (FE) methods and experimental techniques. In this chapter, the main goal is to provide a critical survey of the earlier research on this subject matter addressing all the three different standpoints.

1.2 Non-rotational Loosening

In general, loosening of bolted joints can be classified in two stages: non-rotational and rotational loosening. Non-rotational loosening can occur due to the partial plastic deformation of the joint interfaces (under the bolt head and nut face, between the engaged threads and between the clamped members) after being assembled, which results in a preload loss without any relative rotation between the engaged threads of the bolt and nut. The actual contact area between the surfaces, which is less than the apparent area, consists of asperities that undergo high localized stresses even with the loading under the yield limit of bolt or clamped components. As a result, embedding occurs by the partial collapse of contact surfaces involved. Typically, around 1-5% of the total clamp load can be lost immediately after joint tightening, the amount of which depends on several factors, such as stiffness of joint components, number and condition of the contact interfaces involved, and bearing stress applied. During the first loading, approximately 80% of the preload may be lost after the initial tightening due to embedding, with the remaining 20% lost during subsequent loading (Meyer & Strelow, 1972). A significant portion of the applied external loading to the bolted joint is consumed to reduce the clamping force, yet a proportion of that loading is sustained by the bolt. It is possible

according to the design codes, such as VDI (2003), that the bolt may experience yield because of the external load as it is typically preloaded to a percentage of its yield strength. In high temperature applications, the joint should be preloaded with a lower load than usual because the yield strength of the bolt material is noticeably reduced.

Stress relaxation is another reason for the preload drop of a joint in case of bolting applications at elevated temperatures. It usually occurs due to the material creep over time, and results in a preload drop. To properly measure the stress relaxation of bolts, the British Standards Institute (2006) proposed a standardized method where a sample bolt is preloaded to a certain elastic strain for a specific time duration and temperature, then finally the residual stress is measured after allowing the bolt to relax.

Another problematic effect is thermal expansion in bolted joints. With the elevated temperature, the bolt and the clamped components expand at different rates when exposed to heat, depending on the materials. For example, if the material of the clamped components has higher expansion coefficient than that of bolt, the bolt tension will increase noticeably following an increase in the clamping force, which can result in fatigue of bolt or damage of the joint components in case of excessive thermal expansion difference or thermal cycling are present. In the case of bolt and joint components of similar material, trouble may still occur if both components experience different heat rates.

The surfaces under the bolt head and nut face in a joint usually have high pressures that can create dents on softer clamped members when tightened. Therefore, the asperities present between these surfaces may collapse resulting in plastic deformation due to the sustenance of any externally applied loads, which causes loss of preload because of bolt tension reduction. The preload can be significantly reduced by around 10 to 41% in a joint undergoing cyclic lateral loading even with lock nuts (Jiang, Chang, & Lee, 2001). According to their findings from FE analysis, cyclic plastic deformation at the root level of the engaged threads allows the stress in the bolt to relax, thus resulting in the reduction of the clamping force.

In some cases, fasteners have coatings with softer materials like Zinc (Zn) to prevent corrosion. Although thicker coated fasteners are better resistant to corrosion, the surface coating becomes thinner due to the occurrence of creep that reduces preload. According to Yang and DeWolf (1999), coating relaxation can be continued through longer period due to creep.

In flanged joints, the gaskets used are typically made of softer materials to ensure sufficient sealing that can deteriorate due to gasket creep with the passage of time, resulting in the loss of clamping force. Nechache & Bouzid (2006) address this issue of creep of the bolt and the components of flanged joint by developing an analytical model and validating it with a 3D FE model. Their model can validate the appropriateness of the initial preload in the applications of elevated temperature.

1.3 Rotational Loosening

Self-loosening or loosening occurred by the relative rotation between the engaged threads of bolt and nut resulting in the gradual reduction of clamping force in a joint is a complex phenomenon and the causes behind its occurrence are not clearly identified. This issue is critical in most mechanical systems as the safety and integrity of their structures and equipment are of major concern. There are different factors involved in the occurrence of self-loosening and investigations have been conducted by several researchers who looked into this issue from different perspectives including analytical, numerical and experimental approaches.

Typically, the analytical models are complex in nature to develop for threaded fasteners because of the intricate design structure and the deformations of the components of the assembly while self-loosening takes place, in addition to the amount of time required to develop the analytical formulas. The benefit of this tedious efforts is the ease of the work in case of restructuring or modifying the models when there are changes in the design parameters. The numerical finite element (FE) modeling of the threaded bolted joint is also a cumbersome task due to its complicated geometry design and the complex nature of the phenomenon where joint undergoes self-loosening when subjected to external cyclic loading. On the one hand, the

drawback associated to the numerical approach is obvious when the modeling is based on the simplification of the complex 3D geometry, which impacts the result in most cases when compared to the real scenario. On the other hand, the interesting part is that some investigations become easier because of the simplification technique to conduct parametric study when needed, such as, axisymmetric analysis instead of performing 3D modeling analysis that saves significant computational time. Although developing test rigs and performing experimental analysis are rather costly depending on the type of mechanical system, it is always preferable to generate real experimental data so that the actual behavior of the system can be understood.

Researchers have been striving to uncover the underlying causes of rotational self-loosening. In fact, the bolt force after tightening continuously decreases under the influence of external loads including self-loosening, eventually resulting in a complete loss of preload or bolt failure, which often leads to hazardous incidents. As a result, the topic “self-loosening” has garnered significant attention from researchers over the years for investigation. In general, the types of external loadings to cause loosening can be several, such as axial, impact, torsional, transverse and bending.

1.3.1 Loosening due to axial vibrations

The ability of axial loading, parallel to the bolt axis, to cause rotational loosening has long been a subject of debate. The first investigation on self-loosening was performed by Goodier and Sweeney (Goodier and Sweeney, 1945) where they experimentally measured the rotation of the nut in a bolted joint using microscopes. They observed a preload reduction of approximately 73% with a rotation of 0.0055 radians (0.31°) after 500 loading cycles. From their observations, they proposed a theory in explaining self-loosening due to axial loading that the radial deformation resulting from the elastic contraction of the bolt diameter and elastic expansion of the nut diameter in the radial direction is the reason to the rotation due to the thread helix angle. As a result, a substantial amount of loosening occurred with many loading cycles accumulated. Several researchers came up with necessary modifications of their experimental test settings since their test was based on quasi-static loading that does not reflect

reality. Sauer et al. (1950) modified their experiment where vibration loadings are applied to bolted joints, as commonly seen as in real-world practice, to observe the impact of the number of loading cycles, different dynamic-to-static load ratios, and condition of nut surface. Rapid loosening was observed within the first 500 loading cycles. However, the amount of further loosening decreased after that, continuing up to around 20000 loading cycles although the loosening rate is higher compared to that of Goodier & Sweeney (1945). The used nuts showed better resistance to loosening compared to the new unused nuts. Also, the higher the dynamic-to-static load ratio, the greater the loosening rate.

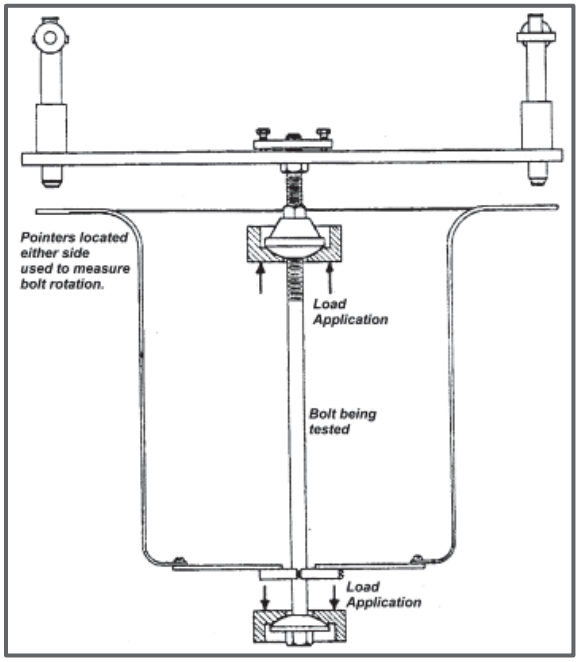

Figure 1.1 Experimental test setup
Taken from Goodier & Sweeney (1945)

Few other researchers also brought changes in the experimental setting of Goodier & Sweeney (1945) and performed their investigations differently. Researchers like Hongo (1964) challenged the idea that rotational or self-loosening could be caused by variations in axial vibration loading. When investigated by projecting a light beam onto a mirror placed on the bolt and observing its oscillation, no relative rotation between the bolt and nut was detected. Loosening under axial loading was also observed in various bolted joints and assessed mathematically based on the tangential strain on the nut surface (Paland, 1966). On the other

hand, Gambrell (1968) investigated a combination of parameters, including thread type (coarse or fine), number and frequency of loading, dynamic-to-static load ratio, initial preload, and surface lubrication, while maintaining consistent loading conditions. Based on his findings, lubrication had no impact on loosening for coarse threads but played a major role for fine threads. Additionally, a dynamic-to-static load ratio greater than unity resulted in a higher loosening rate for fine threads, while ratios below unity had no significant impact on loosening. No loosening was also observed within a certain frequency range (3.3 - 20 Hz) of loading and the loosening rate decreases with increased number of loading cycles. The impact of axial vibration was also experimentally investigated by Sakai (1979) where he demonstrated that material plastic deformation is the primary cause of initial loosening due to preload loss within approximately 200 loading cycles. His indication was towards the axial vibration of bigger amplitude to cause the rotational loosening in the subsequent loading cycles.

An experimental apparatus was developed by Hess & Davis (1996) that consists of a cap screw of 12.7 mm length having 1/4-28 UNF threads inserted onto a base through a 25.4 mm diameter tapped hole with 1/4-28 UNF threads and a shaker to produce axial vibration to investigate loosening. Noticeable twisting motion was found of the cap screw relative to the base caused by axial excitation, especially when the components were lightly loaded. Both the amplitude and frequency of the axial vibration contributed to the twisting motion behavior.

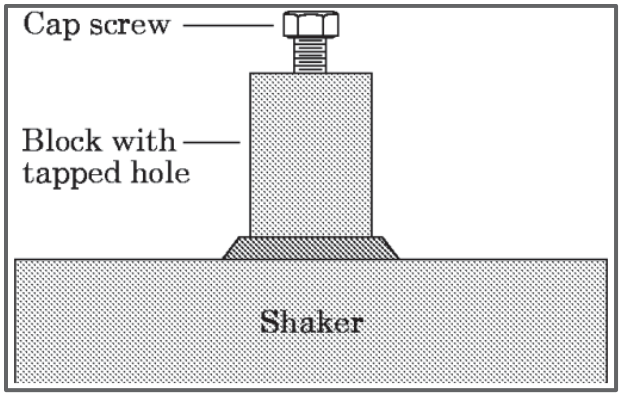

Figure 1.2 Test apparatus with cap screw into a block and shaker
Taken from Hess & Davis (1996)

In another study, a kinematic model was developed by Hess (1996) upon earlier experimental work with his colleague mentioned earlier, which signified the understanding of the twisting of threaded components subjected to gravity and axial vibrations. This demonstrates the potential for various types of motion of the cap screw, including no twisting or twisting in both upward and downward directions. Dynamic modeling analyses were performed in several studies where the threaded cap screw and the base were subjected to axial harmonic loading, either only being loaded by gravity (Hess & Sudhirkashyap, 1996) or with low preload levels between 30 N and 100 N (Basava & Hess, 1998). The latter observed a stable clamping force in the assembly when higher preloads were combined with low-amplitude axial vibration. However, loosening occurred first, followed by tightening as the preload decreased and the vibration amplitude increased, leading to temporary fluctuations in the clamping force. Nevertheless, the clamping force remained stable after numerous loading cycles over time. It is important to note that the above theoretical and experimental studies of Hess and his colleagues were based on assemblies with low preload levels (30-100 N), which is not a realistic scenario in practical applications.

There are other studies that raise doubts about the occurrence of rotational or self-loosening under axial vibration loading. Nassar et al. (2011) conducted finite element and experimental study to observe the loosening phenomenon in bolted joints subjected to cyclic axial separating loads on the clamped members at different radial locations from the bolt axis. They observed no increase in bolt tension with a lower separating force applied eccentrically to the clamped members, but a noticeable drop in clamping force. An immediate increase in bolt tension was observed when the clamped members were separated or nearly separated (see Figure 1.3b). Loosening occurred by the reduction of clamping force, as the joint members underwent nonlinear deformation from the bending effect caused by the axial separating force (see Figure 1.3a). In a follow-up study, the same group (Yang et al., 2012) investigated the impact of axial cyclic separating load on a joint by preloading the bolt beyond its elastic limit. By selecting a preload that exceeds the elastic limit of the bolt, it was found that higher thread friction can be achieved, which helps to reduce loosening caused by a drop in the clamping force (see Figure

1.4). However, in both studies, no loosening due to relative rotation between the bolt and nut was observed because of axial vibration.

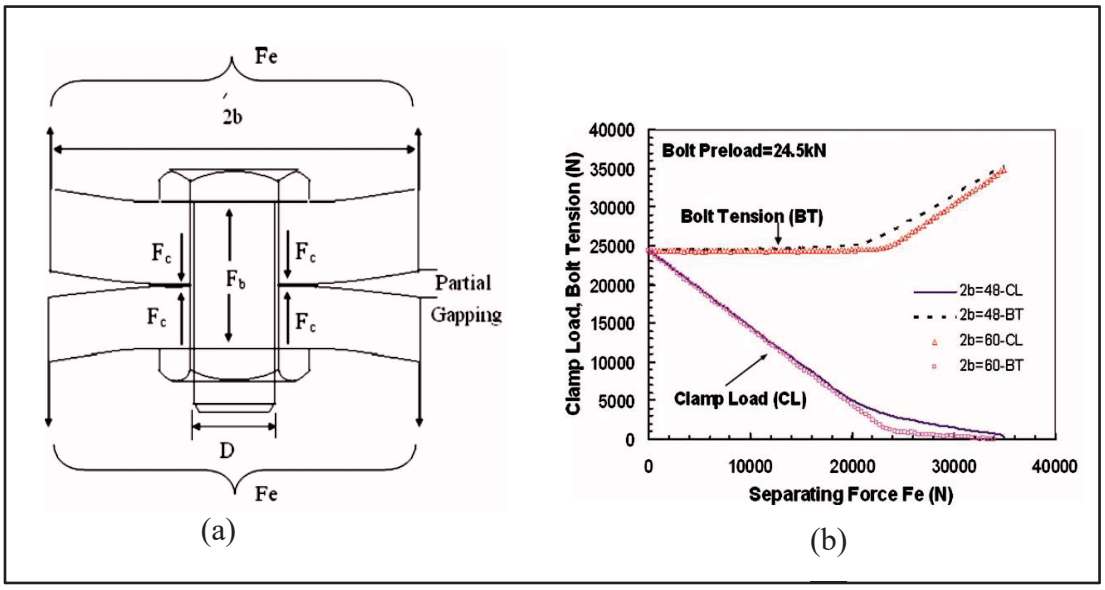

Figure 1.3 (a) Schematic of joint having axial separating load off center; (b) Variation of clamping force/bolt tension
Taken from Nassar et al. (2011)

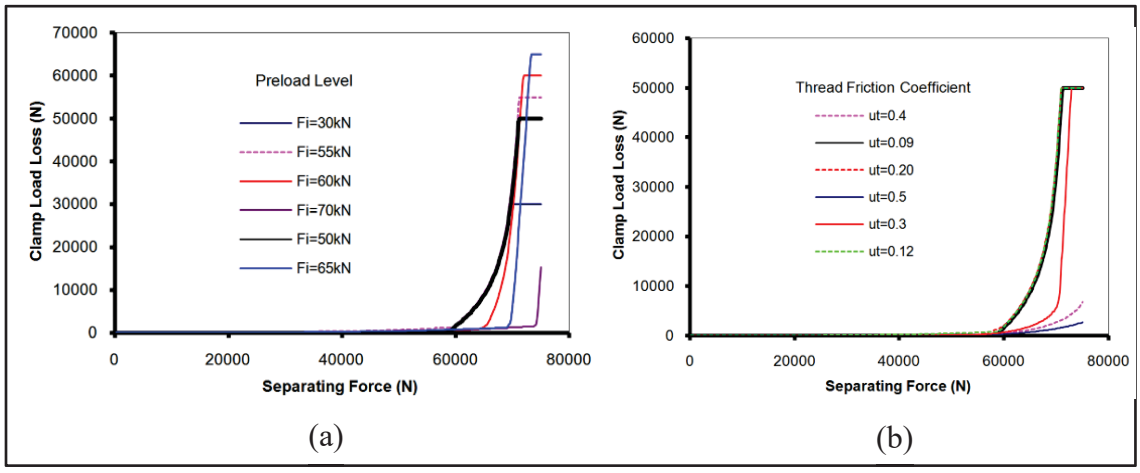

Figure 1.4 (a) Effect of preload at $\mu_t = 0.09$ and (b) effect of thread friction coefficient at preload F_i = 50 kN on the loss of clamping force
Taken from Yang et al. (2012)

Liu et al. (2016, 2017) conducted consecutive studies on loosening by the loss of clamping force due to fretting wear in the engaged thread and contact surface damage when the joint is

subjected to axial excitation forces. In both cases, they found that loosening occurs due to an initial reduction in clamping force caused by plastic damage to the threads, followed by further loosening due to fretting wear. They investigated loosening mechanisms with various coatings, comparing both experimental and numerical results. No rotational loosening due to dynamic axial loading was observed, even as the number of loading cycles increased. Sakai (2011) previously proposed a formulation of critical condition of rotation loosening based on the separation of the clamped members due to axial excitation, where he also noted that rotational loosening is a rare event when axial vibrational loading is involved.

1.3.2 Loosening due to torsional vibration

Torsional vibration loading in bolted joints describes the oscillatory motion resulting from twisting or rotational forces applied to the joint. Loosening of joints by this type of loading occurs when torque is applied to the bolt, causing it to rotate back and forth around its axis. In practice, there are many instances where multiple clamped members are connected to a single bolt and subjected to torsional vibration. Sakai (1978) investigated the self-loosening of bolted joints under torsional vibration both theoretically and experimentally, identifying a minimum relative rotational angle of the clamped components required for self-loosening to occur. According to his findings, no rotational loosening occurs below that minimum rotational angle, and any loosening that happens after a large number of loading cycles is due to fretting wear.

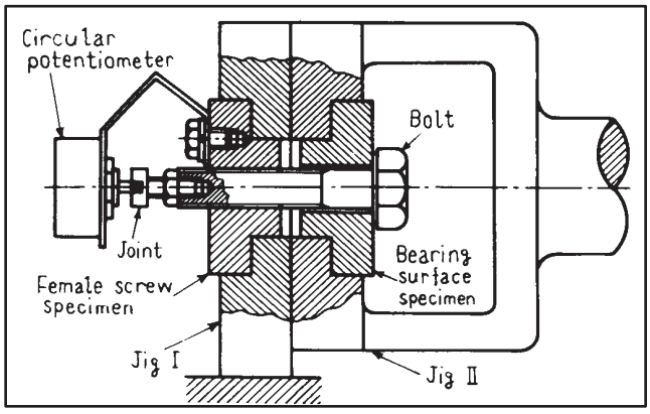

Figure 1.5 Experimental setup to measure relative rotational angle between bolt and nut
Taken from Sakai (1978)

The effects of torsional loading on joint loosening were experimentally observed by Clark & Cook (1966), who identified a functional relationship between bolt force, applied vibration torque, and the number of loading cycles prior to loosening. Strain gauge was used to measure the preload during tests. The tests were carried out on a typical bolt inserted into a tapped hole of a bar that was subjected to a repeated angular displacement. Their findings also indicate a minimum angular displacement beyond which bolt loosening is likely to occur. Better resistance to loosening was observed when the bolt had higher preloads.

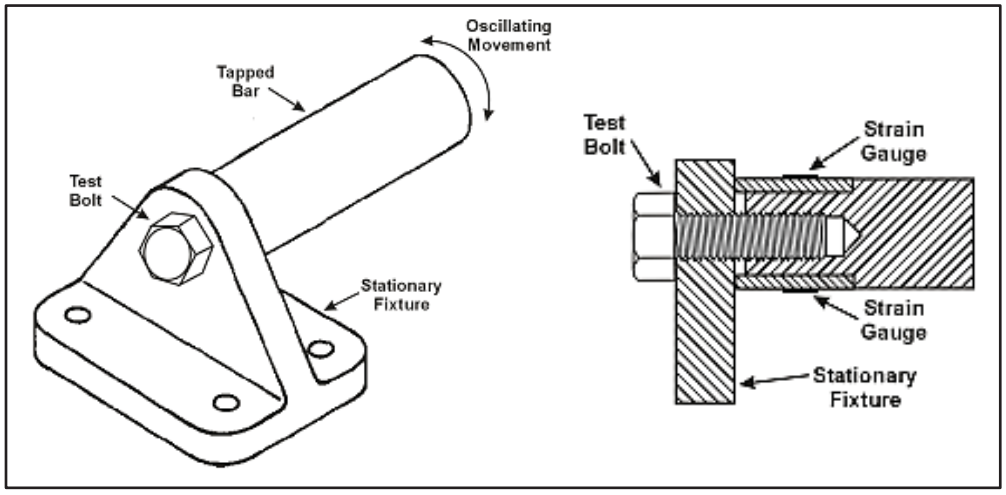

Figure 1.6 Test setup
Taken from Clark & Cook (1966)

Yokoyama (2012) carried out a finite element (FE) analysis to validate Sakai's (1978) work on the initiation and progression of loosening under torsional vibration. In addition to maintaining specific conditions between the thread contact torques during loosening and tightening, as well as the bearing slip torque, a similar conclusion was reached regarding the limiting rotational angle of the moving clamped member required for loosening to occur. Li et al. (2021) conducted analytical and FE modeling on the loosening mechanism, refining Sakai's (1978) theory by removing the constraint of the nut. They demonstrated two distinct failure types: loosening of the bolt and loosening of the nut. Their findings claimed minimum impact of rotational vibration on self-loosening.

1.3.3 Loosening due to impact loading

When a bolted joint is subjected to impact loads, the load is applied so rapidly that there is insufficient time for its gradual distribution, leading to highly localized stress. These loads are dynamic and of high magnitude, occurring over very short intervals, which causes a sudden increase in stress within the joint. The initial experiment on self-loosening due to impact loading, developed by the Elastic Stop Nut Corporation of America (ESNA) and later standardized as the NASM1312-7 test (National Aerospace Standard, 1997), were conducted by Baubles, McCormick, & Faroni (1966). The sample fasteners were tightened onto spool-like arbours that reciprocated inside a slotted fixture (see Figure 1.6), vibrating at a frequency of 30 Hz using a modified fatigue testing machine and at 60 Hz using an electromagnetic shaker. Their theory on the joint loosening due to impact loading stated that the fastener must resonate at the loading frequency for the loosening to occur, though no influence of the loading direction and frequency was noticed.

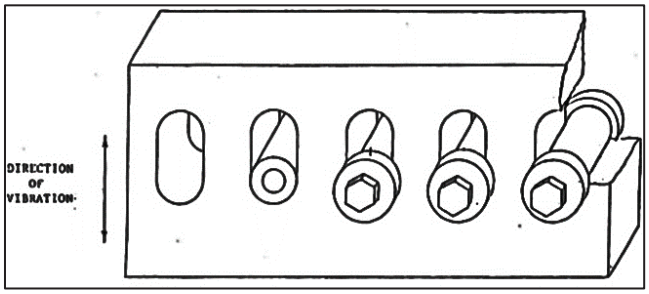

Figure 1.7 NASM1312-7 impact test fixture
Taken from National Aerospace Standard (1997)

Koga (1970) conducted experimental tests on cyclic impact loading in bolted joints and developed a theory stating that compressive waves generated by the thread pressure flanks on one side of the bolt are converted into tensile stress waves upon reflection from the free end of the bolt, ultimately reaching the pressure flank on the opposite side. Loosening occurs when the tensile stress waves are sufficient to overcome the clamping force between the engaged threads. Based on his research, another study (Koga, 1973) proposed a theory that considered the three-dimensional geometry of bolted joints under cyclic impact loading to examine the influence of thread profile angles (see Figure 1.7). Through numerical analysis of several

metric bolts, it was observed that loosening was more pronounced at thread profile angles of 60° and 55°. He recommended using angles between 62° and 63° to achieve the most secure fastening for bolts with certain pitch-to-diameter ratios.

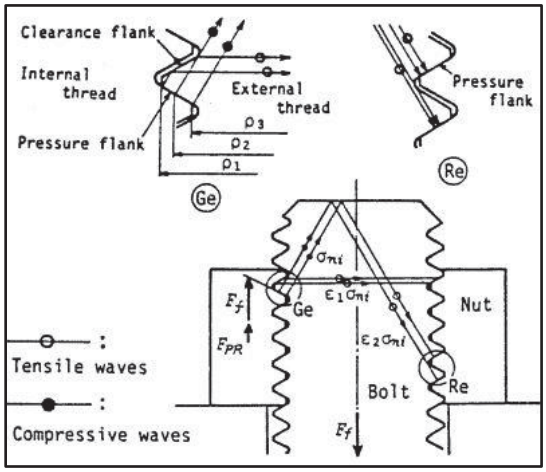

Figure 1.8 Propagation of stress waves between threads by impact loading
Taken from Koga (1970)

Daadbin & Chow (1992) conducted an analytical investigation into self-loosening caused by impact loading on a bolted joint, identifying key factors such as initial preload, impact loading duration, friction characteristics at contact surfaces, and thread lead angle as critical contributors to loosening. They suggested that loosening due to preload reduction can be minimized if the impact load is applied over a longer duration on a joint with finer threads and higher friction at the contact surfaces. An experimental investigation was conducted by Dong & Hess (1999) on self-loosening of dimensionally non-conforming bolted joints subjected to repeated shocks. They found that bolted joints with dimensional conformance are more prone to loosening compared to non-conforming joints, especially in cases where there are specific combinations of undersized pitch and major bolt diameter, or oversized pitch and minor nut diameter. A three-dimensional FE analysis of a bolted joint subjected to dynamic impact loading is performed by Shoji & Sawa (2008), finding no significant difference in loosening caused by impact loading compared to that caused by vibration.

1.3.4 Loosening by transverse loading

Loosening of bolted joints due to transverse loading, also referred to as lateral or shear loading, occurs when a load is applied perpendicular to the bolt axis. This type of loading induces relative motion between the joint components, which can progressively diminish the clamping force, ultimately leading to the bolt loosening.

Early research on self-loosening focused on studying the effects of impact and dynamic axial loading. Junker (1969) was the first to identify the primary cause of complete joint loosening and experimentally demonstrated that self-loosening is more pronounced in joints subjected to dynamic transverse loading compared to dynamic axial loading. His findings shifted the perspective and direction of most researchers at the time, leading many of them to design and conduct their experimental tests using his rig, known as the "Junker test machine".

Figure 1.8 illustrates Junker's experimental test rig that was developed with a fixed base, a movable plate and multiple sensors to get data of preload, transverse force and lateral displacement.

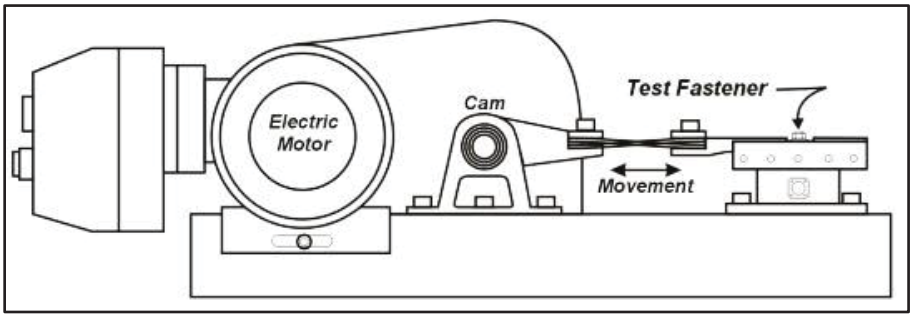

Figure 1.9 Junker's test rig
Taken from Junker (1969)

Cyclic transverse loading was applied by the movable plate to the joint using an eccentric cam mechanism, which was driven by a motor. To reduce friction between the contact surfaces, needle-type roller bearings were placed between the fixed base and the movable plate. The results of the bolt preload showed a significant drop in relation to the number of loading cycles,

with the amplitude of transverse vibration identified as the primary cause of loosening, while the frequency of movement had no effect. A quantitative comparison of the performance of fasteners with different designs was conducted in terms of loosening resistance using this test machine. Based on his testing method and findings, the classical theory known as the "complete slippage theory" was established, which states that the frictional forces on the contact surfaces of engaged threads must be overcome for self-loosening to take place.

Many researchers adopted Junker's theory due to its popularity and began testing various parameters related to the self-loosening mechanism using their own modified test rigs. Finkelston (1972) experimentally examined the impact of thread pitch, as the helix angle of the thread directly influences the loosening or pitch torque of a bolted joint. His tests on 3/8 in. UNF (fine) and 3/8 in. UNC (coarse) self-locking nuts confirmed that loosening is more pronounced in coarse-threaded fasteners. Also, loosening was found to be less pronounced with higher initial preload, lower amplitude of transverse loading and flexible clamped parts.

The phenomenon of self-loosening was theoretically described in two different stages of transverse loading by Yamamoto & Kasei (1977). The first stage involved the inclination of the bolt thread toward the nut thread, followed by the slipping between the engaged surfaces in contact. The subsequent stage referred to the slippage between the nut face and the contact surface of the vibrating plate, which causes the nut to rotate in the loosening direction due to the spring back resulting from the elastic torsion of the bolt shank. Self-loosening occurred as these stages repeated with the progression of the loading cycle.

Sakai (1978) conducted a theoretical investigation on the loosening of a transversely loaded bolted joint resulting in the relative slip between the clamped members. He found that the minimum bearing friction coefficient required to cause bolt loosening was 0.03. The report also provided an analytical formula for critical slippage, which is the minimum slip between clamped members needed to cause relative slip on the bearing surface to meet the condition of bolt loosening. This was verified experimentally. However, the analysis indicated that more precise experimental measurements are needed to determine the bolt loosening angle

accurately. Haviland (1981) identified additional factors, beyond shear loading, that contribute to loosening due to transverse movement. For instance, slippage can occur due to differences in temperature leading to differential thermal expansion, joints made of dissimilar materials, or bending of the joint. A relationship between the applied transverse load and the axial tension of a joint was analyzed by Tanaka, Hongo & Asaba (1982) using numerical FE modeling and calculation were performed on stress distribution of the thread contact surface. Axial tension significantly increased with larger loads, resulting in a further shift of the contact surface from the joint hole. Kasei, Ishimura & Ohashi (1988) conducted a theoretical investigation into self-loosening and found that it can occur in the absence of slippage at the bearing contact surface. According to them, this can be considered as the initial stage with minimal loosening; however, a significant loss of clamping force can occur immediately following this stage. Vinogradov & Huang (1989) proposed a dynamic model to examine the impact of dynamic excitation frequency on self-loosening. They identified the non-uniform distribution of preload across the thread contact surface as the triggering factor for loosening.

Zadoks et al. (1997) conducted a theoretical analysis on the self-loosening mechanism under transverse loading with a two-degree-of-freedom dynamic model and by using Hertz contact stress theory to formulate a relationship between contact force and deformation between clamped mass and bolt shank. They found that the impact between the clamped mass and the bolt shank was the major reason for self-loosening. Additionally, slippage was found to occur both between the engaged threads and between the bolt head and the clamped part due to the impact on the joint. For self-loosening to occur, the pitch torque in the loosening direction must exceed the sum of the bearing and thread friction torques. Nassar et al. (2006) conducted both analytical and experimental investigation to observe the impact of bolt tension and thread pitch on self-loosening of threaded bolted joints subjected to cyclic transverse excitation. They identified a threshold preload value for a given loading amplitude that prevents self-loosening. Beyond this threshold, loosening due to preload loss depends on the thread pitch, with finer threads offering better resistance to loosening compared to coarse threads. This work strongly supported the experimental findings of Dong & Hess (2000), which demonstrated the influence of thread non-conformity on self-loosening. In another study, Nassar et al. (2009) developed

an analytical model that calculates the friction torques and shear forces generated by transverse loading, considering the local bending effect near the bolt head, along with stress distributions and relative slippage at the bearing and thread contact surfaces.

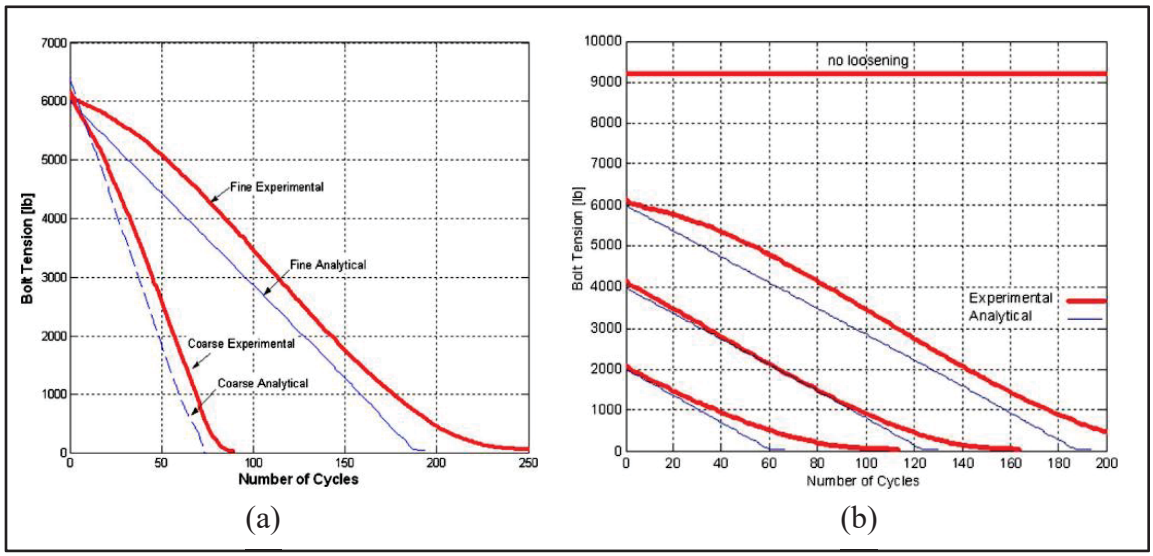

Figure 1.10 Effect of (a) bolt preload and (b) thread pitch on self-loosening
Taken from Nassar et al. (2006)

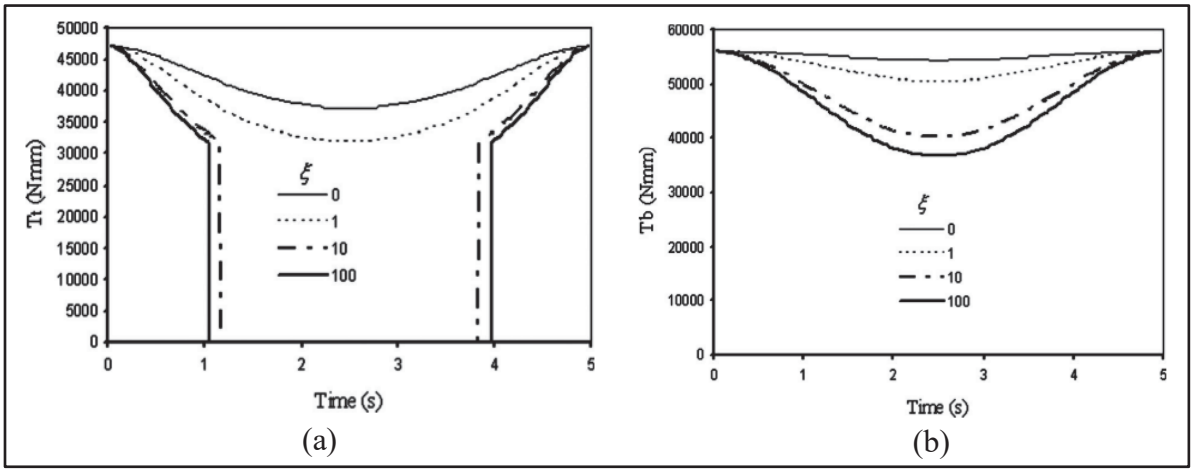

Figure 1.11 Effect of bending on (a) critical thread friction and (b) critical bearing torque under transverse cyclic excitation
Taken from Nassar et al. (2009)

Zaki, Nassar & Yang (2011) developed an analytical model to determine the threshold preload in countersunk bolts, where they also found the impact of the type of thread pitch on self-

loosening of the joint under transverse loading. Fine threaded fasteners were found to be more resistant to loosening compared to those with coarse threads (see Figure 1.11a). Also, the threshold preload became higher after increasing the excitation amplitude (see Figure 1.11b).

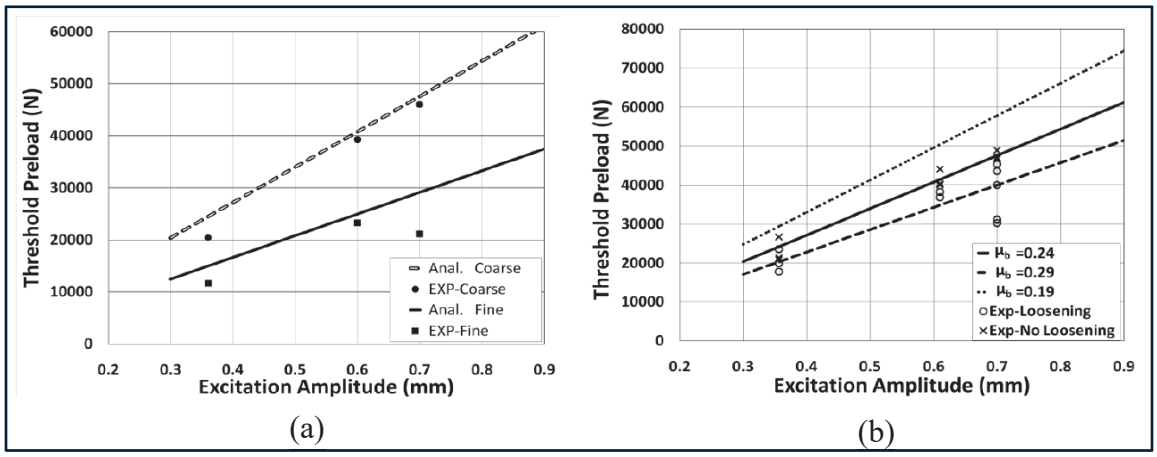

Figure 1.12 Effect on threshold preload of (a) thread pitch, (b) excitation amplitude
Taken from Zaki, Nassar & Yang (2011)

Another study was conducted by Zaki, Nassar & Yang (2012) to investigate the effect of conical angle and thread pitch on loosening of countersunk fasteners subjected to transverse cyclic displacement. They again observed that the thread pitch has a major role in the reduction of the loosening rate, where a decrease of the pitch from 1.95 mm to 1.27 mm resulted in 85% decrease in loosening. Also, loosening was reduced with the increase of the conical angle.

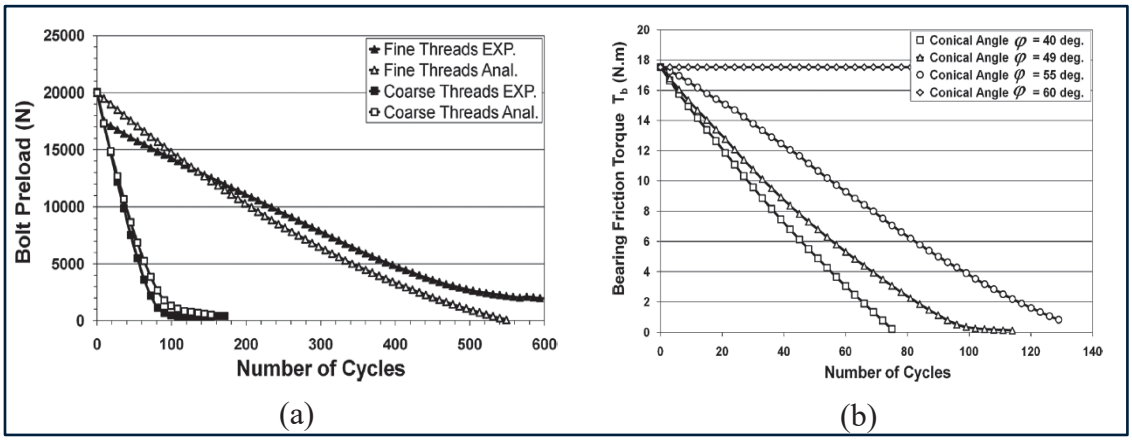

Figure 1.13 Effect of (a) thread pitch and (b) conical angle
Taken from Zaki, Nassar & Yang (2012)

A three-dimensional FE modeling analysis was conducted by Pai & Hess (2002) to investigate self-loosening under dynamic transverse loading caused by slips at the contact surfaces under the bolt head and between engaged threads. Their observations indicated that localized slips at the joint contact surfaces could lead to self-loosening without the need for complete slippage. They also confirmed through another experimental study (Pai & Hess, 2002) that self-loosening can be initiated by localized slips, which require nearly half the shear force needed for complete head slip.

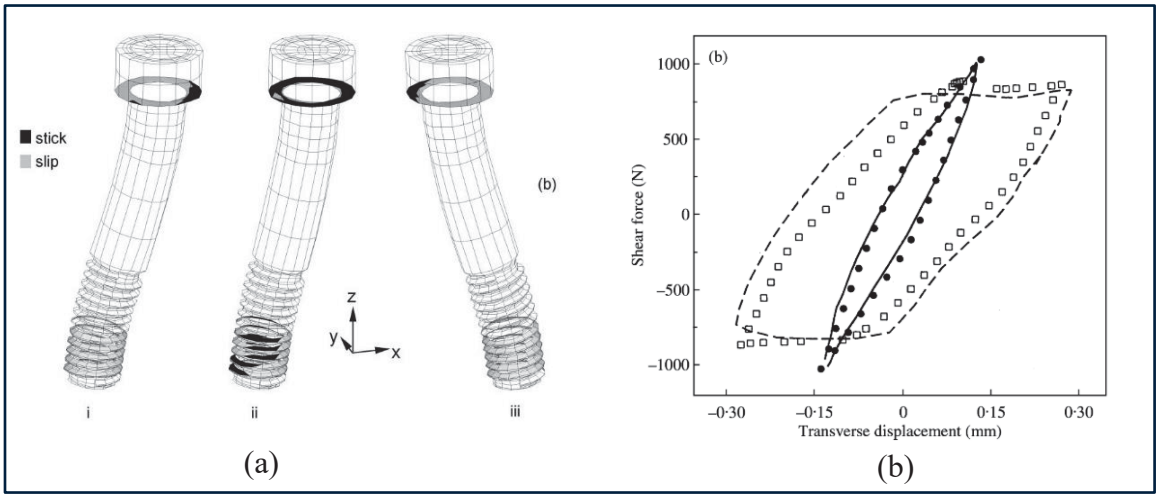

Figure 1.14 (a) Slip-stick phenomenon at contact surfaces, (b) Experiment vs FE hysteresis curves: complete thread and local head slips, EXP (–), FE (•); complete thread and complete head slips, EXP (---), FE (□)
Taken from Pai & Hess (2002)

Housari & Nassar (2007) conducted an analytical study on the effects of bearing and thread friction coefficients on loosening under cyclic transverse excitation, incorporating surface coatings and lubrication (see Figure 1.14). This was followed by experimental validation. They used phosphate and oil coatings (first set), which resulted in a 10% difference between experimental and analytical loosening rates (23 N/cycle experimentally and 20.5 N/cycle analytically). For the second set, with an olefin molysulfide solid film coating, the difference was only 2% (184 N/cycle experimentally and 181 N/cycle analytically). Additionally, the loosening rate was analyzed by varying the bearing and thread friction coefficients and reduced loosening was observed after increasing both parameters.

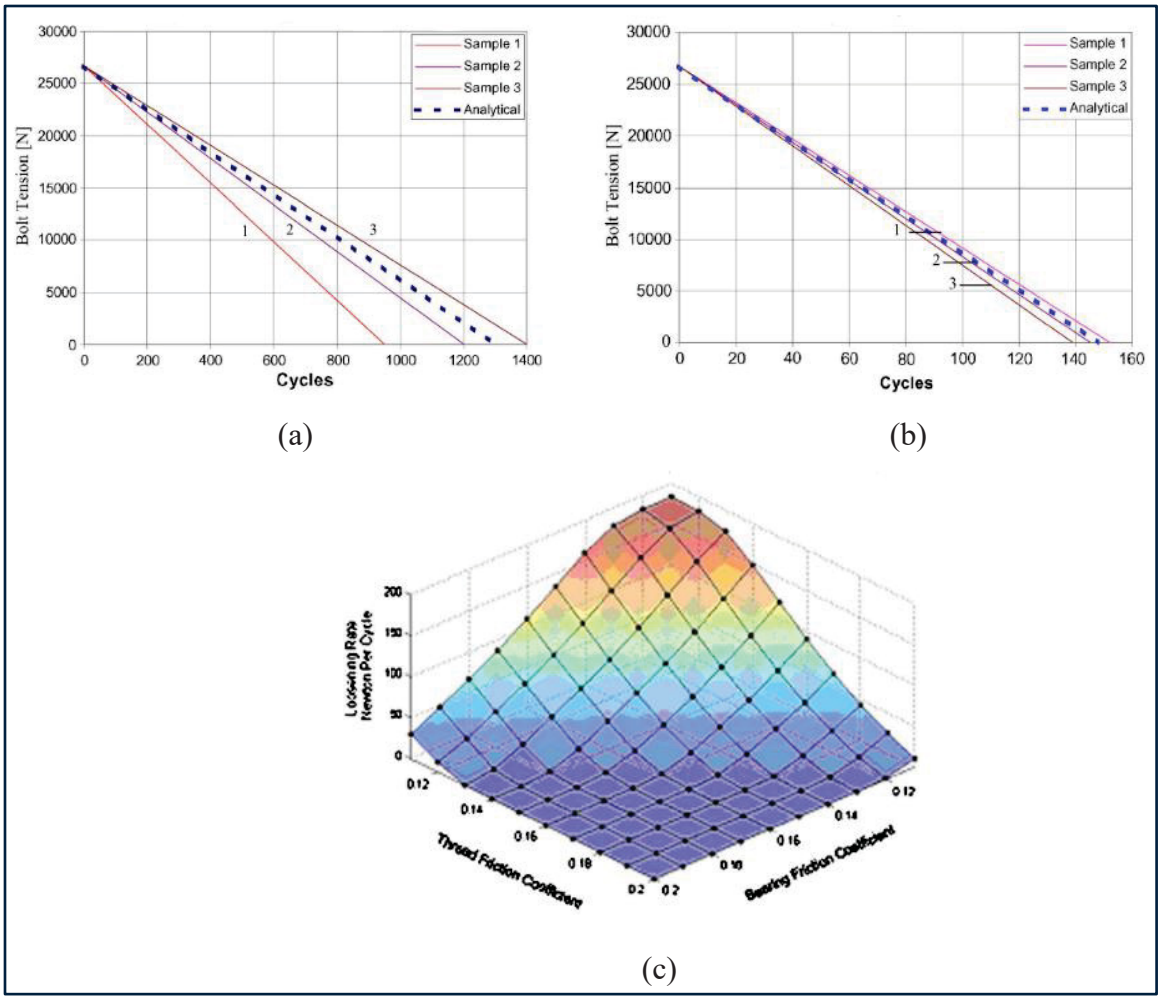

Figure 1.15 (a) experimental and analytical loosening curve for phosphate and oil coated bolt; (b) for olefin and molydisulfide solid film lubricated bolt; and (c) effect of bearing and thread friction coefficient on self-loosening rate
Taken from Housari & Nassar (2007)

A number of studies have been conducted to understand the self-loosening mechanism caused by local slippage using analytical and FE methods. Izumi et al. (2005) carried out a series of FE analyses, identifying self-loosening initiation from the gradual accumulation of local slippage, specifically occurring through complete thread slip without any slippage at the bearing surface. They showed in another study (Izumi, Kimura & Sakai, 2007) that a slight amount of rotational loosening, also known as micro slip, can start with around 50-60% of the transverse loading causing slip in the bearing surface.

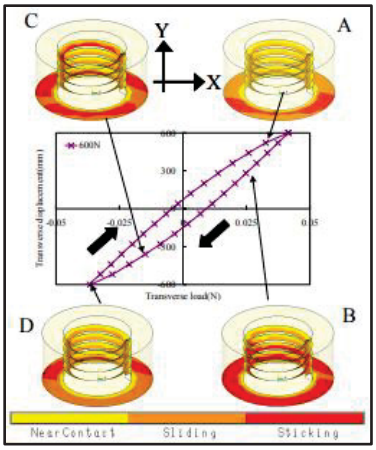

Figure 1.16 Contact conditions during self-loosening
Taken from Izumi, Kimura & Sakai (2007)

Self-loosening caused by the accumulation of micro-slip was further analytically studied by Kasei (2007), validating the findings with experiments on an M10 × 1.25 bolt. Loosening was triggered by rotational movement due to the force restored from the elastic torsion of the bolt shank. Self-loosening under cyclic transverse loading was investigated using three-dimensional FE modeling analysis by Zhang, Jiang & Lee (2007), with an elastic material behavior. Microslip in engaged threads and surface contact pressure variations significantly contributed to initiate loosening by rotation.

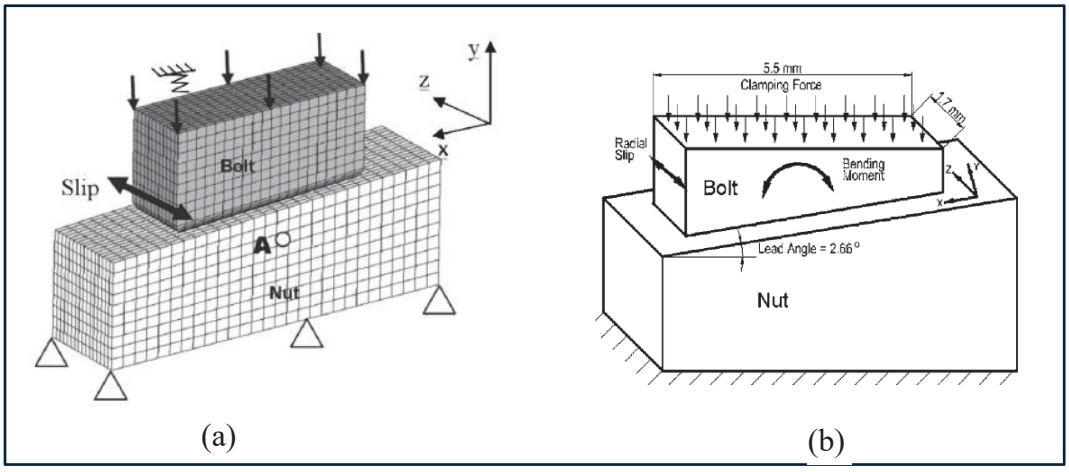

Figure 1.17 (a) Micro-slip model for thread contact; (b) cyclic contact pressure variation to initiate loosening and clamping force
Taken from Zhang, Jiang & Lee (2007)

The analytical model developed by Yokoyama, Izumi & Sakai (2010), which formulated the behavior of bolted joints under transverse vibration, found that self-loosening due to local slippage on the thread surface was amplified by the reaction moment influenced by the bolt bending displacement. Dinger and Friedrich conducted studies on self-loosening caused by localized slippage under repeated loading. They demonstrated by conducting a numerical FE analysis (Dinger & Friedrich, 2011) that loosening occurs through gradual rotation and sliding between engaged threads, driven by shank torque generated from the thread pitch torque. In another study, Dinger (2016) proposed a FE method to investigate the self-loosening of bolted joints subjected to a combination of torsional and vibration loading, identifying the critical conditions for rotational loosening to occur due to the accumulation of localized slippage. To have a detailed understanding of the contact slip states, Chen, Gao & Guan (2017) studied the self-loosening of joint by using a three-dimensional elastic FE modeling analysis. Their method incorporated relative rotation angles and velocities, rather than relying on the traditional Coulomb friction law, to analyze the slip states. They suggested that bolt loosening occurs due to a creep slip phenomenon at the contact surface, despite some contact facets remaining stuck. A very recent study on vibration induced self-loosening was conducted by Gong, Liu & Ding (2020) to investigate the nonlinear localized slip in the threads by using a modified Iwan model. Three component forces in the circumferential, radial and perpendicular directions of the thread were generated from the acting force on it, where the radial component was dominant in accumulating local slippage of the thread contact surface. However, the other two components had zero influence.

Given the hazardous consequences of self-loosening due to cyclic loading, especially in critical structures and machinery where safety and performance are paramount, researchers have been focused on identifying the critical conditions to mitigate this issue. Nishimura et al. (2007, 2013) developed an analytical formula of critical relative slippage (S_{cr}) to evaluate the minimum relative displacement between the bolt head or nut and clamped member in contact due to applied lateral load. They considered bolt bending deformation and the asssociated constraint conditions of the geometry and the inclination compliance (k_w) of the bolt head to

develop the formula. The critical relative slippage (S_{cr}) was found to be decreasing as bolt axial tension decreases, as illustrated in Figure 1.17.

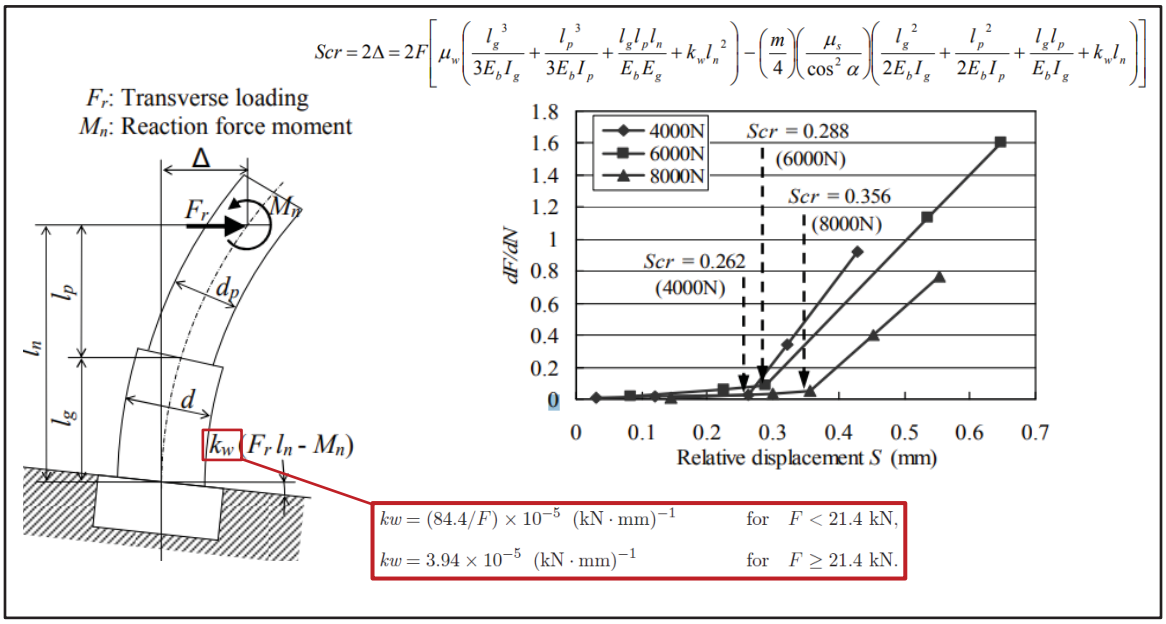

Figure 1.18 Critical relative slippage (S_{cr}) considering inclination compliance of nonlinearity Taken from Nishimura et al. (2007; 2013)

Nassar and his colleagues conducted studies to identify the critical conditions for self-loosening that are discussed earlier, such as the minimum required preload under specific vibration amplitudes based on thread type (Nassar & Housari, 2006), as well as the bearing and thread friction torques under large transverse amplitudes (Housari & Nassar, 2007). An analytical equation was developed by Yang & Nassar (2011) to evaluate the variation of preload per cycle due to cyclic transverse loading. Under a specific loading amplitude, a sharp drop in preload was observed with lower initial preload, whereas the preload remained stable at higher values.

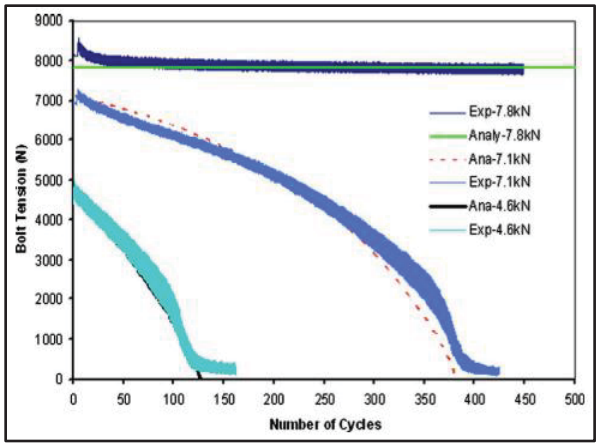

Figure 1.19 Clamp load variation for three different preloads
Taken from Yang & Nassar, 2011)

Though the analytical model was able to correctly predict the clamp load loss per cycle when compared to experimental results, they recommended more explicit analytical solution and proposed another criterion to study self-loosening of preloaded cap screws under cyclic transverse loading (Yang, Nassar & Wu, 2011). They used beam bending theory in their model and included the effect of engaged thread height on the yang (non-uniform) and engaged thread end bending angle (see Figure 1.19). The criterion was based on maximum shear force of bearing ($F_{bs,max} = \frac{3EI}{KL^3}\delta_0$) and thread friction ($F_{ts,max} = \frac{3\beta' EI}{KL^3}\delta_0$) formulas to predict the self-loosening resistance condition as T_b (bearing friction) + T_t (thread friction) – T_p (pitch) ≥ 0.

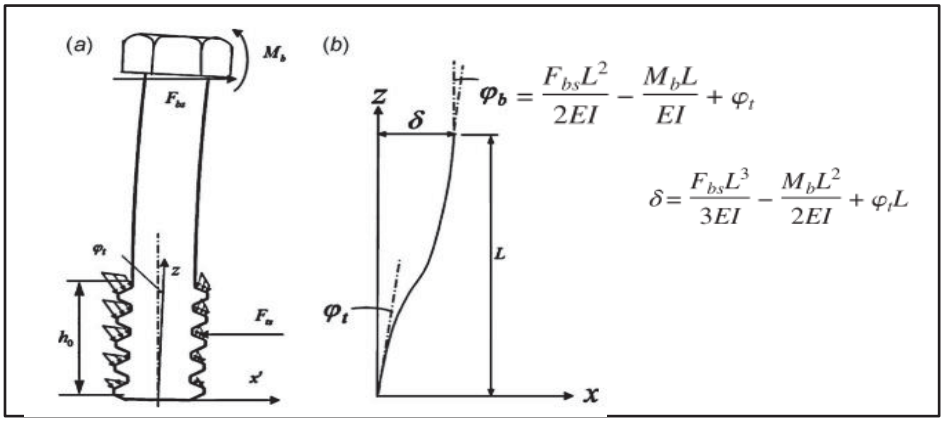

Figure 1.20 Force diagram of bolt with bolt bending deflection and angle
Taken from Yang, Nassar & Wu (2011)

Zaki, Nassar & Yang (2010a) investigated bearing and thread friction coefficients to find the critical preload, by comparing thin and thick coated bolts with Magni 565 and found that thin coated bolts are better resistant to self-loosening than bolts with thick coating (e.g., 210 N/cycle for thick and 187.5 N/cycle for thin). They found better loosening resistance with higher combinations of friction coefficients at bearing and thread contact surfaces.

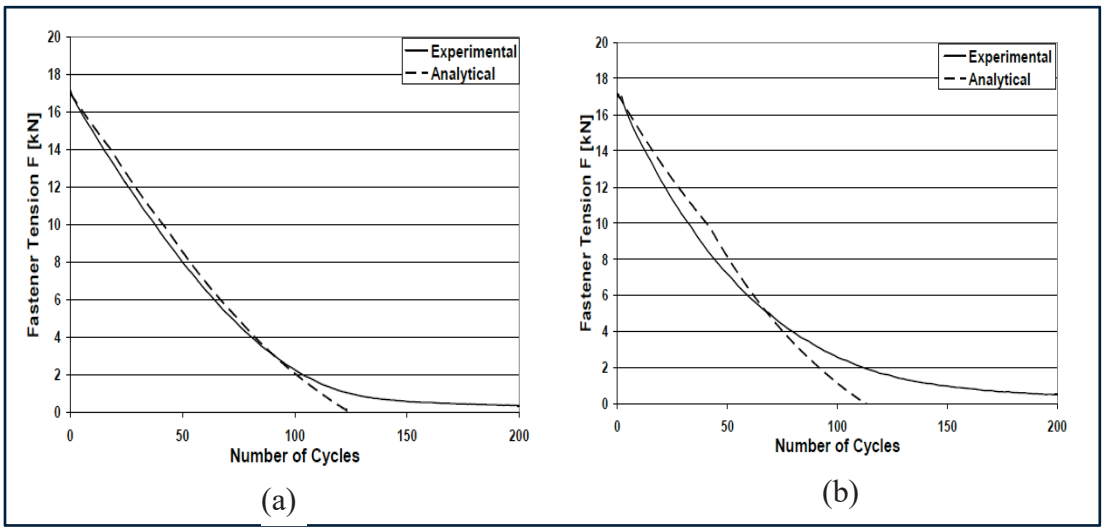

Figure 1.21 Self-loosening behavior-(a) thin vs (b) thick coated bolts at 17.5 kN preload
Taken from Zaki, Nassar & Yang (2010a)

They also conducted analytical investigation on developing critical condition of loosening based on parameters such as bearing and thread friction coefficients (Zaki, Nassar & Yang, 2010b) and threshold preload in countersunk bolts by considering thread pitch and vibration amplitude (Zaki, Nassar & Yang, 2011).

Studies have been performed to investigate different parameters and factor that influence loosening of bolted joints subjected to transverse loading. Sanclemente & Hess (2007) conducted experiments on loosening due to repeated transverse loading to have a quantitative understanding of the influence of certain parameters. Higher preload, lower modulus of elasticity of joint material, larger bolt nominal diameter, fine thread and hole with tight fit were found to be the conditions influencing loosening resistance. Zhang, Jiang & Lee (2006) investigated self-loosening by examining the effects of varying the loading direction and

clamped length. Through experiments on an M12×1.75 bolt and nut, they found that an increase in the grip length resulted in a higher self-loosening endurance limit. Loosening became more pronounced as the loading direction shifts from parallel to perpendicular to the joint axis.

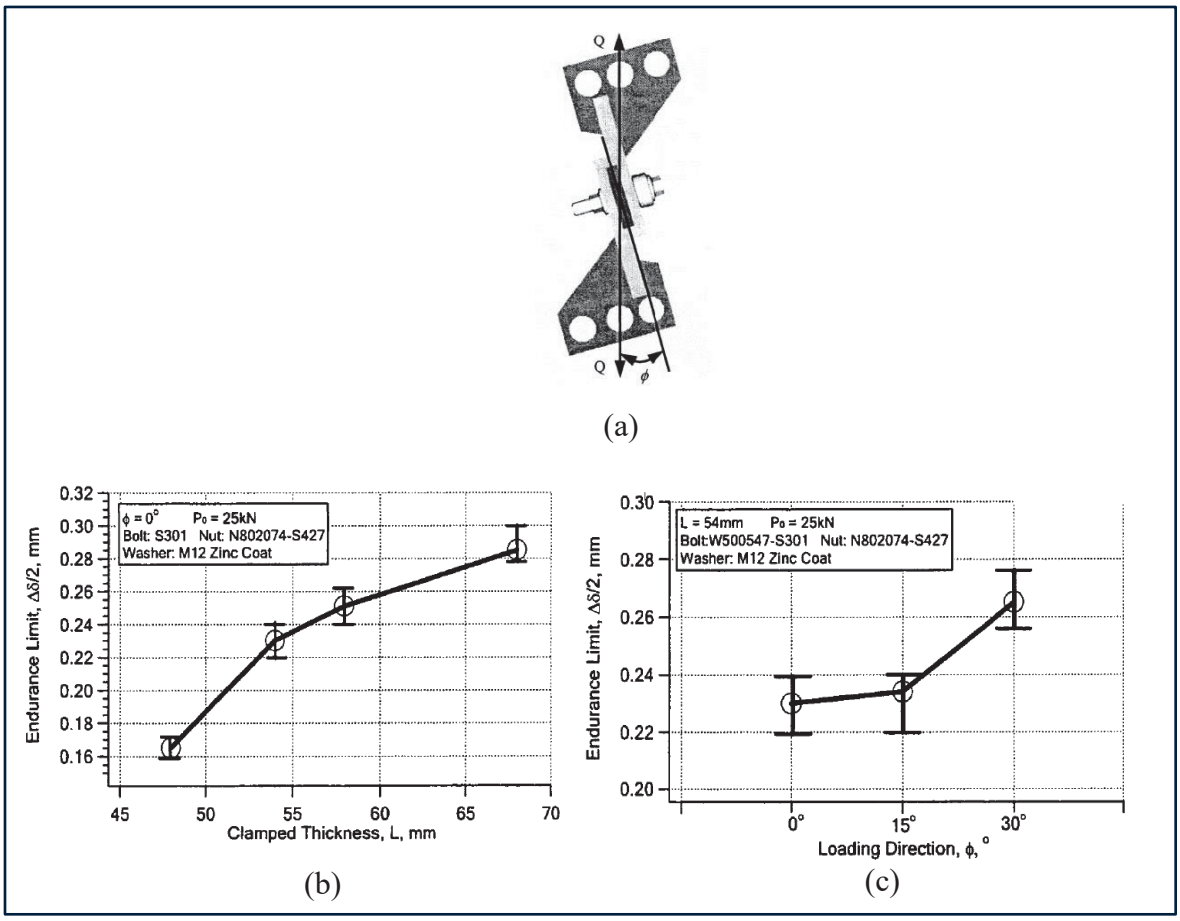

Figure 1.22 (a) Apparatus to adjust loading direction, (b) effect of clamped length, and (c) effect of applied load direction
Taken from Zhang, Jiang & Lee (2006)

An experimental study was performed by Noda et al. (2016) to examine the effect of a slight pitch difference between bolt and nut threads, which leads to a significant increase in prevailing torque, enhancing loosening resistance. After conducting fatigue experiments with different pitch differences under various stress amplitudes, they noted that selecting an appropriate pitch difference can enhance the fatigue life of bolts.

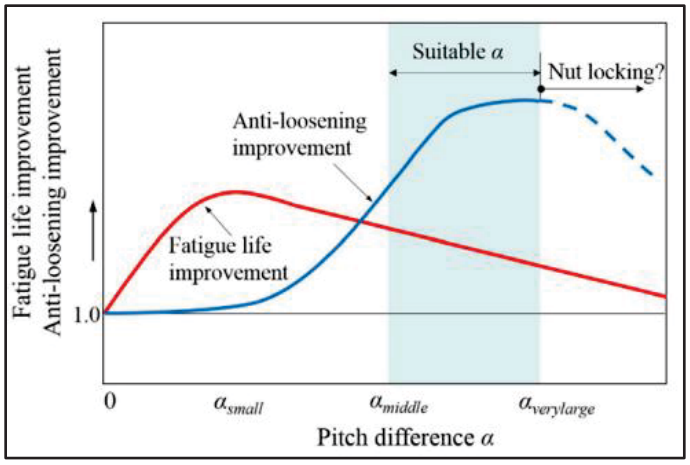

Figure 1.23 Improvement of fatigue life and anti-loosening performance. Taken from Noda et al. (2016)

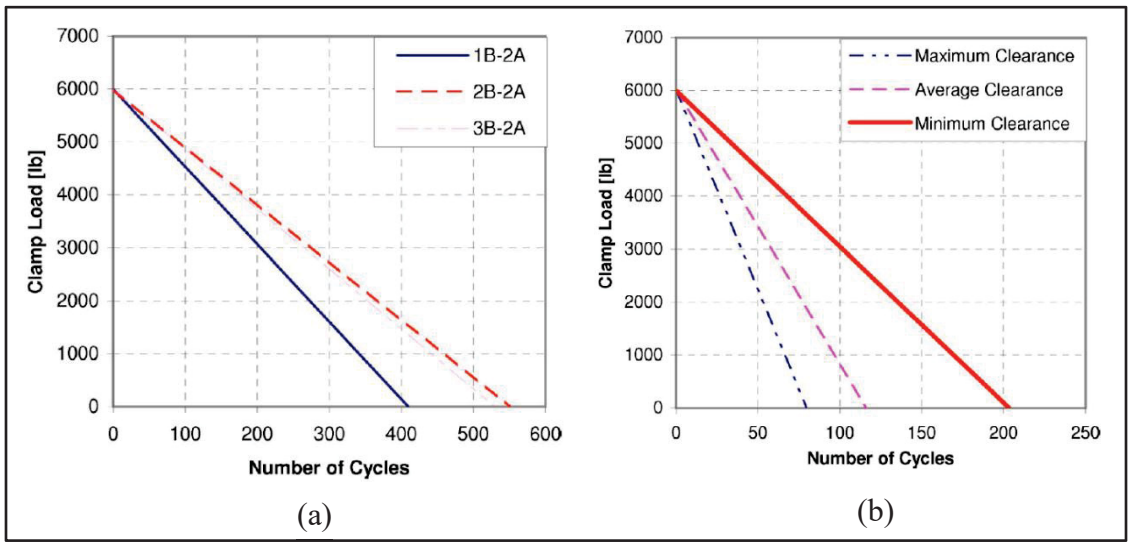

Figure 1.24 Effect of (a) hole clearance (3%) and (b) thread fit (1B-2A). Taken from Nassar & Housari (2006)

Nassar and colleagues investigated several parameters to assess their effects on the self-loosening of various types of joints. Nassar & Housari (2006) analyzed both analytically and experimentally the influence of hole clearance and thread fit on the loosening behavior of fasteners under transverse cyclic loading (see Figure 1.23). They found that increasing hole clearance reduced the number of cycles needed for complete loosening, though it had no effect in case of smaller displacement amplitudes, as the bolt head cannot slide enough to reach the critical displacement for self-loosening. Additionally, a tighter thread fit increases resistance

to self-loosening. Their recommendation was to minimize hole clearance and maintain a tighter thread fit to prevent self-loosening.

In 2011, Yang & Nassar conducted several studies to examine the influence of various parameters on joint self-loosening. They first introduced an analytical model to investigate the effect of non-parallel contact surfaces (wedge angle effect) beneath the nut and bolt head, which was then validated through experimental results (Yang & Nassar, 2011a). A modified test rig, based on Junker's self-loosening test rig, was used to accommodate a zinc-coated M12×1.75 bolt with an 82 mm grip length. After testing five wedge angles at three different preloads, they observed a reduction of loosening with larger wedge angles, even at lower preloads. Additionally, higher preloads provided better resistance to loosening (see Figure 1.25).

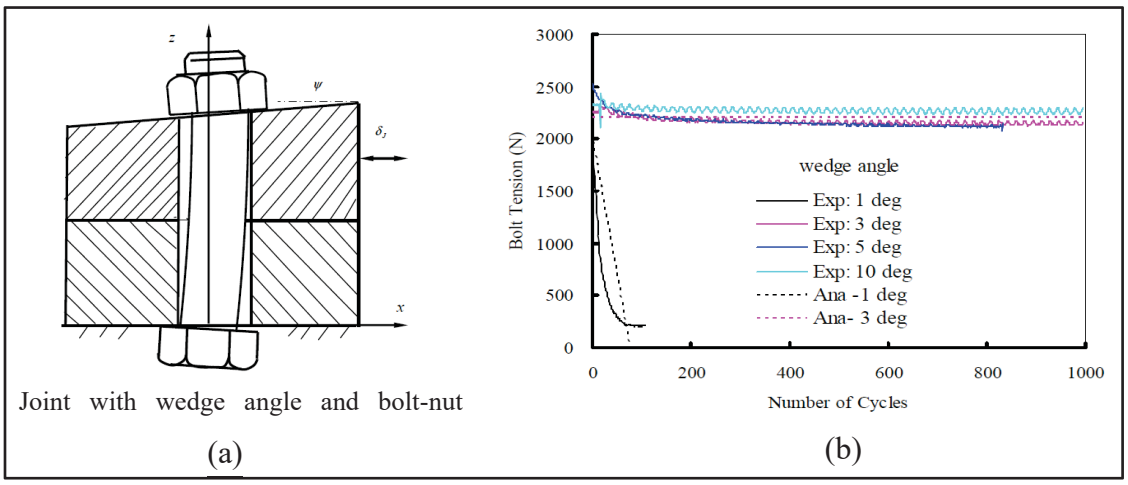

Figure 1.25 (a) Bolted joint with wedge angled contact surfaces; (b) test results for different wedge angles at 2.2 kN preload
Taken from Yang & Nassar (2011)

The authors conducted another analytical study (Yang & Nassar, 2011b) on the self-loosening phenomenon by varying the thread profile angle as well as the thread and hole clearances. They performed experiments using a plain M10×1.5 class 8.8 bolt in their previously developed test rig for validation. The results indicated that self-loosening was more pronounced with larger

thread and hole clearances, while higher thread profile angles exhibited a reduced tendency for loosening (see Figure 1.26).

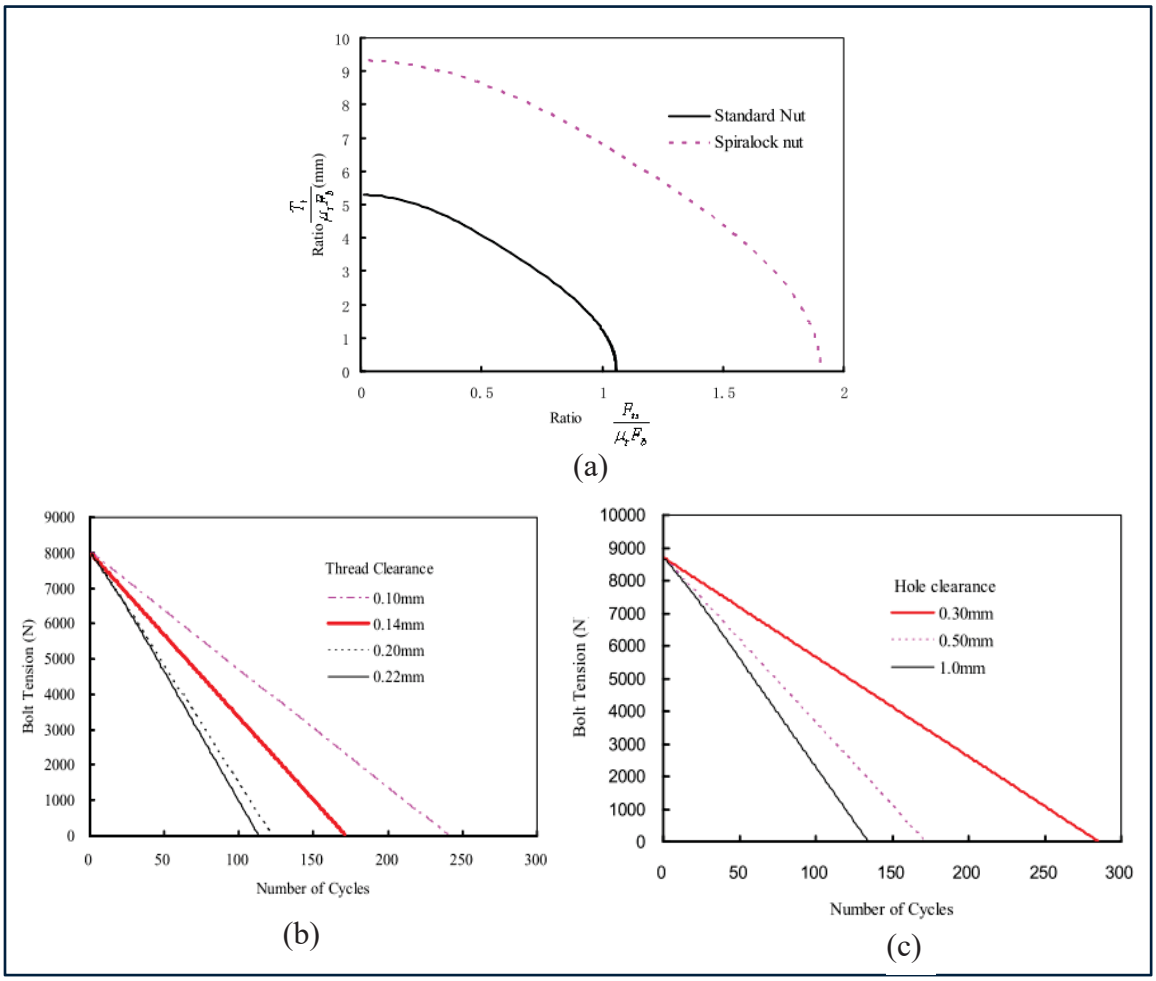

Figure 1.26 Effect of (a) thread profile angle for Spiralock and standard nuts; (b) thread clearance; and (c) hole clearance on loosening for M10×1.5 bolt
Taken from Yang & Nassar (2011b)

Nut of various designs and features can enhance or reduce their ability to resist self-loosening under dynamic transverse loading. Proper selection of nuts should consider factors like load conditions, material compatibility, and ease of assembly and disassembly. Shoji, Sawa & Yamanaka (2007) conducted study with FE modeling and developed their modified Junker test rig to experimentally investigate loosening by examining various types of nuts as well as washers under different preload levels below the bolt yield stress. Overall, the eccentric nut

showed better loosening resistance with less preload loss. The normal nut loosened easily than the others, and larger friction between nut and plate enhanced the loosening more. The authors also concluded that the alternating shear stress (frictional stress) caused by the relative slip between nut and bolt thread surfaces due to cyclic transverse loading is highly responsible for the occurrence of self-loosening.

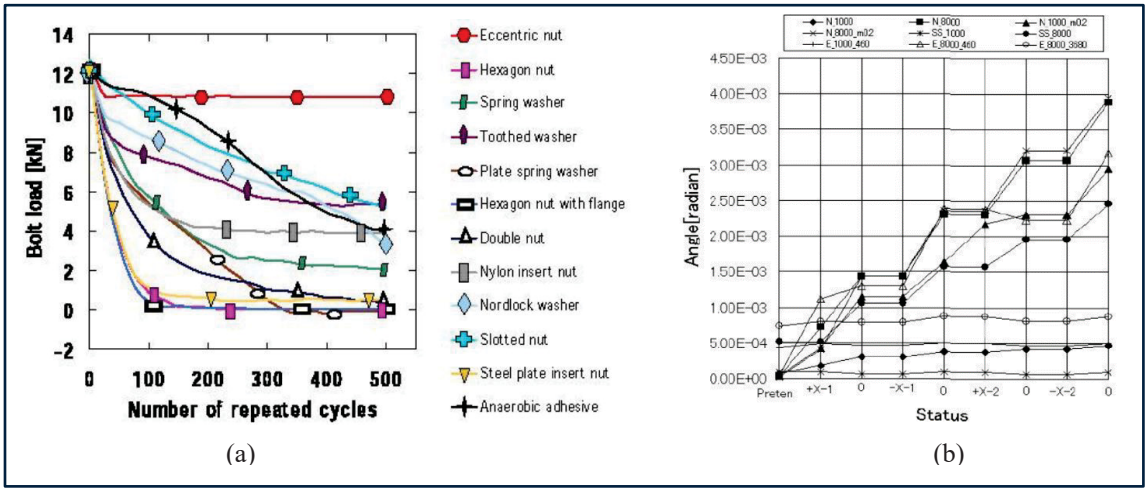

Figure 1.27 Variation of (a) bolt load from 12.5 kN and (b) nut rotation
Taken from Shoji, Sawa & Yamanaka (2007)

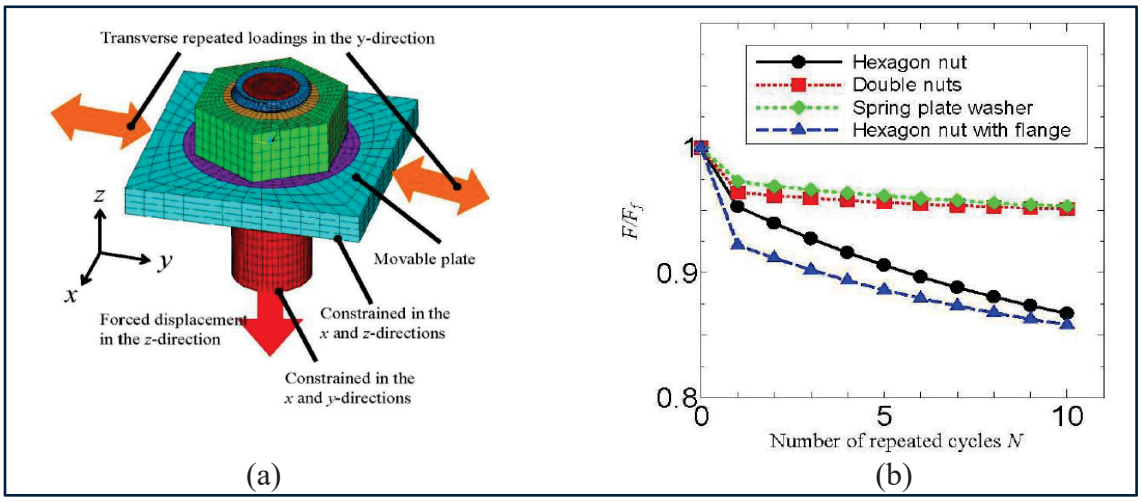

Figure 1.28 (a) FE model of bolted joint, and (b) effect of different nuts and washers
Taken from Sawa, Ishimura, & Nagao (2012)

Sawa and co-workers conducted numerical FE analysis and experimental validation to study the impact of introducing double nut, spring plate washer and flanged hexagon nuts on the loosening behavior of bolted joints (Sawa, Ishimura, & Nagao, 2012). An M10×1.5 bolt with a load cell and the fixed plate was used on their modified Junker test rig. Steel balls were inserted between the mating plates to reduce friction, although this introduced the possibility of altering parameters such as grip length and joint stiffness. Their investigation also explored the impact of an inclined bearing surface on loosening behavior (Sawa, Ishimura & Karami, 2010). The analysis showed that larger incline angles led to a greater reduction in bolt axial force, while eccentric nuts demonstrated better resistance to loosening compared to hexagon nuts.

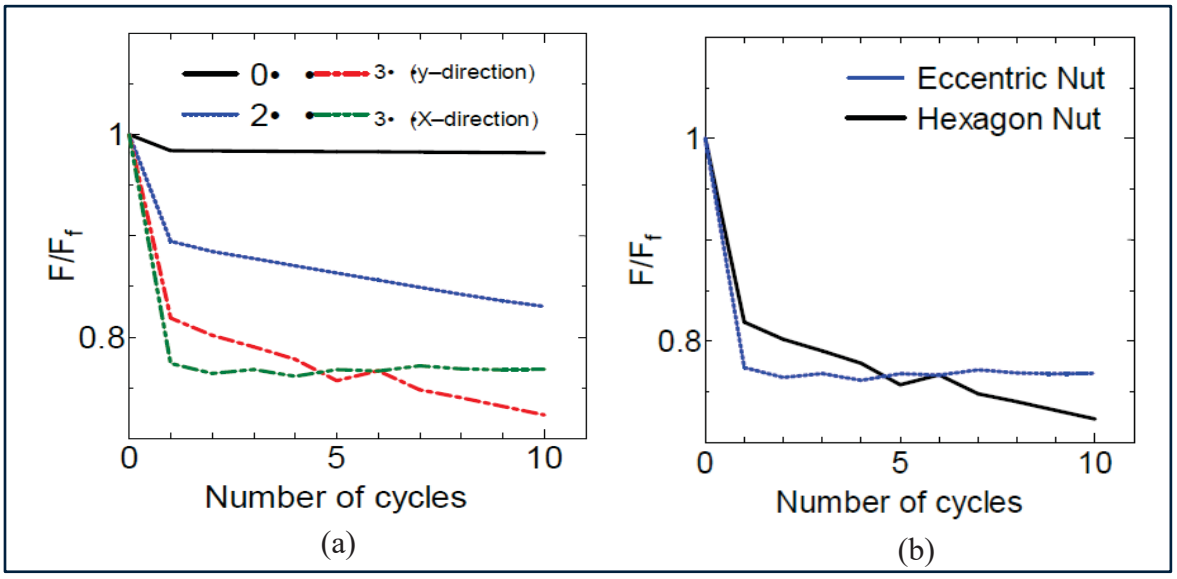

Figure 1.29 (a) Effect of bearing angle inclination, and (b) eccentric vs hexagon nut at 3 degree bearing inclination angle
Taken from Sawa, Ishimura & Karami (2010)

Naruse & Shibutani (2010) used finite element (FE) analysis to assess the equivalent stiffness of clamped members in bolted joints, considering both axial and bending stiffness, as well as the contact conditions between members and bearing surfaces. They compared their results with the VDI 2230 (2003) standard and found that the code overestimated axial and bending stiffness by 11% and 22%, respectively. They also noted variations in compliance based on member thickness. In a subsequent study, Naruse & Shibutani (2012) re-evaluated the helix

angle (*tanφ*) of the equivalent cone of compressive stress fields considering the thickness ratio, to improve VDI 2230 unsafe estimations. For members of similar thickness, the additional correction term was unnecessary, making the original formula (previous version) from the code preferable. This adjustment led to a more accurate prediction of axial and bending compliance compared to VDI 2230. However, the authors cautioned that estimating axial stiffness based on node displacement could introduce errors due to the questionable selection of nodes.

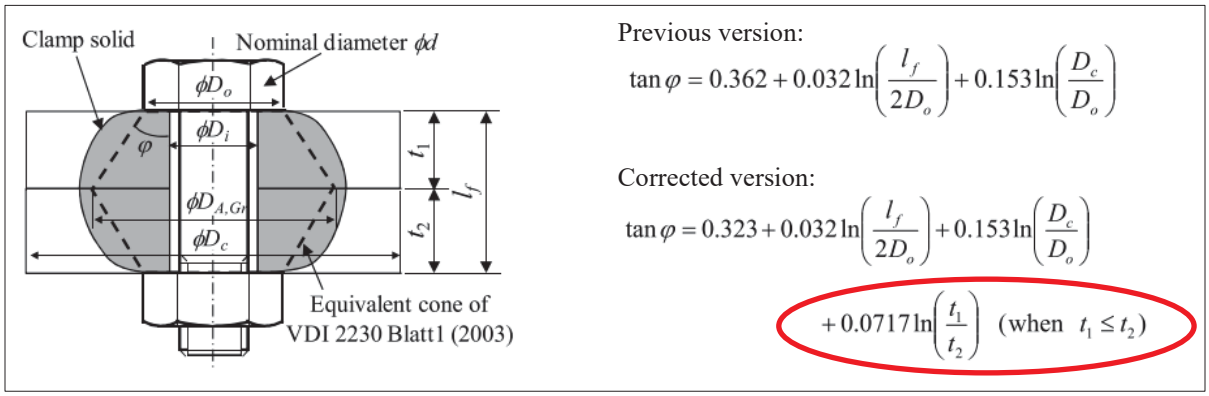

Figure 1.30 Helix angle formulae for equivalent conical compressive stress field of joint assembly
Taken from Naruse & Shibutani (2012)

Fort, Bouzid & Gratton (2019) challenged the model (Nassar & Yang, 2009) and detailed a comprehensive study including an improved analytical model for bolted joints experiencing self-loosening due to transverse loading by highlighting the effect of plate thickness. A FE modeling analysis was performed to support the analytical model. A modified Junker test rig was developed to conduct loosening tests with cyclic transverse movement of joint with M12×1.75 hex bolt and nut, and therefore to validate the analytical model results. They showed that the self-loosening can be more realistic and better understood if it is represented based on the excitation displacement. The model was in good agreement with numerical and experimental results.

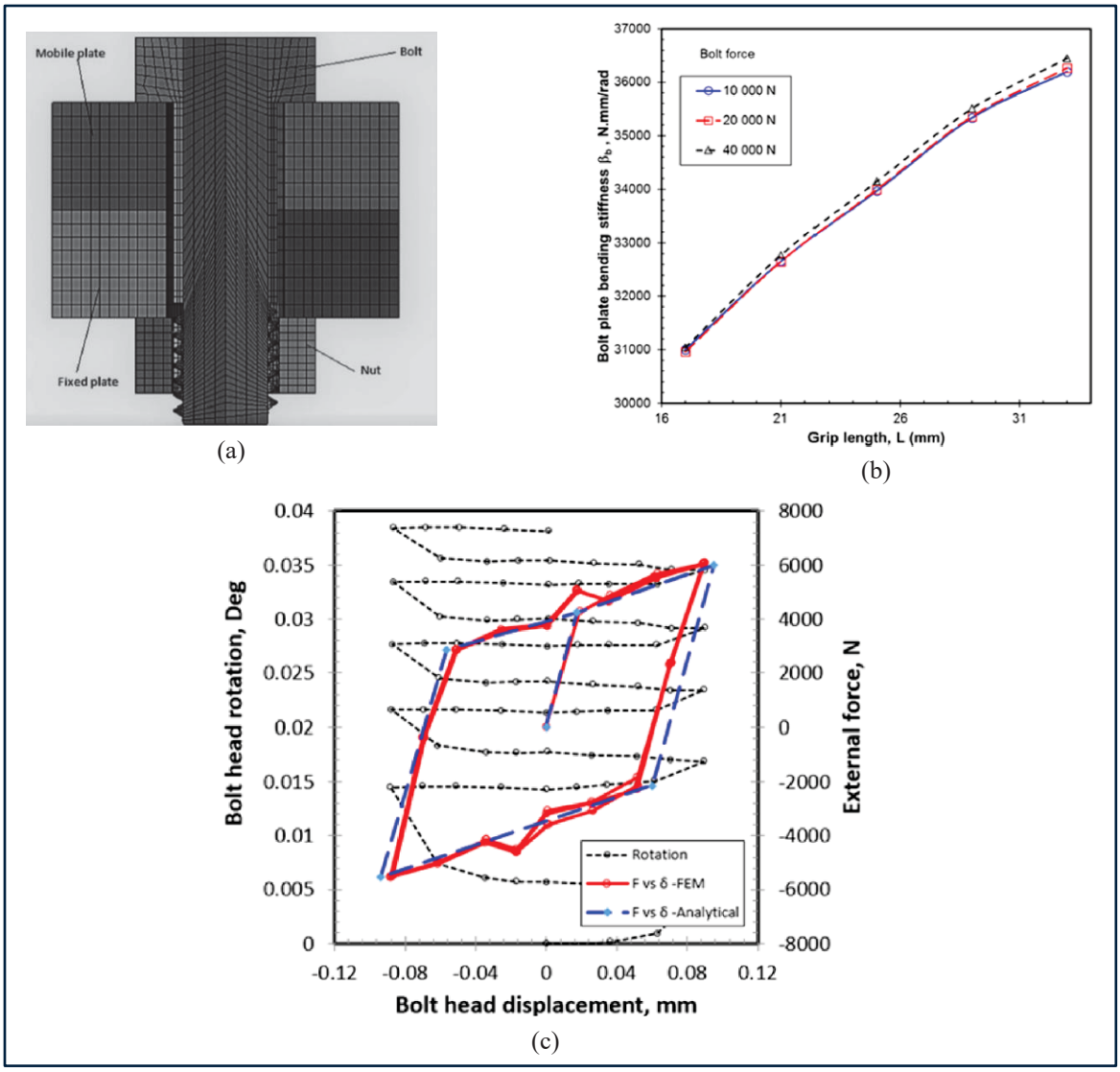

Figure 1.31 (a) FE model of bolted joint; (b) bending stiffness under bolt head vs grip length for three clamping forces; and (c) bolt head rotation and external load vs bolt head displacement for grip length of 17 mm
Taken from Fort, Bouzid & Gratton (2019)

1.4 Objective of the study

The primary objective of this study is to investigate the self-loosening of bolted joints, aiming to identify its underlying mechanism and assess the contribution of various factors that

influence its occurrence. This objective can be accomplished through the following specific sub-objectives:

1. A key factor that significantly affects the loosening behavior of bolted joints is the stiffness of the joint and its individual components. While calculating the stiffness of the bolt is relatively straightforward, determining the stiffness of the clamped members is more complex and has been the focus of various studies. Existing research often relies on numerical finite element (FE) methods, which involve selecting an arbitrary number of nodes in the contact region, leading to potential inaccuracies. Therefore, the first sub-objective is to develop a more precise FE-based methodology for evaluating the stiffness of bolted joints, with particular emphasis on the clamped members. This approach involves developing an axisymmetric FE model to evaluate a wide range of bolts, from M6 to M36, with varying joint grip lengths. The method establishes a unique relationship for the stiffness of clamped members based on the contact width under the bolt head or nut, offering an improvement over existing models. By identifying the overestimation of stiffness in traditional methods found in the literature, this approach serves as a more accurate reference for evaluating stiffness in bolted joints with complex three-dimensional threaded geometries.
2. The second sub-objective of this project is to quantify the contributions of various torque components in response to the externally applied torque on the joint, including pitch torque, bolt or nut bearing friction torque, and thread friction torque. The goal is to examine how these torques vary during the tightening, untightening, and static phases. This involves developing an analytical model to evaluate these torque components, relative rotation between the bolt and nut, joint stiffness and interrelationship among the coefficient of friction and nut factor. The model is validated against an experimental study by Eccles (2014). Additionally, a three-dimensional FE model of a M12 x 1.75 hex-threaded bolted joint is developed to simulate the loading cycles, further validating the analytical model.
3. The third sub-objective is to perform experimental tests using a pre-developed test rig that replicates the self-loosening phenomenon in bolted joints under cyclic transverse loading. These tests are conducted with an M12 x 1.75 hex bolt and clamped members of various sizes and materials, under different tightening conditions. The clamped members include

steel and High-Density Polyethylene (HDPE), with varying grip lengths for comparison. This experimental approach provides an in-depth understanding of the effect of joint rigidity on stage-II self-loosening by revealing a range of preload loss patterns across tests, which offers valuable insights into loosening behavior for comparative analysis.

CHAPTER 2

EXPERIMENTAL SETUP OF SELF-LOOSENING MACHINE

This chapter details the design and development of the experimental setup used to test the self-loosening phenomenon in bolted joints, along with all related components.

2.1 Introduction

Experimental investigation on self-loosening of bolted joints is essential to ensure the reliability, safety, and longevity of bolted joints in practical applications. It enables the examination of self-loosening in realistic conditions, such as dynamic loading, vibration, and temperature fluctuations. Analytical models or simulations alone may not fully capture the complexities of the loosening behavior in real-world environments. Experimental data helps validate the analytical models that predict the conditions under which bolted joints loosen, which leads to improved predictive capabilities for engineers. Also, the parameters, such as materials, component dimensions, thread designs, and coatings affect the susceptibility to self-loosening, where experimental investigations help identify the optimal combinations to reduce this risk.

The test rig in this project must be capable of conducting tests with external cyclic transverse displacement to measure preload, along with other key parameters such as lateral force, transverse displacement, nut rotation relative to the bolt, and the number of cycles. With these considerations, a dedicated experimental test rig is developed at the Static and Dynamic Sealing Laboratory of ÉTS and is based on an existing fatigue test machine. The latter was modified to conduct self-loosening experiments according to the project requirements. The test rig shown in Figure 2.1 is comprised of the following components:

1. Support structure.
2. Universal joints and grips.
3. Adjustable crank system.
4. Lever with a spring-loaded fulcrum and three load application points.
5. Mobile mounting structure.

6. Adjustable stem.
7. Electric motor.
8. Simple control panel for power (ON/OFF) and frequency adjustment.
9. Mechanical cycle counter with a precision of 10 cycles.

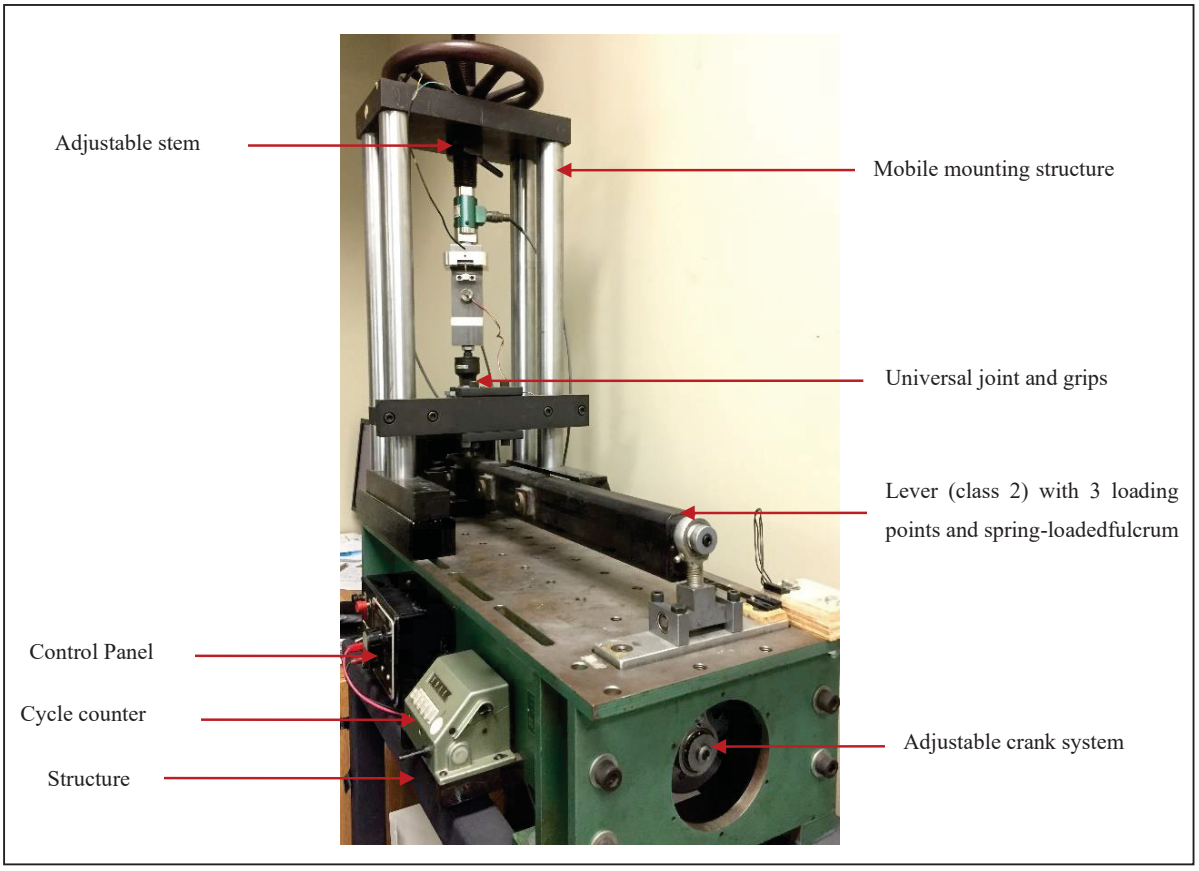

Figure 2.1 Experimental setup developed at Static and Dynamic Sealing Laboratory (SDSL) of ÉTS

Certain components of the rig, including the support structure, mobile mounting structure, lever, adjustable stem, and electric motor, remain unchanged. The mechanical cycle counter has been replaced with a digital magnetic counter. The electric motor controls the speed and adjusts the frequency of the loading cycles. The control system is integrated with the rig's control panel to capture outputs and display them through LabView program.

The test specimens (bolt, clamped members, and nut) are mounted between the load cell and the universal joint, with the entire assembly positioned as close as possible to the fulcrum point

of the test rig to maximize load capacity. Typically, the motor and crank system generate displacement at one end of the lever, which creates the transverse load. The test rig can provide lateral displacement up to 0.25 inches, with a maximum frequency of 5000 cycles per minute and a maximum transverse force of 5000 lbs.

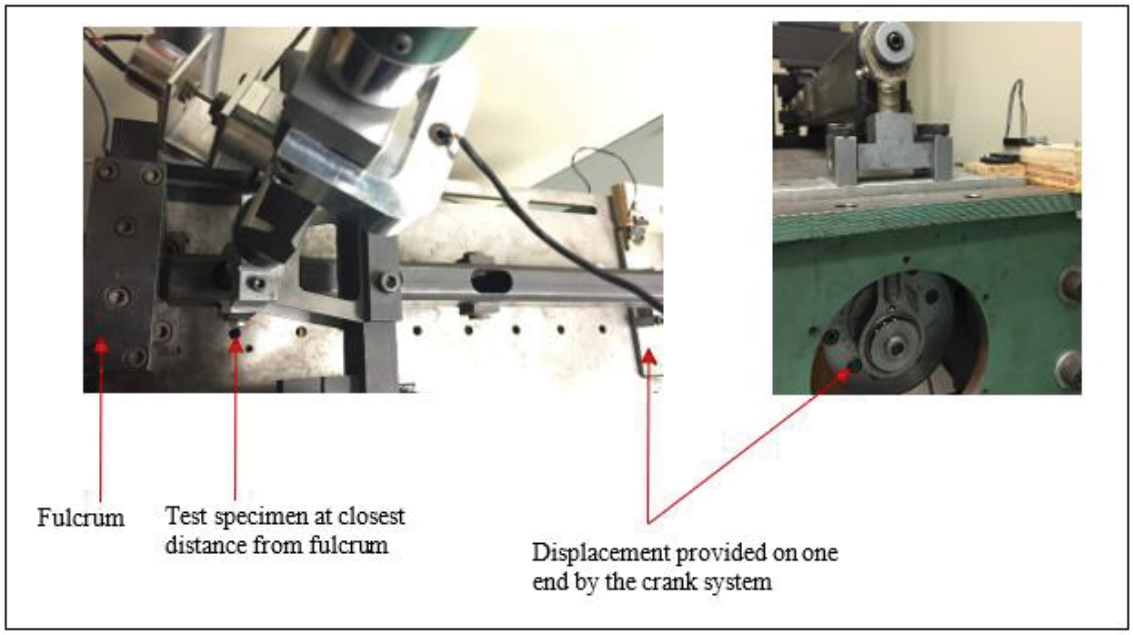

Figure 2.2 Transverse load produced by the displacement on one end of the lever

The experimental tests for self-loosening require measurements of the bolt axial load, lateral displacement, transverse force, number of cycles and relative rotation between the bolt and nut. Other parameters such as temperature and time are also recorded for further references and analyses. Selecting appropriate sensors - such as strain gauges for axial load, LVDTs (Linear Variable Differential Transformers) for displacement, and RVDTs (Rotary Variable Differential Transformers) for rotation - presents challenges due to limitations in the test setup, including restricted space and dimensional constraints of the machine.

2.2 Strain gage for preload (axial load)

To effectively secure the mating parts (clamped members) while maintaining the clamping force between the bolt and nut, bolt preload is a critical parameter. Proper preload ensures the bolt axial load capacity, which maintains joint integrity and safeguards against potential leakage failures. In the existing test rig, a cylindrical strain gauge (KYOWA KFG-3-120-C20-11), designed specifically for measuring bolt strain, is installed in a 2 mm diameter hole in the bolt (see Figure 2.3). Since the use of a load cell alters the joint geometry, it affects the grip length and thus the joint stiffness. However, installing the KYOWA strain gauge into the through-hole of the bolt changes the stiffness by less than 3% for an M12 bolt in practice, which can be considered negligible.

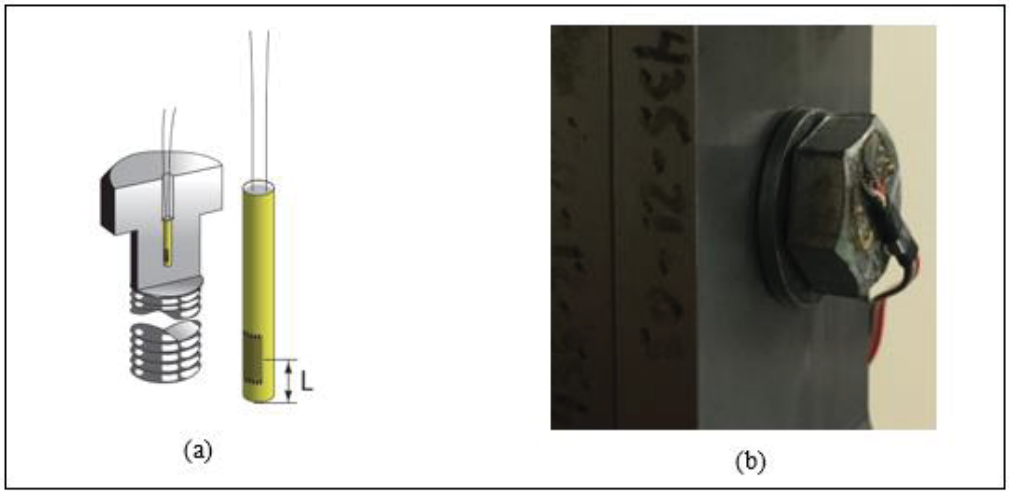

Figure 2.3 (a) KYOWA Strain gauge (see APPENDIX I), (b) Strain gauge inserted into bolt

The M12 bolts were drilled with a 0.1 mm tolerance at the bolt head end using an automatic CNC machine to accommodate strain gauge installation. This installation was challenging because the gauge needed to be positioned as vertically straight as possible. Additionally, the gap between the gauge and the inner wall of the bolt hole was carefully filled with epoxy glue to prevent bubbles and ensure transmission of the deformation from the bolt to the strain gauge through the hole wall (see Figure 2.3a). All four SFC grade 8.8 bolts equipped with strain gauges were calibrated using the MTS 810 tensile test machine up to 50% of their yield strength

(see Figure 2.4). Among the four M12 bolt samples, the one demonstrating the best stability is selected for use in the joint (see Figure 2.3b). Enhanced fabrication tolerance and installation accuracy have resulted in better calibration outcomes.

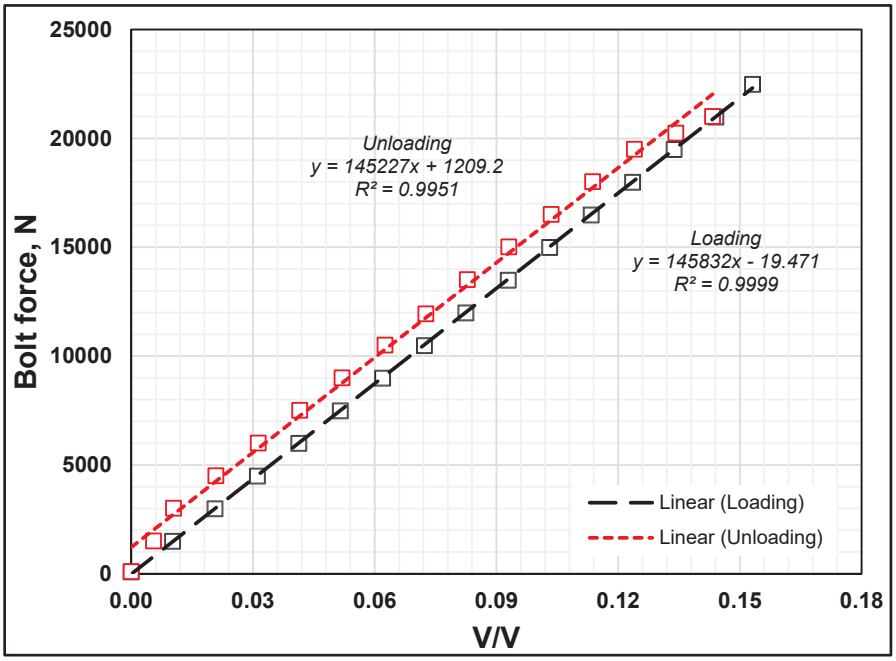

Figure 2.4 Calibration of M12 bolt with KYOWA strain gauge

2.3 RVDT (Rotary Variable Differential Transformer) for rotation

In the study of self-loosening in bolted joints, the relative rotation between the bolt and nut is a key factor, as it signals the onset of stage-II loosening. This indicates the difference between the overall rotations of the bolt and the nut.

$$Diff.(Rot)_{rel} = R_{bolt} \sim R_{nut} \ (\text{if } R_{nut} = 0 \text{ for example, } Diff.(Rot)_{rel} = R_{bolt}) \qquad (2.1)$$

Figure 2.5 depicts the CP-2UT RVDT from Midori Precisions, the rotation sensor used in the existing test rig, connected to the bolt end via its shaft. The surface of each bolt end is machined with a recess that fits into the sensor shaft slot, ensuring a contact free of sliding. The nut is secured to the nut holder using three M3 bolts, and the U-shaped sensor holder is attached to the nut holder with an additional three M3 bolts, forming a rigid structure capable of directly

measuring the relative rotation between the bolt and nut. However, the nut holders vary based on the bolt length.

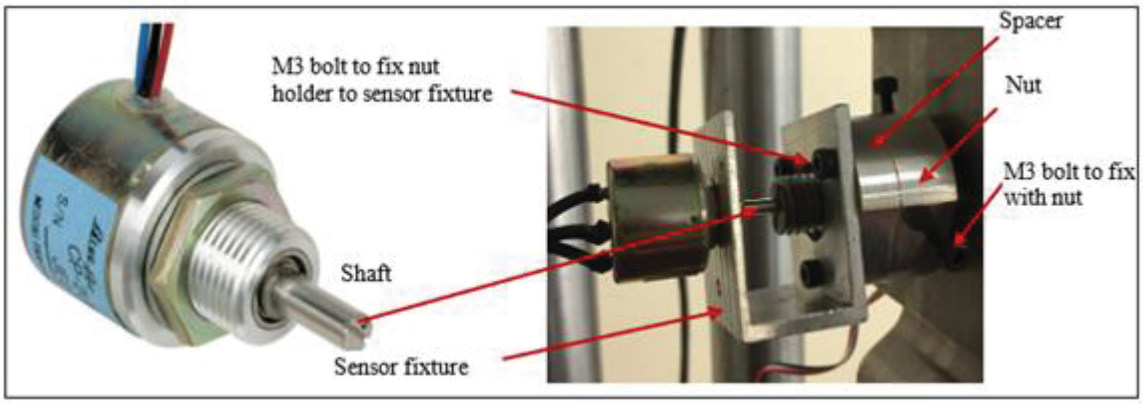

Figure 2.5 RVDT (CP-2UT) connected to bolt end via shaft (see APPENDIX II)

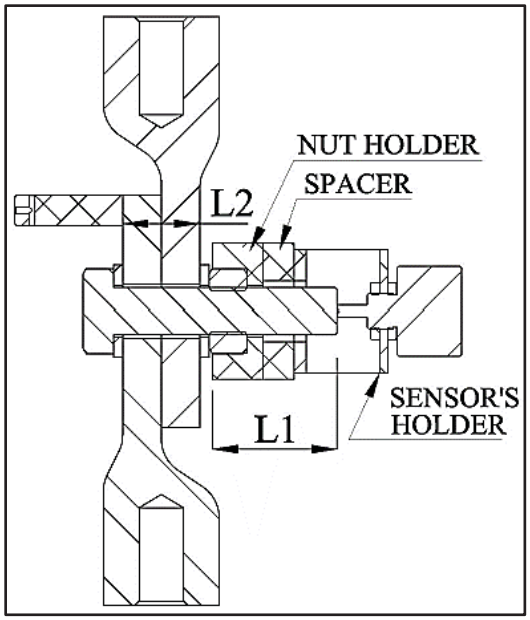

Figure 2.6 Section view of the rotation fixture

Additionally, for plates of different thicknesses, if the value of L2 increases (see Figure 2.6), the nut holder, spacer, and sensor holder shift together along the bolt's length, causing the bolt end to lose contact with the sensor shaft. To address this issue, spacers of various sizes were made, depending on the plate thickness, to be inserted between the nut holder and the sensor holder. The RVDT is accurately calibrated, as illustrated in Figure 2.7. A wide range of angular

displacements can be measured, with a perfect linear range between 60 and 140 degrees, which is more than sufficient for testing self-loosening by nut rotation.

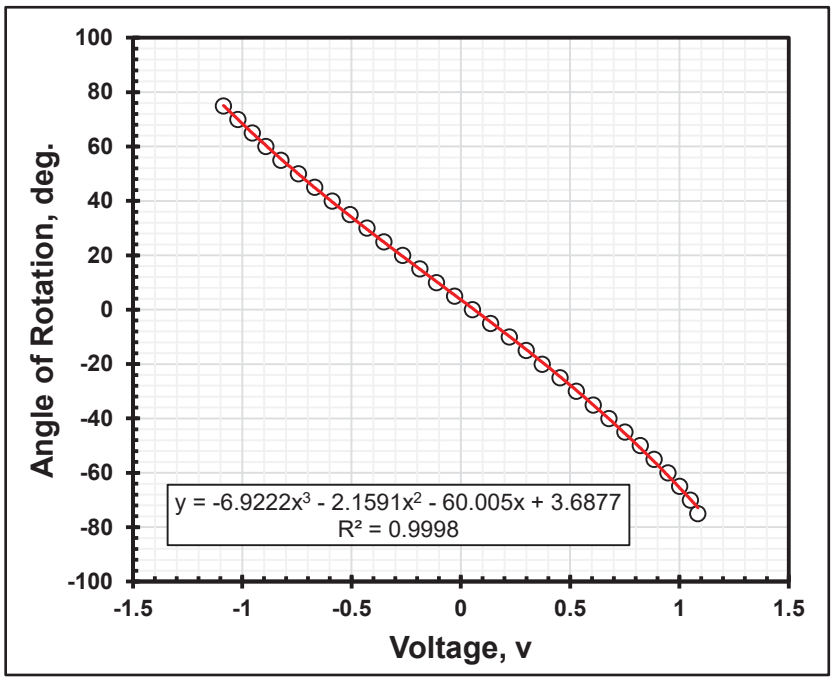

Figure 2.7 Calibration of RVDT (CP-2UT)

2.4 Force transducer for transverse displacement

Selecting the appropriate force transducer is crucial for measuring the externally applied transverse or lateral force. In this experiment, the GSE load cell 5410-8k with a capacity of 8000 lbf is an ideal choice, as it fits perfectly within the test setup, considering the dimensional constraints of the other components. The sensor is positioned between the stem at one end and one of the clamped members at the other end using its female threaded holes on both sides, as shown in Figure 2.8.

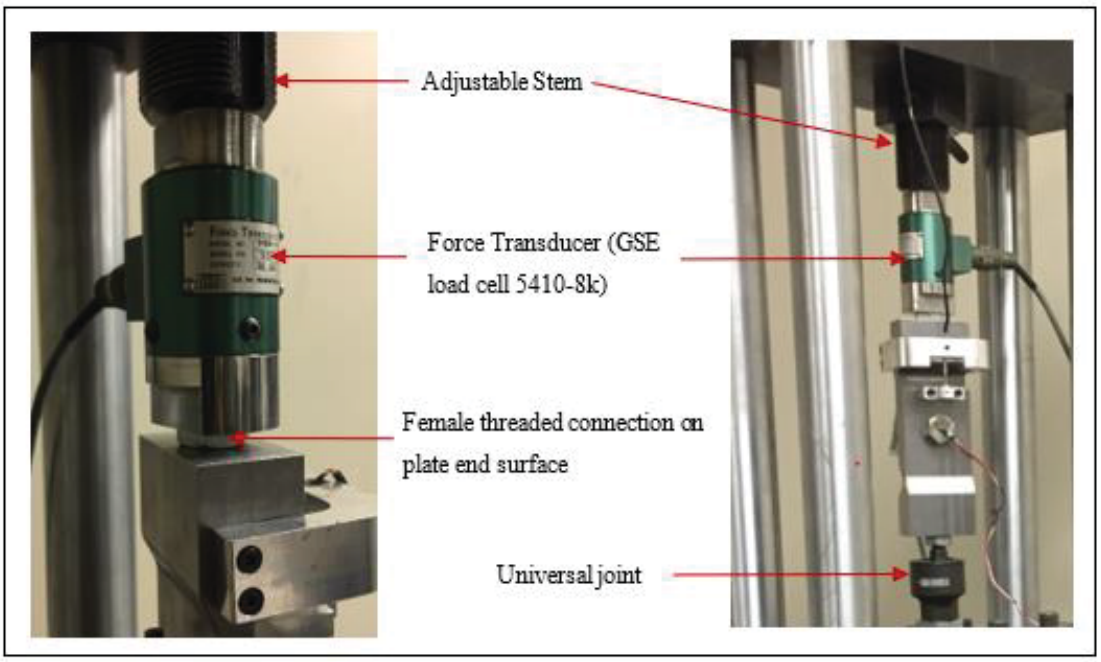

Figure 2.8 Force transducer (GSE load cell 5410-8k) in the test setup

A 12.7 mm (1/2 in.) male threaded connector is needed to attach the force transducer to the nearest clamped member via its female threaded hole. Since the test samples also include clamped members of thickness smaller than 12.7 mm, connecting a male threaded rod by creating a female threaded hole in the smaller members is challenging. Therefore, the clamped members are designed so that the end surface is sufficiently thick to ensure that the remaining section (T_1 and T_2 as shown in Figure 2.9), after connecting the rod, can withstand the stresses generated by the transverse displacement. However, the sudden transition between the thicker and thinner sections may generate excessive residual stress, potentially leading to premature fatigue of the clamped members. To address this problem, a fillet is added at the transition, with a radius chosen to ensure that the contact area between the two clamped members remains flat during the test. All these tasks are carefully managed to ensure that the plate mating surfaces are aligned with the machine axis.

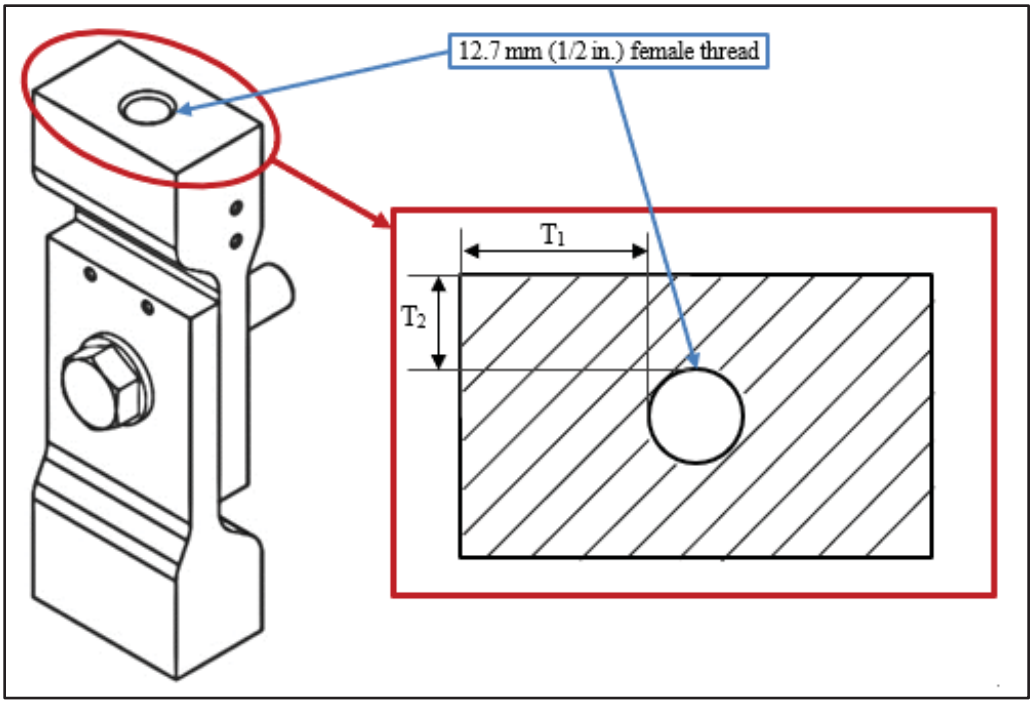

Figure 2.9 Extended portion of the clamped member

A universal joint is installed between the lower clamped member and the actuator lever, replacing a standard threaded connection, as it would be challenging to align the axis with the upper clamped member already fixed to the force transducer. This reduces possible bending moment on the clamped members during the application of transverse displacement.

2.5 LVDT (Linear Variable Differential Transformer) for lateral displacement

This study employs displacement control for self-loosening tests. Therefore, a magnetic contactless sensor (Macro CD 375-025 LVDT) with a nominal range of ±0.63 mm is used, which comprises a fixed casing and a movable core in the rig. This LVDT is renowned for its lightweight design, infinitesimal accuracy, and, most notably, its unlimited mechanical lifespan due to the frictionless movement of the core. It operates by detecting changes in electrical current caused by alterations in the magnetic field, which allows for precise measurement of displacement.

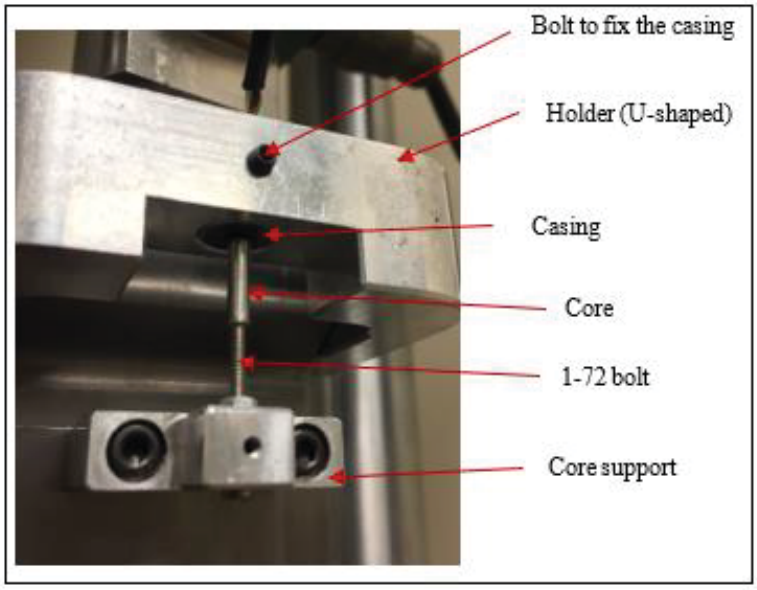

Figure 2.10 LVDT fixture details

Figure 2.10 shows the details of the LVDT fixture. As illustrated in Figure 2.11, when the core is in its central position (primary winding), the voltage induced in both secondary coils is identical due to the equal magnetic flux coupled to each coil. As the core moves toward either up or down, more magnetic flux is coupled to the corresponding secondary coil, generating a higher voltage in that coil. This difference in voltage between the two secondary coils allows the core's position to be determined.

The LVDT casing is secured by a U-shaped holder mounted on the upper clamped member and fastened with an M3 bolt. The core, which has 1-72 UNF female threads at both ends, is mounted on a support (holder) using a 1-72 bolt. The core support is mounted on the lower clamped member, with M3 bolts securing both holders to their respective clamped members. The LVDT is then calibrated, and the results are presented in Figure 2.12.

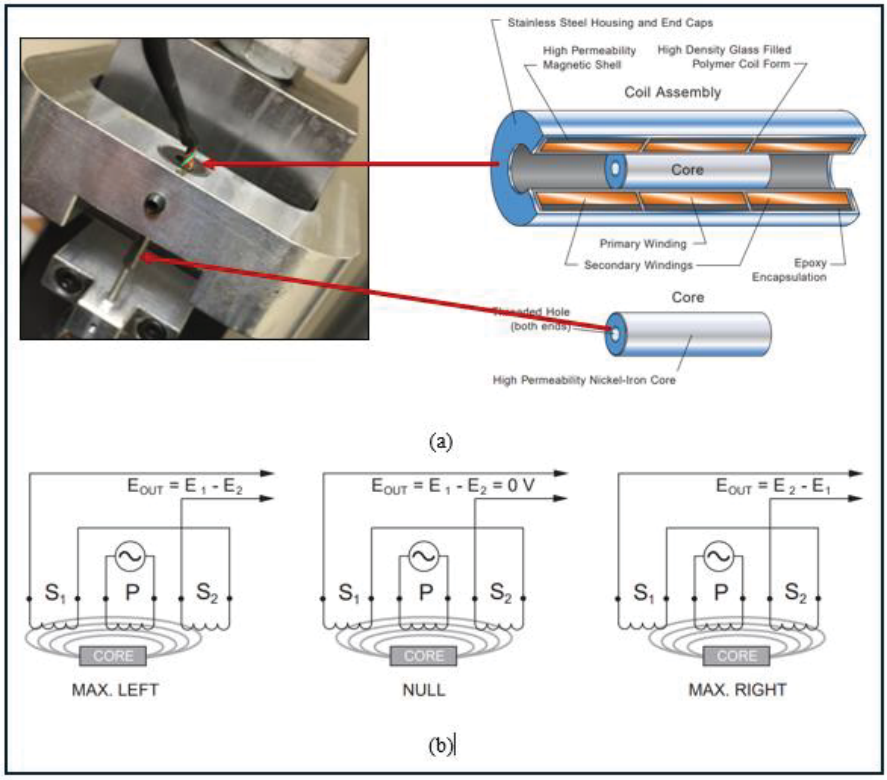

Figure 2.11 (a) Structure and position of LVDT, (b) working principle of LVDT

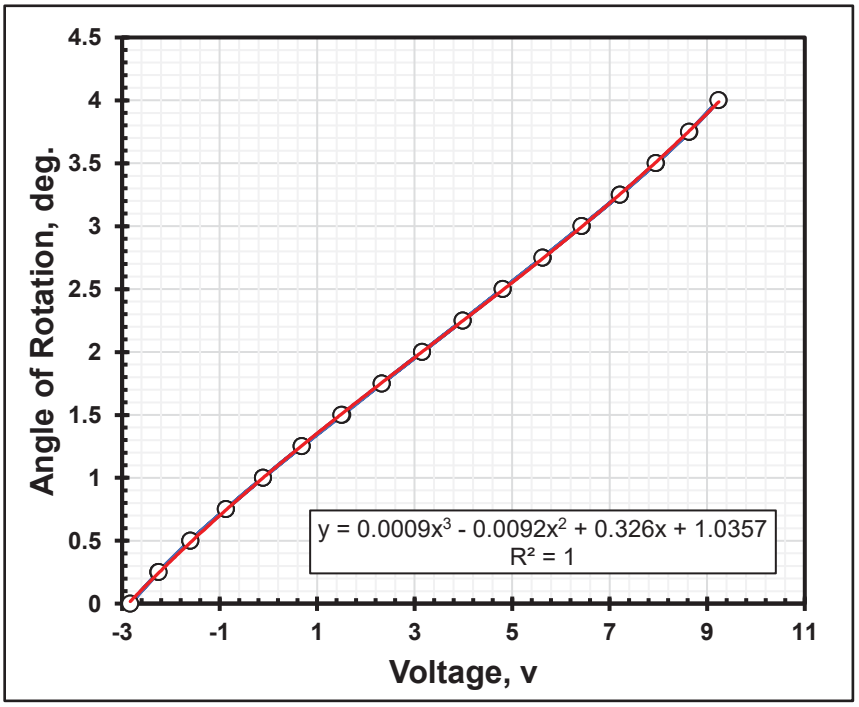

Figure 2.12 Calibration of LVDT (Macro CD 375-025)

2.6 Magnetic cycle counter

Accurately measuring and recording the number of cycles at the start of the stage-I loosening test is essential for correlating it with other measured parameters. The machine was originally equipped with a mechanical cycle counter, connected to the motor shaft through a set of gears. However, that counter could only register every ten cycles, rather than each individual cycle, and had difficulty synchronizing its output with the data acquisition system. To address this, the counter was replaced with a magnetic cycle counter. The fixed part is mounted on the machine body, while the mobile part, a permanent magnet, is attached to the actuator lever, as shown in Figure 2.13. The magnetic counter generates a signal each time the magnet passes through the sensor's magnetic field, once per cycle, providing an accurate count of individual cycles.

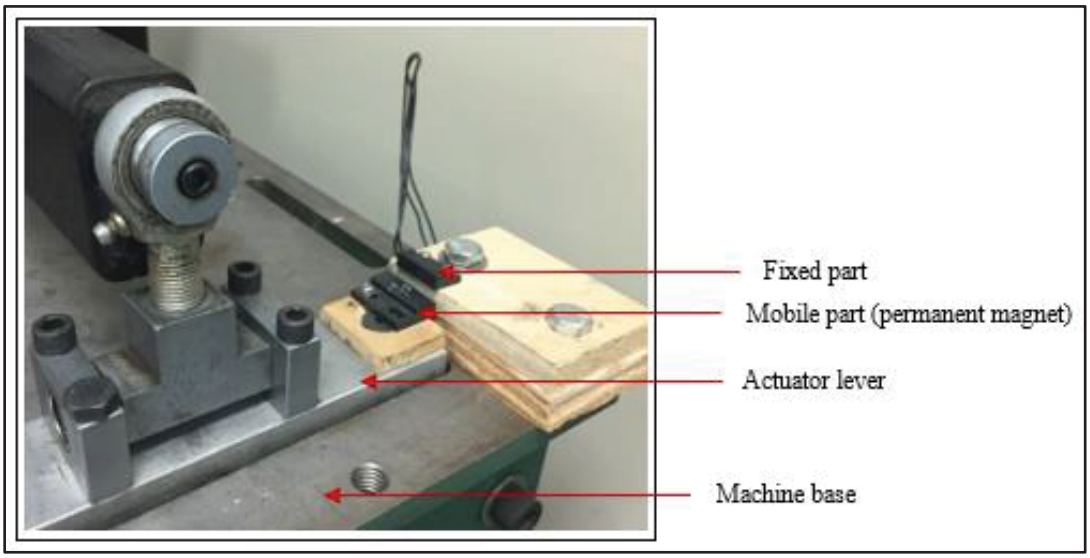

Figure 2.13 Position of the magnetic cycle counter

2.7 Test specimen

In this project, the assembly consists of one bolt, one nut, two washers (one on each side), and two clamped members, as shown in Figure 2.14. The design and installation approach for the clamped members, as described earlier, ensures that the contact surface is coaxial with the shared axis between the force transducer and the universal joint.

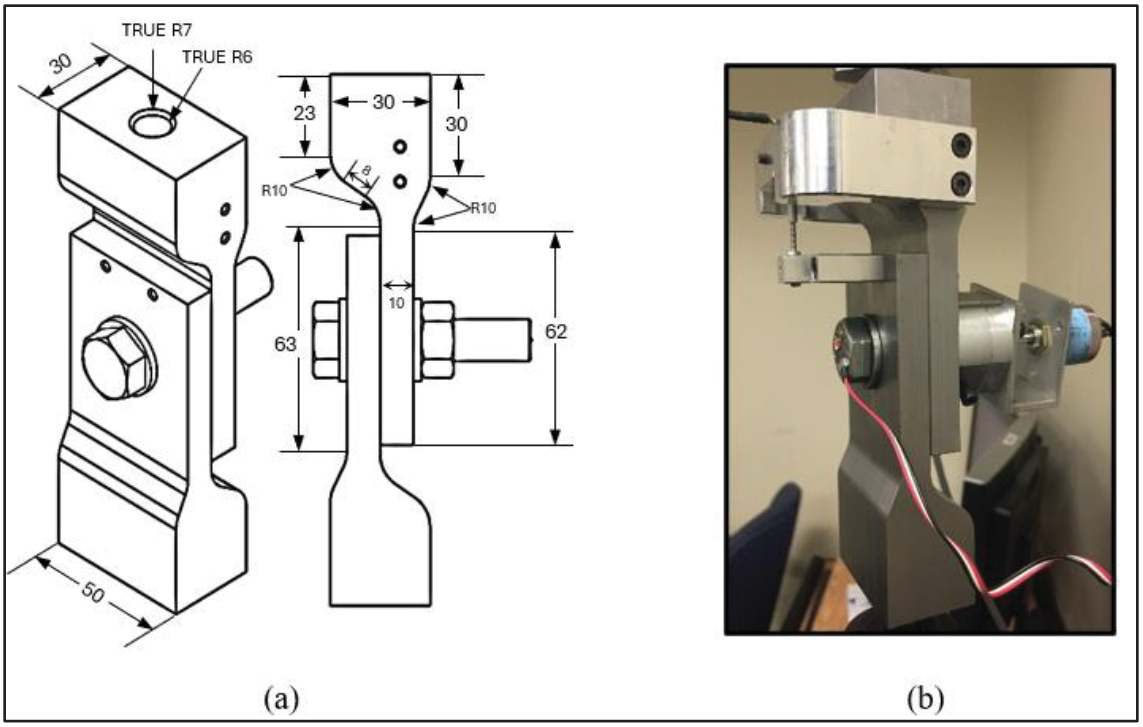

Figure 2.14 (a) Schematic of the bolted joint, (b) joint in test rig

Since M12 hex bolts and nuts are used in the experiments, the diameter of the holes in all clamped members is set to 13.6 mm to accommodate and fasten the bolts.

The test samples for the clamped members are made from two different materials: steel and high-density polyethylene (HDPE), to investigate the effect of materials on joint loosening (see Figure 2.15). To conduct tests with higher preloads for steel clamped members of different thicknesses, two single-row flat roller bearings (INA-HYDREL Flat Cage Assemblies FE series) are placed between the clamped members to reduce the initial friction in the beginning of loading cycles. Figure 2.16a illustrates a 3D printed housing made of hard plastic, which is used to properly position and align both roller bearings. The dimensions of the rectangular slots and the hole are carefully maintained during the 3D printing so that the bolt goes through easily and both roller bearing fits perfectly into the slots without titling when the components are clamped and tightened together (see Figure 2.16b).

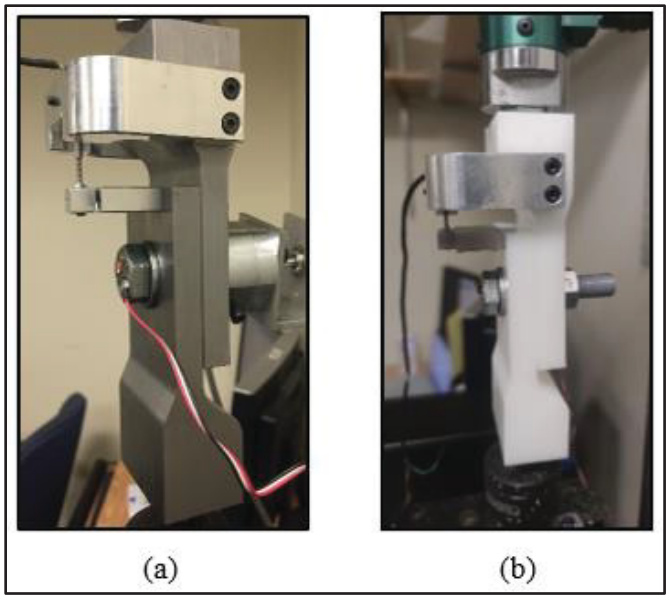

Figure 2.15 Clamped members: (a) Steel, (b) HDPE

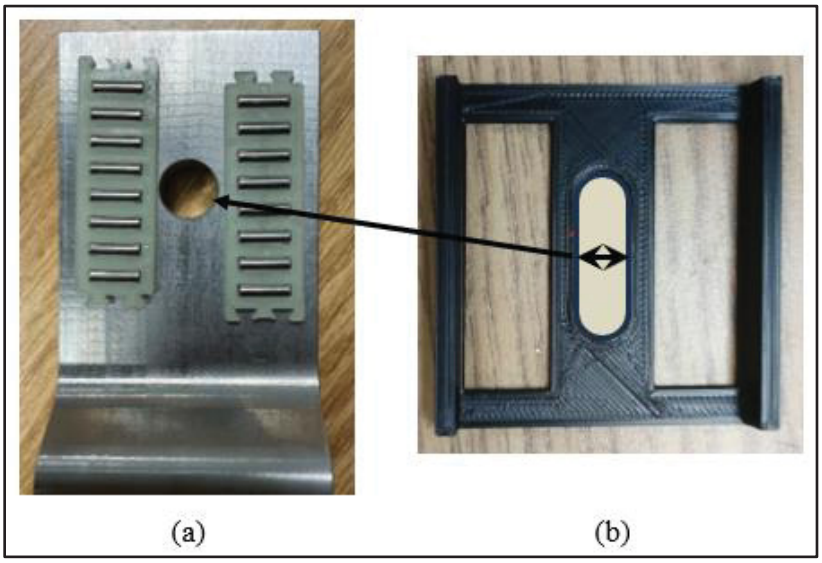

Figure 2.16 (a) Roller bearings (INA-HYDREL FE series) on contact face of steel clamped member, (b) 3D printed hard plastic housing

2.8 Data acquisition system

To directly monitor and record the data from the experimental tests, a data acquisition system is specifically designed for this project and consists of a main analog to digital board and individual electrical circuit boards, one for each instrument (see Figure 2.17). All the

measuring devices are connected to a computer via the main board (PCB). The electrical signals measured from all sensors attached to the different components of the test rig are lateral displacement, preload, transverse force, rotation, number of cycles, time and temperature.

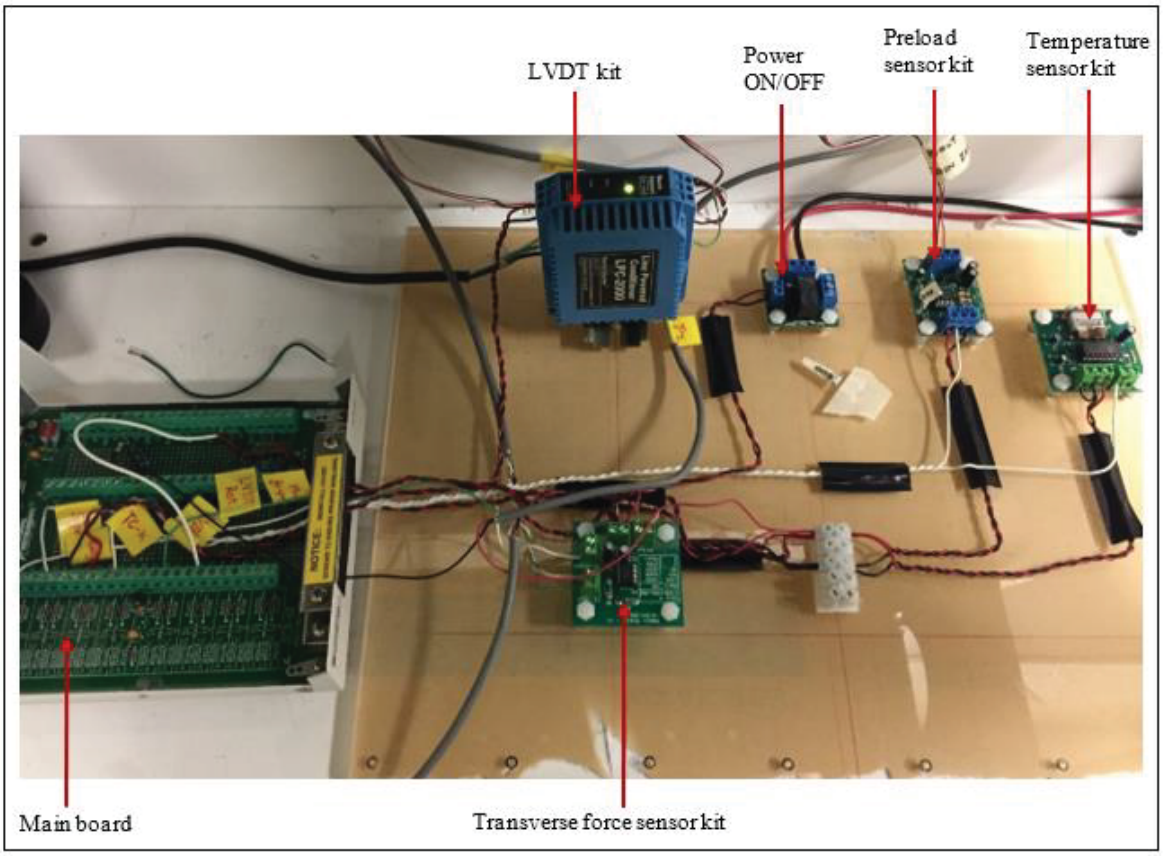

Figure 2.17 Data acquisition system: main board and electrical components

The entire system is programmed by the LabView software, the user interface of which is shown in Figure 2.18. The program continuously tracks and captures real-time data from all sensors connected to the test rig, transforming and organizing this data into their appropriate units.

Figure 2.18 LabView user interface of the data acquisition system

CHAPTER 3

ON THE RE-EVALUATION OF THE CLAMPED MEMBERS STIFFNESS OF BOLTED JOINTS

Rashique Iftekhar Rousseau [a], Abdel-Hakim Bouzid [b] and Zijian Zhao [c]

[a, c] Department of Mechanical Engineering, École de technologie supérieure,
1100 Notre-Dame St. West, Montreal, Quebec, H3C 1K3
[b] ASME Fellow, Department of Mechanical Engineering, École de technologie supérieure,
1100 Notre-Dame St. West, Montreal, Quebec, H3C 1K3

Paper published in the Transactions of the Canadian Society for Mechanical Engineering Journal, March 2024.
(48(1): 75-83, DOI: 10.1139/tcsme-2023-0092)

3.1 Abstract

To address the structural integrity of bolted joints and verify their capacity to withstand external loads and relaxation resulting from thermal expansion difference and creep, proper evaluation of the axial stiffnesses of bolt and clamped members are of vital importance. A number of finite element (FE) based methods are available for the calculation of the stiffnesses of joint elements, most of which rely on the displacement of arbitrarily selected nodes that has led to the improper evaluation of joint stiffness values. In this paper, the stiffness of clamped members is evaluated by a simple FE methodology using a known bolt stiffness evaluated separately. Two load cases, one based on the application of external force (mechanical loading) and the other on temperature (thermal loading), are conducted using the FE method to validate the obtained results. The proposed methodology is also compared with other FE models and analytical methods obtained from the literature. The new technique is based on axisymmetric FE modeling and is applied to bolted joints with bolts ranging from M6 to M36 having various

grip lengths. Finally, the stiffnesses of the bolt and clamped members can be determined accurately, and a general formula is proposed to evaluate the stiffness of clamped members.

NOMENCLATURE

θ	Half of the apex angle of conical frustum, °
α_b	Coefficient of thermal expansion for bolt material, K^{-1}
α_m	Coefficient of thermal expansion for clamped member material, K^{-1}
Δ	Change in a parameter
γ	Contact radii ratio
δ	Displacement of the bolt at symmetry plane, mm
υ_b	Poisson's ratio of bolt material
υ_m	Poisson's ratio of clamped members material
A, B	Material constants
A_b	Bolt stress area, mm^2
A_m	Effective contact area of the clamped members, mm^2
d	Nominal diameter of bolt, mm
d_{hd}	Diameter of the bolt head, mm
d_h	Diameter of the hole of clamped members, mm
d_m	Outer diameter of the clamped members, mm
d_w	Outer diameter of the washer, mm
E_b	Modulus of elasticity of bolt material, GPa
E_m	Modulus of elasticity of clamped members material, GPa
F_b^i	Initial bolt force, N
F_b^f	Final bolt force, N
F_e	External separating force, N
F_m^i	Initial clamping force, N
F_m^f	Final clamping force, N
K_b	Bolt stiffness, N/mm
K_m	Stiffness of clamped members, N/mm
K_j	Joint stiffness, N/mm

L Grip length of the joint, mm

L_{eq} Equivalent bolt length, mm

ΔT Difference between final and initial temperature

T_H Length added to equivalent bolt length from bolt head, mm

T_N Length added to equivalent bolt length from nut, mm

P Bolt force, N

H Thickness of bolt head, mm

N Thickness of nut, mm

w Bolt bearing contact width, mm

3.2 Introduction

The stiffnesses of the bolt and clamped members of a bolted joint have a major impact on the bolt load and the overall joint behavior due to loading. As bolted joints are subjected to various types of loading, including external, thermal, and creep loads, their stiffness values play a major influential role in controlling load retention. Therefore, because of their use in predicting the load variations within a preloaded bolted joint, these parameters need to be determined accurately. In a typical bolted joint, there are two or more clamped members in between a bolt and a nut that are compressed with the preload generated by the initial tightening process. During their lifetime, the tightened clamped members can endure different loadings. It is thus important to have accurate values of the bolt stiffness K_b and the stiffness of clamped members K_m to predict the amount of preload in the joint subjected to different loadings. Both stiffnesses play an important role in controlling the loads in the bolt being under tension and in the clamped members being under compression. Hence, it is equally important to accurately evaluate the stiffness K_m as well as K_b. Unlike K_b, it is not straighforward to estimate K_m due to the three-dimensional stress distribution and the complex calculation of the effective contact area of clamped members A_m. Some earlier studies relied on some arbitrary approximations, and no exact analytical solution has been proposed yet. Identifying separately the stiffness of each component of a joint, such as the bolt head and nut, besides the stiffness of the shank, is

important to properly evaluate K_b without underestimating the calculation of K_m (Sawa & Maruyama, 1976).

Rotscher (1927) first developed a model of a symmetrical bolted joint where he assumes that the members flexibility contribution comes from two conical frusta of vertex angle 2θ (each) developed from the midplane of the joint. The stiffness of clamped members was evaluated in another study (Stuck, 1968) using a half-apex angle of $\theta = 45^\circ$, which overestimates the clamping stiffness according to Little (1967). A simplified assumption was given by Shigley and Mitchel (1983) by introducing a washer of 1.5 times the diameter of the corresponding standard bolt ($d_w = 1.5d$) to provide compressive force on the clamped members.

$$K_m = \frac{\pi E_m d \tan\theta}{2\ln\left[\frac{(L\tan\theta + d_w - d)(d_w + d)}{(L\tan\theta + d_w + d)(d_w - d)}\right]} \tag{3.1}$$

In another study by Shigley & Mischke (1989), the half-apex angle θ was considered as one of the most influential variables in estimating the stiffness of clamped members. A value of θ equal to 30° was recommended for better results.

$$K_m = \frac{0.577\pi E_m d}{2\ln\left[5\left(\frac{0.577L + 0.5d}{0.577L + 2.5d}\right)\right]} \tag{3.2}$$

Juvinall & Marshek (2000) estimated the effective contact area of the clamped members for the evaluation of the stiffness of the clamped members. Nassar & Abboud (2008) developed an analytical model to calculate the stiffness of clamped members of an axisymmetric bolted joint where the members contact stress distribution is based on a fourth-order polynomial in the radius. Equations. (3.3) and (3.4) give the stiffness for the larger and smaller outer diameters of clamped members, respectively.

$$K_m = \frac{\pi E_m d \tan\theta}{2\left[\ln\left(\frac{\gamma + 3}{\gamma d + L\tan\theta + 3d}\right)\left(\frac{\gamma d + L\tan\theta - d}{\gamma - 1}\right)\right]} \qquad [d_m \geq L\tan\theta + \gamma d] \tag{3.3}$$

and

$$K_m = \frac{\pi E_m \tan\theta}{2\left[\frac{1}{d}\ln\left(\frac{\gamma+3}{d_m+3d}\right)\left(\frac{d_m-d}{\gamma-1}\right)+\frac{4\left(\gamma d+L\tan\theta-d_m\right)}{\left(d_m+3d\right)\left(d_m-d\right)}\right]} \qquad [d_m < L\tan\theta+\gamma d] \tag{3.4}$$

Here, γ is the contact radii ratio, i.e., the ratio of maximum to minimum contact radii under the bolt head. Several numerical studies were conducted using the finite element (FE) technique to estimate the stiffness of clamped members. Maruyama, Yoshimoto & Nakano (1975) compared FE analysis of axisymmetric bolted joints with experimental tests showing the impact of the ratio of member diameter to bolt diameter on the stiffness of clamped members. The estimated member stiffness showed reasonable agreement between numerical and experimental results because of the incorporation of the deformations of bolt head and nut into the calculations. Lehnhoff, Ko & Mckay (1994) developed a FE model to estimate the stiffness K_m, the results of which were compared to the one produced by the basic theoretical formula. Only the results for the half apex angle $\theta = 30^\circ$ that was highly recommended by Shigley & Mischke (1989) showed deviance from their FE results, which encouraged smaller cone angles to be used while considering the clearance between the bolt and hole in the theory. Grosse and Mitchell (1990) showed the nonlinear characteristics of the stiffness K_m in an axisymmetric joint due to its compression relief when subjected to an external axial separating load. They claim that the axial stiffness of the joint is highly influenced, particularly by bending and rotation of clamped members and also by interfacial friction and the thread geometry. Wileman, Choudhury & Green (1991) performed a FE analysis to evaluate the stiffness of clamped members considering an axisymmetric bolted joint. They derived the following exponential expression based on the FE data resulting from the displacement of the topmost node located on the centerline of the washer.

$$K_m = E_m d_h A \exp\left[B\left(\frac{d_h}{L}\right)\right] \tag{3.5}$$

Here, A and B are constants, the values of which are 0.78952 and 0.62914, respectively, for steel, cast iron, aluminum, and copper. This study aimed at providing a nondimensional parametric analysis where different materials and aspect ratios defined by the hole diameter over the joint grip length (d_h/L) were considered. The approach of Wileman, Choudhury & Green (1991) was later extended by Musto and Konkle (2006) to calculate the stiffness of two

clamped members of different materials, specifically steel and aluminum. They understood that the former approach (Wileman, Choudhury & Green, 1991) can lead to inaccurate stiffness results for members of dissimilar materials. Equation (3.5) is based on the principle of conical frusta stress distribution, which may change when dissimilar materials are used. Pedersen and Pedersen (2008) also highlighted the use of bolt hole diameter instead of bolt nominal diameter in estimating the stiffness of clamped members. These aspect ratios ranged between 0.1 and 2.0, where the grip length remained constant and the washer diameter d_w was equal to 1.5d. Due to the consideration of an infinitely rigid washer to which the compressive force was employed to produce uniform displacement of the clamped members nodes in contact, an unrealistic estimation of the members stiffness resulted, which was also reported in Zadoks & Kokatam (2001) and Guillot (1997).

Lehnhoff & Bunyard (2001) conducted an axisymmetric FE analysis of a bolted joint and observed a noticeable effect of bolt thread on the stiffnesses of bolt K_b and clamped members K_m. A decrease in the bolt stiffness due to bolt thread bending and a reduced cross-sectional area were reported, whereas the stiffness K_m was increased due to reduced initial deflection after the initial joint tightening. In addition, the stiffness K_m is material-dependent and affects the overall joint stiffness considerably.

Alkatan et al. (2007) introduced a 3D FE method to evaluate joint stiffness based on the deformation energy principle. Their method considered different geometrical parameters, materials, and friction coefficients for axisymmetric loading. Another study by Sethuraman & Kumar (2009) considered the same material and clamped member thickness for the estimation of the corresponding members stiffness K_m. They predicted that K_m lies within a range bounded by an upper and a lower limit determined by two different axisymmetric FE models; the first one is based on a uniform displacement analysis (UDA) and the second one is based on a uniform pressure analysis (UPA) or average nodal displacement method, respectively. The uniform displacement was simulated by considering an infinitely rigid washer, whereas the uniform pressure on the bolt bearing surface was obtained by making the washer very soft.

In this study, the stiffnesses of the bolt and clamped members are accurately evaluated using a FE methodology, and the results are compared to those from earlier FE methods and some well-established analytical models. The thicknesses of both clamped members are kept the same, but the grip lengths are varied during the analysis. The paper presents first the FE methodology to evaluate the stiffness of the bolt separately and then that of the clamped members. After that, the proposed methodology is validated by comparison with the stiffnesses obtained from two different load cases involving the application of mechanical and thermal loading. Axisymmetric bolted joints with seven different-size metric hex bolts of ASME B18.2.3.5M (ASME, 1989*a*) and members of different thicknesses are considered in the study. The proposed methodology is finally compared with previously developed FE methods and existing analytical models.

3.3 Proposed methodology: finite element analysis

Figure 3.1 illustrates the schematic of a conventional bolted joint with its various functional components: a bolt, a nut, and two clamped members. The FE model in this study is developed on the assumption of an axisymmetric bolted joint using the ANSYS Workbench (ANSYS, 2019), where both clamped members are identical, having the same thickness and being made of the same material. Consequently, the contact plane between the members is a plane of symmetry. Seven different-sized bolts with a simplified design having circular bolt heads and no thread in the shank are considered. Also, no washer is included under the bolt head to simplify the analysis and to be able to compare with the literature. The nut is not considered as part of this study since only the stiffness of the clamped members is of main interest. All these assumptions allow for the formation of a symmetrical bolted joint with respect to its midplane as well as its axis (z); therefore, the upper half of the joint above the midplane and the half of the upper half about the z axis are sufficient to conduct the analysis without any generality loss. The purpose of these assumptions is to save unnecessary computational costs, as complex 3D modeling is lengthy and time-consuming.

Table 3.1 shows the material properties of the bolt and clamped members. All these components are considered to be composed of homogenous, isotropic, and linearly elastic materials. Thus, the modulus of elasticity and the Poisson's ratio of bolt and clamped members are equal ($E_b = E_m$ and $\upsilon_b = \upsilon_m$). SA-193 B7 and SA-285 steels are selected for the bolt and clamped members, respectively.

Table 3.1 Mechanical and thermal properties of bolt (SA-193 B7) and clamped members (SA-285)

Properties	Bolt Material	Member Material
Ultimate tensile strength [MPa]	860	450
Yield strength [MPa]	720	165
Young's Modulus [GPa]	206.8	206.8
Poisson's ratio	0.3	0.3
Coefficient of thermal expansion [K^{-1}]	0.000015	0.000012

Table 3.2 Aspect ratios used for analyses and bolt dimensions according to the standard Taken from ASME (1989a)

Bolt Size	Hole Diameter d_h [mm]	Equivalent Head Diameter d_{hd} [mm]	Head Thickness H [mm]
M6	6.5	10.78	4.38
M8	8.5	14.01	5.68
M10	11	16.16	6.85
M12	13	19.39	7.95
M16	17	25.86	10.75
M20	21	32.32	13.4
M36	37	59.26	23.55
Aspect Ratio d_h/L (for all bolt sizes)			
0.35, 0.38, 0.40, 0.44, 0.48, 0.53, 0.58, 0.66, 0.75, 0.88, 1.05, 1.31, 1.50, 1.75, 1.91			

Since the bolt head is hexagonal in practice, it is simulated by a cylinder with a diameter that is taken as the average of the diameters of the standard bolt head across the flats and across the corners. The aspect ratio of the hole diameter to the grip length d_h/L ranges between 0.35 and 1.91 to cover the possible grip lengths of M6, M8, M10, M12, M16, M20 and M36 bolts. Table 3.2 shows the dimensions of all seven bolts used in this study, which are based on the ASME B18.2.3.5 M standard for Metric Hex Bolts (ASME, 1989*a*). The outside diameter of the clamped member d_m for the study is 109 mm, which is large enough to cover most practical cases in general. This value is selected so that the stiffness of clamped members is not affected.

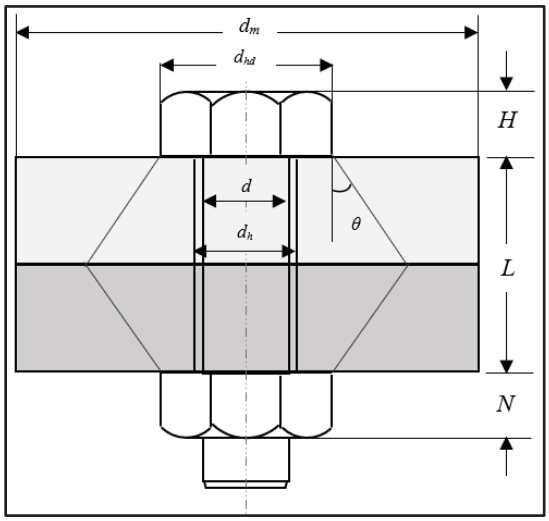

Figure 3.1 Schematic of a bolted joint with the assumption of conical frusta

In this study, the main focus is to estimate stiffness of the bolted joint components, and for that reason, the results of forces and displacements are taken into consideration. Therefore, only static elastic analysis is considered for the study. The model basically has 2D rectangular isoparametric 8-node elements with a global size of 0.2 mm. The contact region between the bolt head and clamped member is modeled using contact and target elements with a friction coefficient of 0.2. The mesh refinement of the FE model is continuously improved by increasing the number of elements, in particular near the important contact zones of interest until a convergence of 1% on the stiffness of clamped members is obtained. The final model, after mesh refinement, retains 8,700 elements and 26,793 nodes (see Figure 3.2).

Most of the numerical studies account for the average displacement of the number of arbitrarily selected contact nodes that are located at the bolt bearing surface in contact with the clamped member for the estimation of the member stiffness K_m. Those nodes are selected between the radius of the bolt hole and an arbitrary radius of the bolt bearing surface. The node selection for this contact region is different from one study to the other. Some prefer to choose the nodes up to half of the bolt bearing contact width, whereas others consider additional nodes beyond the end point of the contact surface. The considerations of the average nodal displacement method are able to give a range within which the actual result of the stiffness K_m lies and can be predicted; however, these approaches give stiffer values, and the concept relies on the number of nodes selected within the bolt bearing surface.

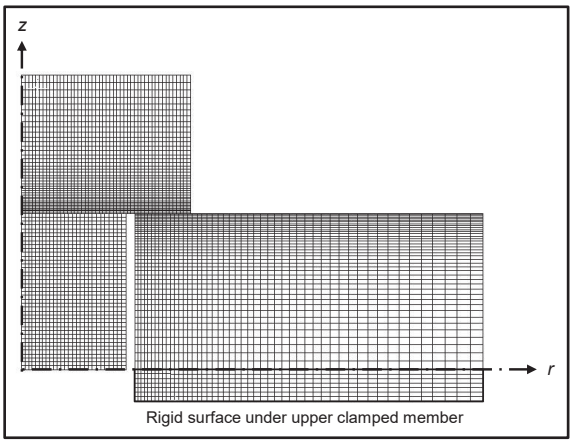

Figure 3.2 Finite Element mesh of the axisymmetric bolted joint

The proposed methodology evaluates the stiffness of clamped members K_m by deducting the estimated bolt stiffness K_b from the overall stiffness of the joint K_j. In the first step, the bolt stiffness K_b is estimated. The bolt with the bolt head and shank is allowed to deform under an applied load with a support at the bolt bearing surface. In this step, the clamped members are not modeled (see Figure 3.3a). A load P in the axial direction is applied in steps to the lower face of the half shank within the elastic range. The corresponding axial displacement δ of these nodes constrained to move together is used to obtain the bolt stiffness K_b using the slope with the following equation (Bickford, 1995).

$$K_b = \frac{1}{2}\left(\frac{\Delta P}{\Delta \delta}\right)_b \tag{3.6}$$

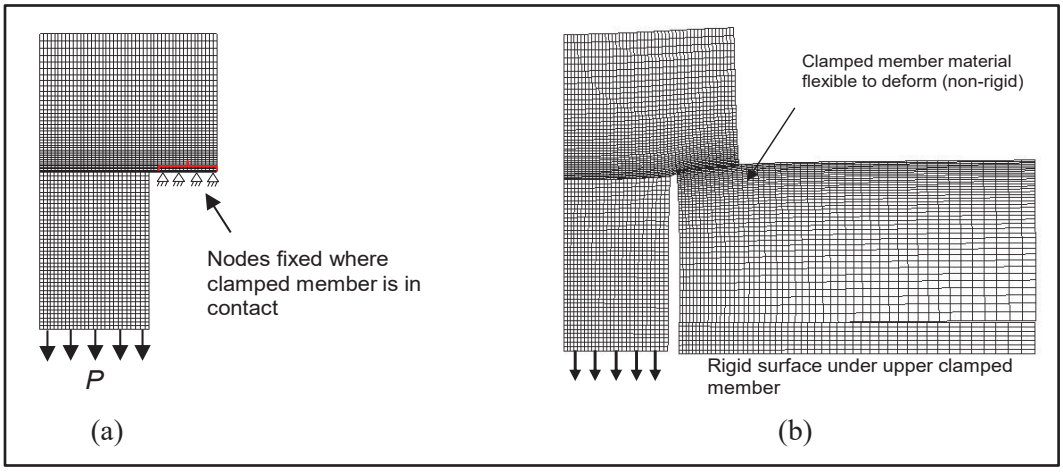

Figure 3.3 (a) Axial displacement of lower face of half shank to measure K_b, (b) Axial displacement of the joint with clamped member to measure joint stiffness

The next step involves the estimation of the total stiffness of joint K_j consisting of the bolt and the clamped members that are in contact (see Figure 3.3b). It is important to mention that a rigid surface is added under the upper clamped member to allow any possible lifting of the latter. Therefore, the corresponding axial displacement δ of all the nodes that belong to the half-shank lower face is also used to calculate the total joint stiffness K_j using the slope in the following equation:

$$K_j = \frac{1}{2}\left(\frac{\Delta P}{\Delta \delta}\right)_j \tag{3.7}$$

Here, the subscripts b and j in equations (3.6) and (3.7) refer to the bolt and the whole joint, respectively. Therefore, the stiffness of clamped members K_m can be deduced from equation (3.8) based on K_b and K_j estimated earlier, where K_b and K_m are considered to be in series.

$$\frac{1}{K_j} = \frac{1}{K_b} + \frac{1}{K_m}$$

$$K_m = \frac{1}{\frac{1}{K_j} - \frac{1}{K_b}} \tag{3.8}$$

This method uses a simple approach to estimate the stiffness of clamped members K_m without having to use the displacements of arbitrarily selected nodes in the bolt under-head contact region, which usually gives an overestimated stiffness of clamped members.

3.4 Validation of the proposed methodology

Because the contact area between the bolt bearing surface and the clamped member in contact is annular and covers several nodes, it is almost impossible to measure experimentally the displacement of each individual node of the clamped member in contact with the bolt bearing surface to finally evaluate the stiffness K_m for the validation of the proposed methodology. Therefore, to validate the stiffness of the clamped members obtained earlier, a resolution of two loading cases to simultaneously evaluate the stiffnesses K_m and K_b is presented in this section. Here, the stiffnesses K_m and K_b are evaluated using the FE results, where two selected loading cases are conducted: (i) mechanical loading: bolted joint subjected to an external separating force; and (ii) thermal loading: bolted joint subjected to a uniformly distributed temperature rise. Also, unlike the first mentioned method, bolt load cases are combined, where K_b and K_m are directly obtained from FE results using the slopes of the curves of the bolt and clamped member forces as a function of the external separating force and temperature, which are detailed in Sections 3.4.1 and 3.4.2.

3.4.1 Mechanical loading: application of an external separating force

An external separating ring load F_e distributed along the perimeter of the outer diameter d_{hd} of the M20 bolt head is applied to loosen the clamped members after the joint is tightened with a preload in steps up to 75% of the bolt yield strength. The decrease in the clamping force of the joint is recorded during the application of F_e.

Both the stiffnesses K_m and K_b can be obtained by the slopes of the curves that represent the change of bolt and clamping forces due to the external loading. The initial equilibrium of the forces after preloading the joint and the final equilibrium of the forces after the application of F_e are given by:

$$F_b^i = F_m^i \tag{3.9}$$

$$F_b^f = F_m^f + F_e \tag{3.10}$$

The compatibility equation requiring the change of bolt extension equal to the change of clamped member compression gives:

$$\frac{F_b^f}{K_b} - \frac{F_b^i}{K_b} = \frac{F_m^f}{K_m} - \frac{F_m^i}{K_m} \tag{3.11}$$

Combining the above three equations gives:

$$\frac{K_m}{K_b} = \frac{F_m^f - F_m^i}{\Delta F_e} \times \frac{\Delta F_e}{F_b^f - F_b^i} \tag{3.12}$$

$$\frac{K_m}{K_b} = \frac{\Delta F_m}{\Delta F_e} \times \frac{\Delta F_e}{\Delta F_b} \tag{3.13}$$

where $\Delta F_m/\Delta F_e$ is the slope obtained from the curve of the clamped member force plotted against the external force, and $\Delta F_b/\Delta F_e$ is the slope obtained from the curve of the bolt force plotted against the external force.

3.4.2 Thermal loading: application of a unifom temperature increase

This loading case is conducted by applying a preload first up to 75% of the bolt yield strength and then uniformly increasing the temperature of the bolted joint, allowing a uniform expansion of all the components. All the properties and conditions are the same. Like the previous loading case, the following compatibility of displacement equation is used to relate the stiffness of the clamped members K_m and the bolt stiffness K_b:

$$\frac{F_b^f}{K_b} - \frac{F_b^i}{K_b} + \alpha_b \Delta T\ L_b = \frac{F_m^f}{K_m} - \frac{F_m^i}{K_m} + \alpha_m \Delta T\ L_m \tag{3.14}$$

where ΔT is the temperature increase between initial and final temperature and $L_m = L_b = L$ is the grip length. Noting that the initial and final forces in the bolt and the clamped members are the same, Equation (3.14) becomes

$$\frac{1}{K_m}-\frac{1}{K_b}=\frac{(\alpha_b-\alpha_m)\,\Delta T\,L}{F_m^f-F_m^i} \tag{3.15}$$

$$\frac{1}{K_m}-\frac{1}{K_b}=\frac{(\alpha_b-\alpha_m)L}{\Delta F_m/\Delta T} \tag{3.16}$$

Here, $\Delta F_m/\Delta T$ is the slope obtained from the curve of the clamped member force plotted against the temperature.

3.4.3 Stiffness determination

A combination of the two load cases described above can be used to obtain simultaneously K_m and K_b. From equations (3.13) and (3.16), the following expression of K_m is obtained.

$$K_m=\left(\frac{\Delta F_m}{\Delta F_e}\Big/\frac{\Delta F_b}{\Delta F_e}-1\right)\times\frac{\Delta F_m/\Delta T}{(\alpha_b-\alpha_m)L} \tag{3.17}$$

Therefore, K_b can be obtained by substituting equation (3.17) into equation (3.13). The two stiffnesses can be compared to the ones obtained directly from the proposed methodology in Section 3.3.

$$K_b=-\left(\frac{\Delta F_b}{\Delta F_e}\Big/\frac{\Delta F_m}{\Delta F_e}+1\right)\times\frac{\Delta F_m/\Delta T}{(\alpha_b-\alpha_m)L} \tag{3.18}$$

3.5 Results and discussion

Figure 3.4 shows the displacement of all the nodes located in the lower face of the bolt half-shank due to the applied load in steps. The displacement is linear as the applied load is kept within the elastic range of the bolted joint.

Figure 3.5 illustrates the changes in the bolt and clamping forces of a M20 bolted joint with five different grip lengths as a function of the external separating force (ring load). Both slopes of F_b and F_m with respect to the external force F_e are almost similar for all grip lengths considered or for the aspect ratios defined as the bolt hole diameter over the grip length, d_h/L.

The slopes of the straight lines are used to calculate the stiffness of clamped members. The variations of F_b and F_m for the same bolted joint are shown in Figure 3.6 when subjected to a uniform temperature variation in steps. Both forces are equal in magnitude but opposite in direction for a particular grip length. The stiffness of the clamped members and bolt are calculated simultaneously by equations (3.17) and (3.18) and the slopes of the curves of Figures 3.5 and 3.6.

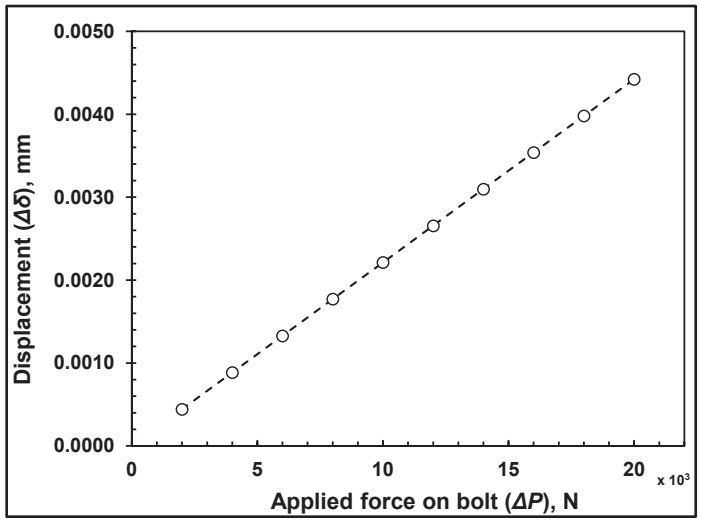

Figure 3.4 Displacement of all nodes of lower face of bolt half shank due to applied load in steps

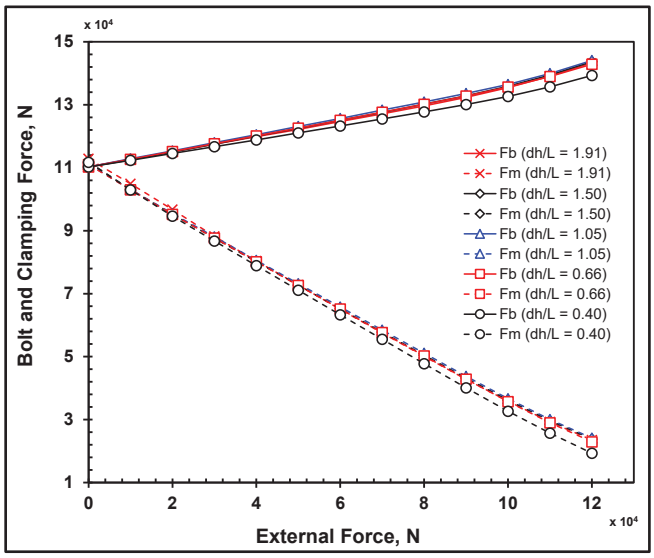

Figure 3.5 Bolt and clamping forces due to external separating force (ring load) for different aspect ratios

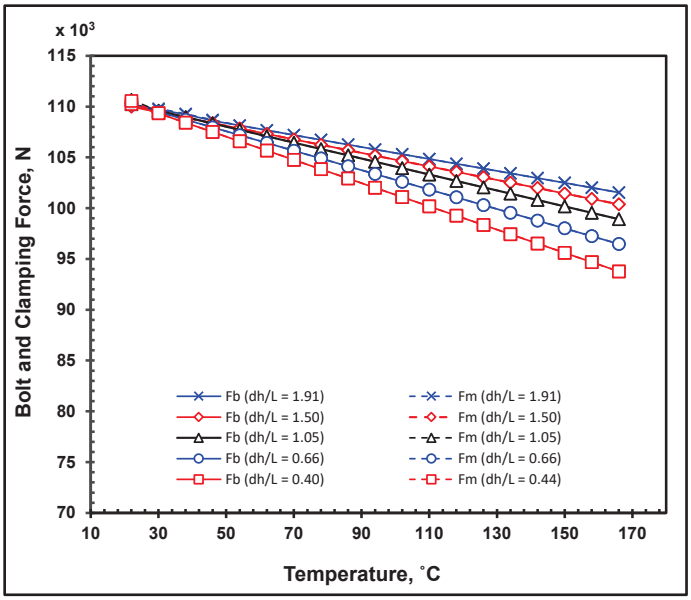

Figure 3.6 Bolt and clamping forces due to joint temperature rise for different aspect ratios

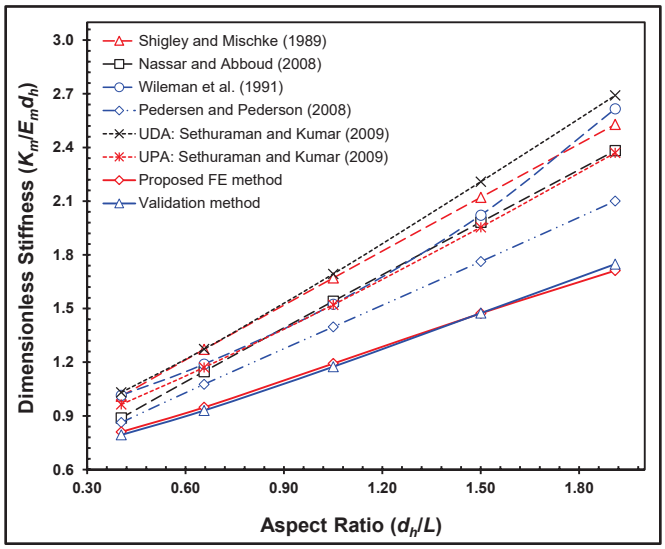

Figure 3.7 Comparison of dimensionless stiffness of clamped members among different methods for M20 Bolt

Figure 3.7 compares the results of the dimensionless stiffness of the clamped members $K_m/E_m d_h$ evaluated using the proposed methodology and validation technique with those obtained from the well-established analytical methods (Shigley & Mischke, 1989; Nassar & Abboud, 2008) and FE models (Wileman, Choudhury & Green, 1991; Pedersen & Pedersen, 2008) discussed in the literature. Also shown are the FE results by Sethuraman & Kumar (2009) based on UDA

and UPA techniques. All the dimensionless stiffness results displayed in the figure are for two equally thick clamped members having different grip lengths used with the M20 hex bolt. Therefore, the dimensionless stiffness of clamped members is given based on the same aspect ratio, d_h/L.

Noticeable differences can be observed among the different methods, particularly with the proposed method, which apparently shows lower stiffness values. It is clear from Figure 3.7 that the dimensionless stiffness resulted from the proposed method and the validation explained earlier agree very well with each other. The stiffness of clamped members Km calculated using the combined loading case from the validation technique is similar to that obtained from the FE results of the proposed method, with a reasonable maximum difference of around 2% at aspect ratio 1.91. The results of the analytical methods proposed by Shigley & Mischke (1989) and Nassar & Abboud (2008) show up to around 48% and 39% maximum differences at the highest aspect ratio with the proposed methods.

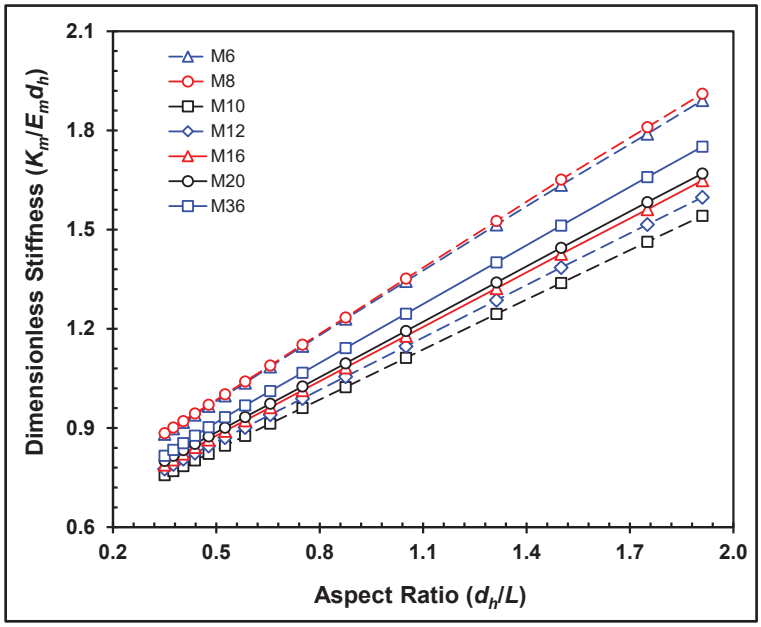

Figure 3.8 Dimensionless stiffness for different bolt sizes using proposed FE method

Figure 3.8 highlights the influence of the variation of bolt sizes on the dimensionless stiffness $K_m/E_m d_h$ obtained using the proposed method. The effect of bolt size is usually not considered

when comparing different methods. From this figure, a significant change in the dimensionless stiffness of clamped members can be observed with the variation of bolt size. The biggest difference is 24% and is obtained with the M8 and M10 bolts. It would appear that the influence of the joint hole is not linear. As the hole diameter (or aspect ratio) decreases, the stiffness also decreases. However, after reaching a certain hole size, the stiffness of the members starts increasing again as the hole size decreases. This is depicted by both Rötscher (1927) and Norton (2000).

By introducing a new aspect ratio defined as the bolt bearing contact width w over the grip length L instead of the one based on bolt hole diameter d_h/L, all the lines are superimposed. The contact width represents half the difference between the diameters of the bolt head and the joint hole, $(d_{hd} - d_h)/2$. Figure 3.9 confirms that all the curves are effectively superimposed when the stiffness is plotted as a function of the new aspect ratio w/L, forming a single line that simplifies the calculation.

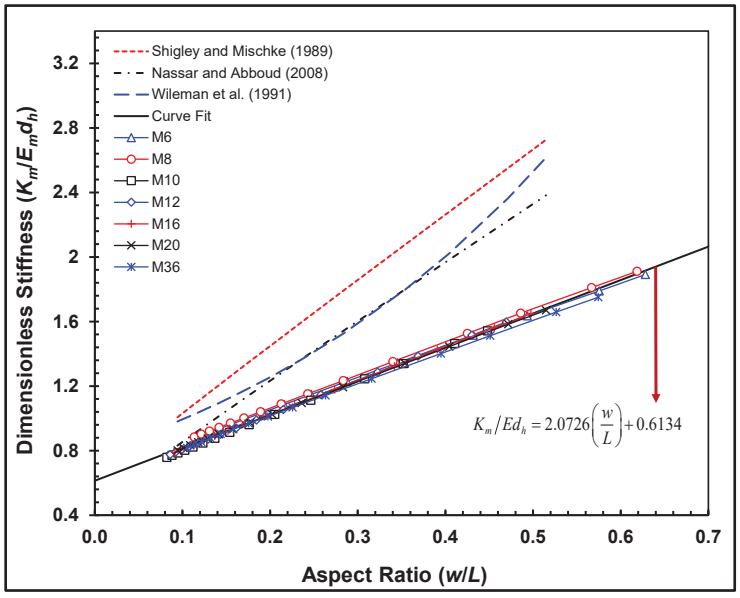

Figure 3.9 Dimensionless stiffness based on new aspect ratio, w/L

Thus, the following generalized expression gives the stiffness of clamped members of a sufficiently wide bolted joint and is obtained from a curve fitting of all the points.

$$K_m = \left[2.0726\left(\frac{w}{L}\right) + 0.6134 \right] E_m d_h \tag{3.19}$$

Figure 3.9 presents the dimensionless stiffness results from the proposed equation (3.19) with a new aspect ratio *w/L* that shows noticeably lower stiffness values as compared to the existing analytical methods (Shigley and Mischke, 1989; Nassar & Abboud, 2008). It can be seen that the maximum differences with Shigley & Mischke (1989), Nassar & Abboud (2008), and Wileman, Choudhury & Green (1991) are around 62%, 42%, and 56%, respectively.

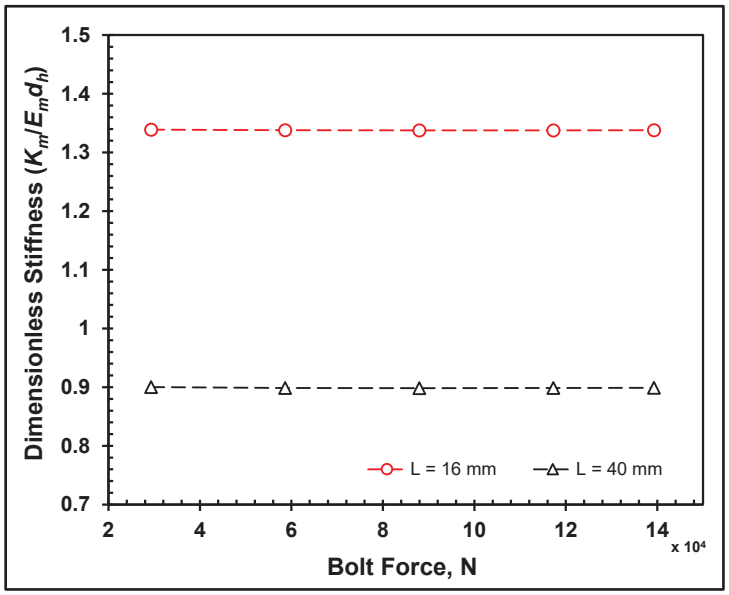

Figure 3.10 Effect of the change of bolt force on the dimensionless stiffness for two different grip lengths

A load sensitivity study was conducted on the M20 bolt, as shown in Figure 3.10, where the bolt force is changed from 20% to 95% of the maximum load that causes yield considering two different joint grip lengths. It is observed that the dimensionless stiffness remains constant, with a lower value obtained for the higher grip length as expected. Figure 3.11 shows the effect of bolt bearing contact width w. A comparison between two M20 bolts, one with hex and the other with heavy hex dimensions, shows that the bigger bolt head diameter results in higher stiffness. There is a 12% increase in the stiffness of clamped members as the size of the bolt head increases. However, with the lower aspect ratio, the difference between the two curves becomes smaller.

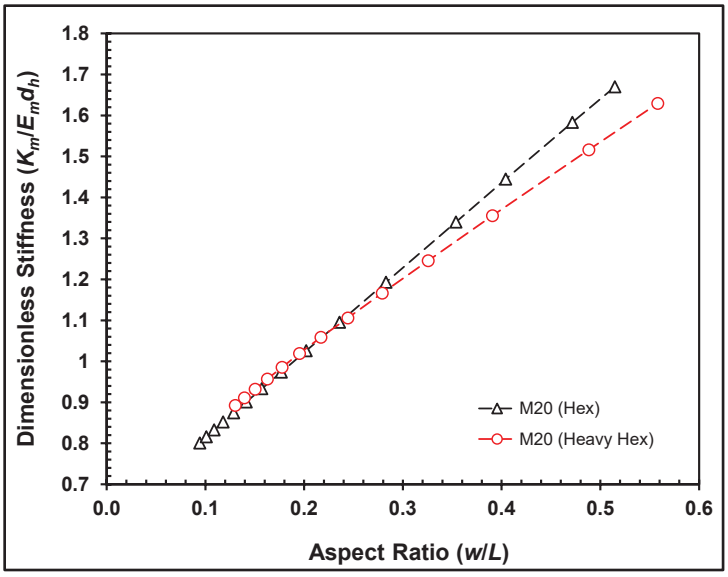

Figure 3.11 Effect of bolt head diameter variation on the dimensionless stiffness considering aspect ratio with *w*

A better result of dimensionless stiffness is thus possible to get from the proposed relationship of equation (3.19), as the maximum difference between these two curves is around 6%. It should be noted that this maximum difference represents unrealistic or uncommon applications, where the bolt bearing contact width is comparatively high in comparison with the grip length and usually the aspect ratio *w/L* is below 0.35.

3.6 Conclusion

The evaluation of the stiffness of clamped members was revisited, and the suggested methodology does not rely on the displacement of arbitrarily selected nodes as done in the earlier studies. In addition, a validation using a simple FE-based method combining two load cases to better estimate the stiffnesses of the bolt and clamped members is suggested. The study shows a noticeable difference with the earlier proposed FE methods based on the UDA and UPA techniques. Also, an observable influence of the bolt size on the dimensionless stiffness of clamped members, which was not referenced in the earlier developed analytical models, is clearly highlighted when the aspect ratio is based on the joint hole diameter. However, this influence vanishes with the new aspect ratio based on the bolt bearing contact width, and as a

result, the curves of the dimensionless stiffness of clamped members lie in a straight line, the relationship of which is given by equation (3.19). Therefore, this suggested equation is the recommended relationship for use in estimating the stiffness of clamped members for sufficiently wide bolted joints. Also, the validation method from combining the two load cases in any specific bolted joint can be used to determine the stiffness of any member, regardless of their width.

CHAPTER 4

THE TIGHTENING AND UNTIGHTENING MODELING AND SIMULATION OF BOLTED JOINTS

Rashique Iftekhar Rousseau [a] and Abdel-Hakim Bouzid [b]

[a] Department of Mechanical Engineering, École de technologie supérieure,
1100 Notre-Dame St. West, Montreal, Quebec, H3C 1K3
[b] ASME Fellow, Department of Mechanical Engineering, École de technologie supérieure,
1100 Notre-Dame St. West, Montreal, Quebec, H3C 1K3

Paper published in the Machines Journal, September 2024.
(12(9): 645, DOI: 10.3390/machines12090654)

4.1 Abstract

Although bolted joints may appear simple and are easy to manipulate, they are challenging to model and analyze due to their complex structural patterns and statically indeterminate nature. Ensuring the structural integrity of these joints requires maintaining proper bolt preload and clamping force, which is crucial for preventing failures such as overload, excessive bearing stress, fatigue, and stripping caused by seizing or galling. Achieving the necessary clamping force involves carefully controlling the input tightening torque, which is divided into the pitch torque and the friction torques at the bolt or nut bearing surfaces and in the engaged threads. The resulting clamping force is critical for generating the required force within the bolt. However, the achieved bolt force depends on several factors, such as friction at the joint's contact surfaces, grip length, and the relative rotation between the bolt and nut during tightening. Friction at the contact surfaces, particularly beneath the bolt head or nut and between the threads, consumes a significant portion of the applied tightening torque - approximately 90%. This paper explores the three existing bolt internal pitch, bearing, and thread friction torques that are generated by the external applied torque in a bolted joint, as

well as their contributions and variations throughout a loading cycle composed of three phases: tightening, settling, and untightening. An analytical model is developed to determine these torque components, and its results are compared with those obtained from finite element (FE) modeling and experimental testing from previous studies. Finally, this study examines the torque–tension relationship during bolt tightening, offering insights into the required accuracy of bolt and clamped member stiffness. The bolt samples used in this study include M12 × 1.75 and M36 × 4 hex bolts.

4.2 Introduction

Among the non-permanent clamping methods, bolted joints are the most popular, as they provide easier features for their assembling and disassembling. Having sufficient clamping force in a bolted joint is very important as it ensures structural integrity and reliability of the clamped products. In the bolted joints, the bolt force generated due to tightening depends on the torque applied on the bolt, which is critical to estimate as it is de-pendent on certain conditions, such as the material specifications, contact surface conditions, and the type of threads. Insufficient torque results in a joint with inadequate clamping force, whereas an excessive amount of torque can be the reason for joint failure, and therefore possible damage to the components can take place. It is thus important to determine the proper installation torque for a bolted joint to ensure sufficient clamping force to avoid joint separation as well as overstretching of the bolt.

Several factors must be considered when determining the input tightening torque, as the clamping force can vary with the identical input torque. These include joint geometry, material strength, inclusion of washers, contact surface conditions, and types of loadings (Li et al., 2019). Frictions at different contact surfaces are highly important to count in, as small variations in friction torques bring significant change in the torque as well as in joint tension. The first torque–tension relationship was presented by Motosh (1976) for threaded joints as follows:

$$T_e = F_b\left(\frac{p}{2\pi} + \frac{\mu_t r_t}{\cos\beta} + \mu_b r_b\right) \tag{4.1}$$

where T_e = external input torque, F_b = bolt load, p = thread pitch, μ_t = thread friction coefficient, μ_b = bolt head bearing friction coefficient, β = thread profile angle (half), r_b = effective bearing friction radius, and r_t = effective thread friction radius. The three components on the right-hand side of equation (1) are three different torque components known as pitch torque T_p, thread friction torque T_t, and bolt head bearing friction torque T_b, respectively. The tension or preload in the bolted joint is developed by the pitch torque component T_p, which provides the clamping force in the joint by stretching the bolt. On the contrary, the other two torque components, T_b and T_t, are used to overcome the friction at contact surfaces: the former being in between the bolt head or nut and the corresponding clamped member surface in contact, and the latter between the engaged threads of the bolt and nut. Though this equation is a strong basis of the torque-tightening method, lack of accuracy of the tightening torque resulted from not considering the thread helix angle, effective radii of bearing and thread contacts, and contact pressure distribution. Usually, almost 90% of the input tightening torque is consumed by the two frictional torque components (Bickford, 1995). Also, the clamping force of a bolted joint highly depends on the friction coefficients at different contact surfaces, as small changes in the roughness percentages of the joint parts can significantly change the predicted amount of clamping force and thus affect the joint stability (Bickford, 1995; Juvinall & Marshek, 2000). Although the values of friction coefficients can be known based on the material being used, in real practice these values change as the contact surfaces and the techniques highly depend on the contact surface geometries, loading, and environmental factors (Kogut & Etsion, 2004). Therefore, it is highly important to properly determine these friction coefficients for the accurate measurement of friction torques that in turn provide the required clamping force of the joint and ensure its integrity. Inaccurate measurement of T_b can lead to joint leakage, separation, loosening, and fatigue failure, whereas T_t can cause material failure because of overstress.

Several studies have been conducted on developing the correlation between the input torque and the clamping force of joints. Nassar & Yang (2008) performed a study on devel-oping an

analytical relationship between tightening torque and clamping force for joint applications where a difference was shown between theoretical and experimental results of clamping force by a torque-angle control technique. In another study, Nassar & Zaki (2009) tested the impact of coating thickness and showed a noticeable effect of the bearing and thread friction coefficients, highlighting the sensitive impact of frictional changes on the torque–clamping force relationship. The torque equation of Motosh discussed earlier was improved by Nassar and his colleagues (Nassar, Barber & Dajun, 2005; Nassar, Matin, & Barber, 2005), where they presented analytical models of effective radii of bearing and thread frictions to calculate bearing and thread friction torques, respectively. The former highlighted the significance of correctly determining the bearing friction coefficient considering four different contact pressure distribution scenarios on a bearing surface, whereas the latter focused on analytically improving the thread friction torque component considering five complex pressure distribution scenarios be-tween the mating thread surfaces in contact. Izumi et al. (2005) highlighted a deviation coming up from the comparison of the preload–tightening torque relationship with that from classical theory due to the underestimation of non-uniform contact pressure at a bolt bearing surface. Contrary to conventional theory, they figured out the starting point of joint loosening as due to the occurrence of complete thread slip before bolthead slip occurs under shear loading, which is a key point to consider in the joint design for preventing early loosening. Huang & Guo (2011) restructured the torque–tension relationship considering all the forces and moments that act in the bolted joints instead of only relying on axial force as carried out earlier in the classic method by Motosh. They used FE modeling to validate their results. Fukuoka (1992) showed the importance of the tightening method with a hydraulic tensioner over the torque method because the former does not get influenced by the helical friction coefficient of mating threads and circumferential friction coefficients on the bolt or nut bearing surfaces, thus giving less error. He evaluated the effective tensile coefficient, the ratio of required clamping force to the initial tension, which has the primary influence of grip length with minimal impact of bolt nominal diameter.

Jiang, Chang, & Lee (2001) experimentally found that the friction coefficients in a bolted joint can be affected by repeated tightening. The bearing friction coefficient does not change much

after repeated tightening, but the thread friction coefficient tends to increase after a certain number of tightening and untightening. Liu et al. (2020) also noticed while investigating the behavior of friction coefficients under repeated tightening that the friction coefficients be-come higher by repeated tightening without lubrication. However, friction coefficients tend to stabilize or decrease with lubrication after repeated tightening. The impact of different types of lubricants was experimentally investigated by Zou et al. (2007) in altering the torque–tension relationship and the friction coefficients of a bolted joint. Among the three, the solid-film lubricant types gave lower friction coefficient values compared to the greases and oils, thus providing a higher clamping force with the same input torque. Grabon, Osetek & Mathia (2018) experimentally studied the impact of tribological factors on the contact surfaces of bolted joints to understand how the actual contact area between surfaces changes during tightening, which is complex to predict. They found higher values for bearing friction coefficient compared to that for engaged thread when tightening and observed a parabolic increase of total tightening torque instead of having linearity as per standard expectation. Nonetheless, a quantitative benchmark to evaluate the tightening performance is lacking, thus making the approach less feasible for industrial applications. Fernando, Pokharel & Gad (2022) formulated the relationship between bolt tension and torque, considering the three-dimensional thread helical geometry and the nut dilation effect, improving upon Nassar's model (Nassar & Yang, 2008). Jiang et al. (2022) developed a model based on Motosh's theory (Motosh 1976) to investigate the distribution of input torque using the energy method, where the effects of parameters such as effective bearing contact radius, thread contact radius, and spiral angle were analyzed. Zhang et al. (2024) introduced an innovative method to enhance the torque–tension relationship of threaded fasteners by incorporating a differential geometric representation of the thread surface and accounting for pressure distribution on contact surfaces.

However, there is still a lack of studies to answer the concerns regarding how various torque components are distributed in the joint contact surfaces and how they act while the joint undergoes tightening and untightening cycles and remains at rest in between. This paper proposed a detailed finite element-based method to evaluate individual contributions of the three torque components: bearing friction torque between the bolt head or nut and the

corresponding clamped member in contact, thread friction torque between engaged threads, and pitch torque in a bolted joint, and their variations during tightening, untightening, and states at rest condition between both cycles. A three-dimensional (3D) M12 × 1.75 hex bolt is modeled, including threads to imitate the joint-tightening and untightening phenomena through bolt and nut relative rotation for analyzing the relationship among the external input torque, resulting bolt force, and rotation between the bolt and the nut. The bolted joint undergoes tightening and untightening cycles with different values of friction coefficients for bearing and thread contacts to observe the correlation between bolt force and input torque.

4.3 Analytical model

It is important to consider the equilibrium condition to properly analyze the assembly of a tightened bolted joint made up of a bolt, a nut, and two clamped members held together by friction. The input torque applied to tighten the joint must be of an amount enough to overcome the torques resulting from the friction forces under the bolt head T_b and in between the engaged threads T_t to resist rotation, as shown in Figure 4.1. Therefore, external input torque $T_e \geq T_b + T_t$ (Fort, Bouzid & Gratton, 2019).

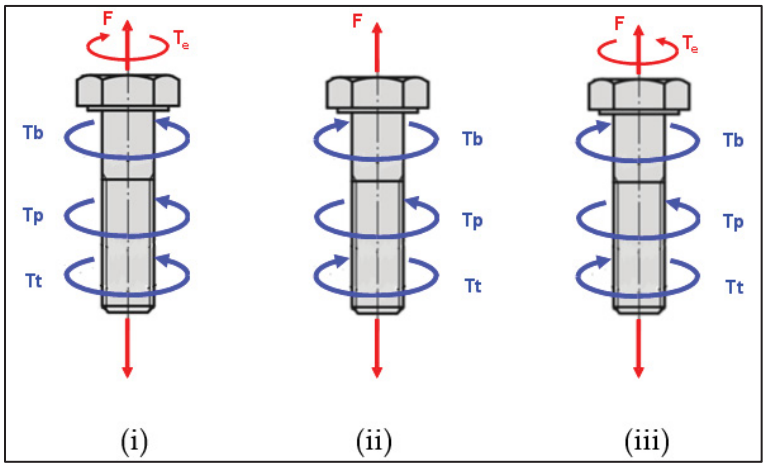

Figure 4.1 Moment equilibrium: (i) tightening, (ii) at rest after tightening, and (iii) untightening

The pitch torque T_p resulting from the contact pressure on engaged threads acts in the loosening direction. Thus, the following equilibrium conditions occur during the tightening and untightening of the joint:

$$\begin{aligned} &T_e \geq T_b + T_t + T_p \text{ (tightening)} \\ &T_b + T_t - T_p = 0 \text{ or, } T_p = T_b + T_t \text{ (at rest after tightening)} \\ &T_e \geq T_b + T_t - T_p \text{ (untightening)} \end{aligned} \tag{4.2}$$

4.3.1 Underhead Bearing Friction Torque

While tightening the bolt, the uniform contact pressure acting under the bolt head is $p_b = F_b/A_b$, where F_b is the bolt tension force, $A_b = \pi(r_{bo}^2 - r_{bi}^2)$ is the area of the bolt underhead, and r_{bo} and r_{bi} are the maximum and minimum radii of the underhead contact surface area. The equilibrium of the elementary forces can be written as

$$\overrightarrow{dF_{Teb}} + \overrightarrow{dF_{Tbf}} = \vec{0} \tag{4.3}$$

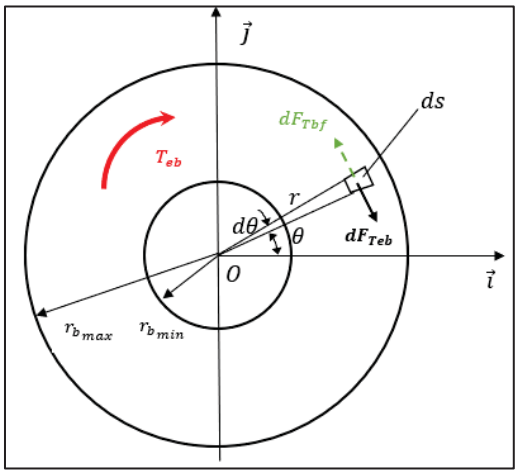

Figure 4.2 Free body diagram of friction on underhead bearing contact surface

where, T_{eb} is the tightening torque in the contact surface area under the bolt head, $\overrightarrow{dF_{Teb}} = dF_{Teb}\vec{v}ds$ and $\overrightarrow{dF_{Tbf}} = \mu_b p_b \vec{v}ds$, as illustrated in Figure 4.2. μ_b is the friction coefficient of the contact surface between the bolthead and the clamped member in contact. $\vec{\imath}$ and $\vec{j}$ are the radial and tangential unit vectors, respectively. The bearing friction torque T_b resulting from

the friction force F_{Tbf} under the bolt head opposes the tightening input torque under head T_{eb}; therefore, $T_b = T_{eb}$. The elementary bearing friction torque dT_b due to $d\overrightarrow{F_{Tbf}}$ is calculated as

$$dT_b = \left(\vec{r} \times d\overrightarrow{F_{Tbf}}\right) \cdot \vec{k} = \mu_b p_b \left(\vec{r} \times \vec{v}\right) \cdot \vec{k} ds = \mu_b p_b r^3 dr d\theta \tag{4.4}$$

where $ds = rdrd\theta$ for the plane contact surface. By integrating equation (4.4) on the contact area, the bearing friction torque T_b can be found as follows:

$$T_b = \mu_b \iint_{\Omega_b} p_b r^3 dr d\theta \tag{4.5}$$

4.3.2 Thread Friction and Pitch Torques

Following a similar approach, the force equilibrium equation with the bolt being tightened is composed of the elementary friction force in the thread contact surface resulting from the tightening input torque T_{et} (see Figure 4.3). In addition, pitch torque is added. Therefore,

$$d\overrightarrow{F_{Tet}} + d\overrightarrow{F_{Tp}} + d\overrightarrow{F_{tf}} = \vec{0} \tag{4.6}$$

where $d\overrightarrow{F_{Tp}}$ is the elementary thread pitch force. $d\overrightarrow{F_{Tp}} = \mu_t p_t \vec{v} ds$ is the elementary friction force and μ_t is the friction coefficient of the thread contact surface. $p_t = (F_b/A_t) \cdot \overrightarrow{w_1}$ is the average contact pressure where $A_t = n\pi(r_{bo}^2 - r_{bi}^2)$ is the thread contact area; r_{to} and r_{ti} are the maximum and minimum radii of the thread contact area, respectively. n is the number of engaged threads. $\overrightarrow{w_1}$ is the unit vector normal to the thread contact surface, which is defined by the cross product of radial and tangential vectors $\overrightarrow{u_r}$ and $\overrightarrow{v_t}$ that are parallel to the thread contact surface. Therefore,

$$w_1 = \frac{\overrightarrow{u_r} \times \overrightarrow{v_t}}{\left|\overrightarrow{u_r}\right|\left|\overrightarrow{v_t}\right|} = \cos\alpha \cos\beta \begin{bmatrix} \tan\alpha \\ \tan\beta \\ 1 \end{bmatrix} \tag{4.7}$$

where α and β are the half of the thread profile angle and the thread helix angle, respectively. $\overrightarrow{u_r}$ and $\overrightarrow{v_t}$ can be found from the local coordinate system ($\vec{u}\vec{v}\vec{w}$), as shown in Figure 4.3:

$$\overrightarrow{u_r} = \begin{bmatrix} \cos\alpha \\ 0 \\ -\sin\alpha \end{bmatrix} \text{ and } \overrightarrow{v_t} = \begin{bmatrix} 0 \\ \cos\beta \\ -\sin\beta \end{bmatrix} \tag{4.8}$$

The elementary thread pitch force in the loosening direction can be written as

$$d\overrightarrow{F_{tp}} = p_t(\overrightarrow{w_1}\cdot\vec{v})\cdot\vec{v}ds \tag{4.9}$$

Here, $ds = rdrd\theta/(\overrightarrow{w_1}.\vec{w})$ is the elementary thread contact surface. The equilibrium equation of torques about the joint axis center O is given by

$$T_{et} = T_t + T_p \tag{4.10}$$

The thread pitch torque T_p can be written as follows:

$$T_p = \iint_{\Omega_t}\left(\vec{r}\times d\overrightarrow{F_{Tp}}\right)\cdot\vec{k} = \tan\beta\iint_{\Omega_t} p_t r^2 drd\theta \tag{4.11}$$

The thread friction torque $d\overrightarrow{F_{Tf}}$ due to the force can be given by

$$T_t = \iint_{\Omega_t}\left(\vec{r}\times d\overrightarrow{F_{tf}}\right)\cdot\vec{k} = \mu_t\cos\alpha\cos\beta\iint_{\Omega_t} p_t r^2 drd\theta \tag{4.12}$$

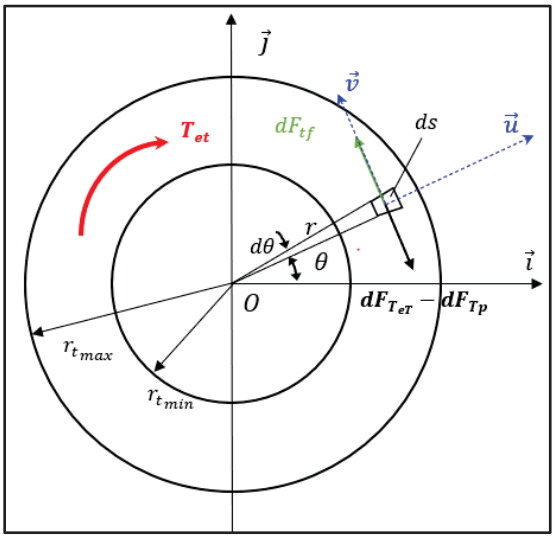

Figure 4.3 Free body diagram of friction on thread contact surface

4.3.3 Stiffness of joint

The total stiffness of the bolted joint, considering all its components are in series, results from the stiffness of the individual components, which can be expressed by the following equation:

$$\frac{1}{k_j} = \frac{1}{k_{sh}} + \frac{1}{k_m} + \frac{1}{k_{tc}} \tag{4.13}$$

where subscripts *j*, *sh*, *m*, and *tc* stand for joint, shank and head, member, and threaded connection.

4.3.3.1 Bolt stiffness

The stiffness of the bolt, including its head and shank, is as follows:

$$k_{sh} = \frac{A_b E_b}{L_{eq}} = \frac{\pi d^2 E_b}{4 L_{eq}} \tag{4.14}$$

Here, $L_{eq} = L + 0.2\{(d^2 + H^2)/H\}$ is the equivalent bolt length with the joint grip length L and the portion resulting from the combination of bolt diameter and head thickness. A few studies came up with different recommendations to calculate L_{eq} based on a single parameter, such as adding 50% of bolt head and nut thickness each (Bickford, 1995), 40% of head and nut diameter each (Meyer and Strelow, 1972), or 60% of head diameter and 70% of nut diameter (Sawa and Maruyama, 1976). A recent study (Rousseau, Bouzid & Zhao, 2021) showed a noticeable impact of the combination of bolt nominal diameter and head thickness on L_{eq} and recommended using 20% of the parameter $\{(d^2 + H^2)/H\}$ to add in the calculation.

4.3.3.2 Stiffness of Threaded Connection

The stiffness of the threaded connection that includes the nut and part of the bolt that is threaded to it can be written as follows (Zhang, Gao & Xu, 2016):

$$k_{tc} = \frac{1}{\lambda\left(\delta_b + \delta_n\right)\sin\beta} \cdot \frac{\cosh \lambda M - 1}{\sinh \lambda M} \tag{4.15}$$

where subscripts *b* and *n* are used for bolt and nut, respectively. *M* is the nut height. $\lambda = \left\{(1/A_b E_b + 1/A_n E_n)/\left(1/k_{by} + 1/k_{ny}\right)\right\}^{1/2}$. $k_{by} = 1/\delta_b sin\beta$ and $k_{ny} = 1/\delta_n sin\beta$ are the stiffness of the unit axial length of the bolt and nut due to the unit force, respectively. δ is the total axial elastic deformation of the thread, which is composed of thread bending deformation δ_1, thread shear deformation δ_2, thread root inclination deformation δ_3, thread root shear deformation δ_4, and radial extended deformation for the nut or radian shrinkage deformation for the bolt δ_5. Therefore, for the bolt,

$$\delta_b = \delta_{1b} + \delta_{2b} + \delta_{3b} + \delta_{4b} + \delta_{5b}$$
$$= 0.034\left(\frac{1-\upsilon_b^2}{E_b}\right) + 1.08\left(\frac{1+\upsilon_b}{E_b}\right) + 0.229\left(\frac{1-\upsilon_b^2}{E_b}\right) + 1.18\left(\frac{1-\upsilon_b^2}{E_b}\right) + 0.056\left(1-\upsilon_b\right)\frac{d_p}{E_b p} \quad (4.16)$$

and for the nut,

$$\delta_n = \delta_{1n} + \delta_{2n} + \delta_{3n} + \delta_{4n} + \delta_{5n}$$
$$= 0.073\left(\frac{1-\upsilon_n^2}{E_n}\right) + 1.15\left(\frac{1-\upsilon_b}{E_n}\right) + 0.294\left(\frac{1-\upsilon_n^2}{E_n}\right) + 1.14\left(\frac{1-\upsilon_n^2}{E_n}\right) + 0.056\left(\frac{d_n^2+d_p^2}{d_n^2-d_p^2} + \upsilon_n\right)\frac{d_p}{E_n p}$$

(4.17)

where υ and E are the Poisson's ratio and Young's modulus, p is the pitch, and d_p and d_n are the pitch diameter of the bolt and the outer diameter of the nut, respectively (Zhang, Gao & Xu, 2016).

4.3.3.3 Stiffness of Clamped Members

The same study (Rousseau, Bouzid & Zhao, 2021) also proposed a more accurate method to calculate the stiffness of clamped members km for bolts of different sizes based on the bolthead bearing contact width instead of joint hole diameter previously used by many studies. The stiffness of the clamped members is expressed as follows:

$$k_m = \left[2.0726\left(\frac{w}{L}\right) + 0.6134\right]E_m d_h \quad (4.18)$$

Here, w and d_h are bearing contact width and hole diameter, respectively.

4.3.4 Angle of Nut Rotation

Assuming no plastic deformation, the angle of rotation of the nut with respect to the bolt to generate a force is given by

$$\theta = \frac{2F_b\pi}{pk_j} + \frac{F_b\left(\frac{p}{2\pi} + \frac{\mu_t r_t}{\cos\beta}\right)}{G_b J_b / L_{eq}} \quad (4.19)$$

where $G_b = E_b/2(1+\upsilon_b)$ is the shear modulus and $J_b = \pi d^4/32$ is the polar moment of area of bolt. The first term of equation (19) refers to the nut rotation due to the axial displacement

of all the joint components, whereas the second term corresponds to the nut rotation caused by the twisting of the bolt shank as a result of the applied external torque.

4.3.5 Nut Factor

The nut factor is an experimentally derived constant that links the external applied torque T_e to the resulting preload F_b. The equation is given by

$$T_e = F_b K d \tag{4.20}$$

The dimensionless nut factor K accounts for factors influencing the generation of the load, including the stiffness of the joint as a result of torsion, bending, and material deformation of all components, but mostly the effect of friction between them. However, for a specific lubricant, it must be determined experimentally, although it may not be a single number. In addition, the preload corresponding to an input torque can only be predicted within a range. Also, the nut factors evaluated in laboratory conditions often show noticeable differences from those existing in real practice; this assessment encompasses various factors including operator proficiency, tool precision, bolting techniques, as well as lubrication and thread conditions (Bickford, 1995).

Therefore, most of the lubricant manufacturers and research laboratories do not use the nut factor but rather rely on test results based on the coefficient of friction in general. It can be calculated using the tightening external torque T_e of equations (4.2) and (4.20) such that

$$K = \frac{T_b + T_t + T_p}{F_b d} \tag{4.21}$$

The pitch, bearing, and thread friction torques T_p, T_b, and T_t are given by equations (4.5), (4.11), and (4.12). From equations (4.1) and (4.20), an expression of the nut factor can be found in terms of the coefficient of friction as follows:

$$K = \frac{\dfrac{p}{2\pi} + \dfrac{\mu_t r_t}{\cos\beta} + \mu_b r_b}{d} \tag{4.22}$$

4.4 Finite element model

Figure 4.4 represents the schematic of the entire bolted joint with its various components, which consists of a M12 × 1.75 hex bolt, a nut, and two clamped members, each with an equal thickness of 10 mm in this case. The thread dimensions of the bolt and nut used in this analysis are based on the British Standard ISO Metric Screw Threads (BS 3643: Part 2, 1981). ANSYS workbench (ANSYS, 2019) is used to develop the complex 3D model with hexagonal geometries of a bolt and nut, including threads (see Figure 4.5). The mechanical properties of the bolt, nut and clamped members are listed in Table 4.1. All the dimensions are based on the standard, including the single-side contact interface between the mating threads to enhance the model's relevance to practicality. Since this study aims at investigating and determining accurate values of the torque components at contact surfaces to ensure proper joint-clamping force and a very small change in the friction coefficient values significantly amplifies these parameters, it is necessary to consider such 3D complex geometry into modeling even though the entire process is computationally expensive and time-consuming. To resolve this issue, a high-performance computer (HPC) is used for running the model.

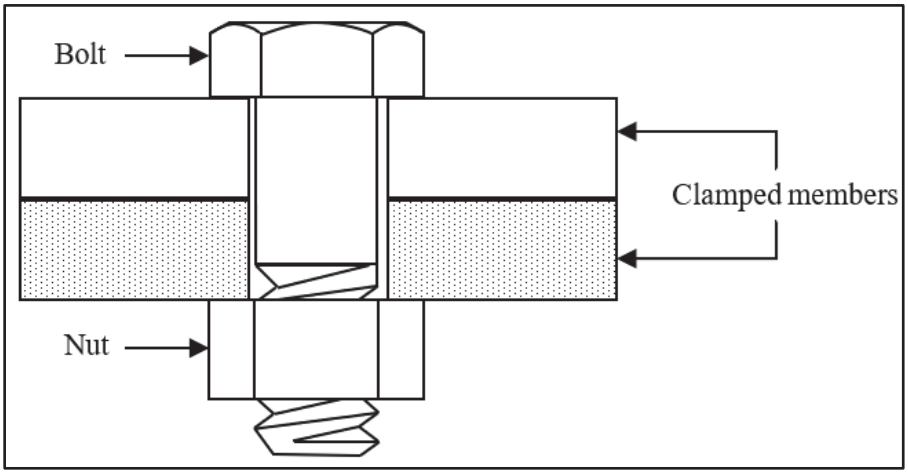

Figure 4.4 Schematic of a bolted joint with its components

4.4.1 Constraints

To prevent spatial displacement of the model, singularity, and rigid body motion, horizontal displacement constraints are applied to two diametrically opposed symmetrical points of the upper and lower plates while allowing axial displacement of the bolt, as shown in Figure 4.5a. The preload is generated in the bolt by application of an external rotation to the nut, while the bolt is fixed in rotation and other degrees of freedom of the nut are restrained. Target and contact elements are used between the clamped members, between the bolt head and the upper clamped member, and between the nut and the lower clamped member. The bolt friction coefficient is set to 0.12, a commonly used value for metal-to-metal contact surfaces of the bolt.

The FE methodology involves tightening of the joint by applying torque T_e to induce the required amount of bolt force F_b and then untightening the joint with reverse torque to bring the clamping force down while recording the levels of the different torque components. Therefore, the joint is first tightened gradually in steps to achieve a clamping force of around 41 kN with a torque of 81 kN/mm. Since the model has a threaded bolt and nut, the preload is achieved by applying a proper amount of rotation to the nut as shown in Figure 4.5b. The next step is to untighten the bolt by applying a rotation to the nut in the opposite direction to loosen the joint to 25 kN. The torque required for the untightening is lower than the tightening torque as the thread pitch torque component T_p acts in the loosening direction (Eccles, 2014).

The model uses a structured hexahedral mesh, which offers advantages not only in reducing CPU time but also in extracting data. Especially the nut bearing and the engaged thread contact surfaces are the important contact regions where sufficient mesh refinements are performed by continuous increment of the number of elements until 1% convergence on the thread contact pressure is obtained in the engaged thread and nut and underhead bearing contact surfaces. The final model consists of 1,72,720 elements in total.

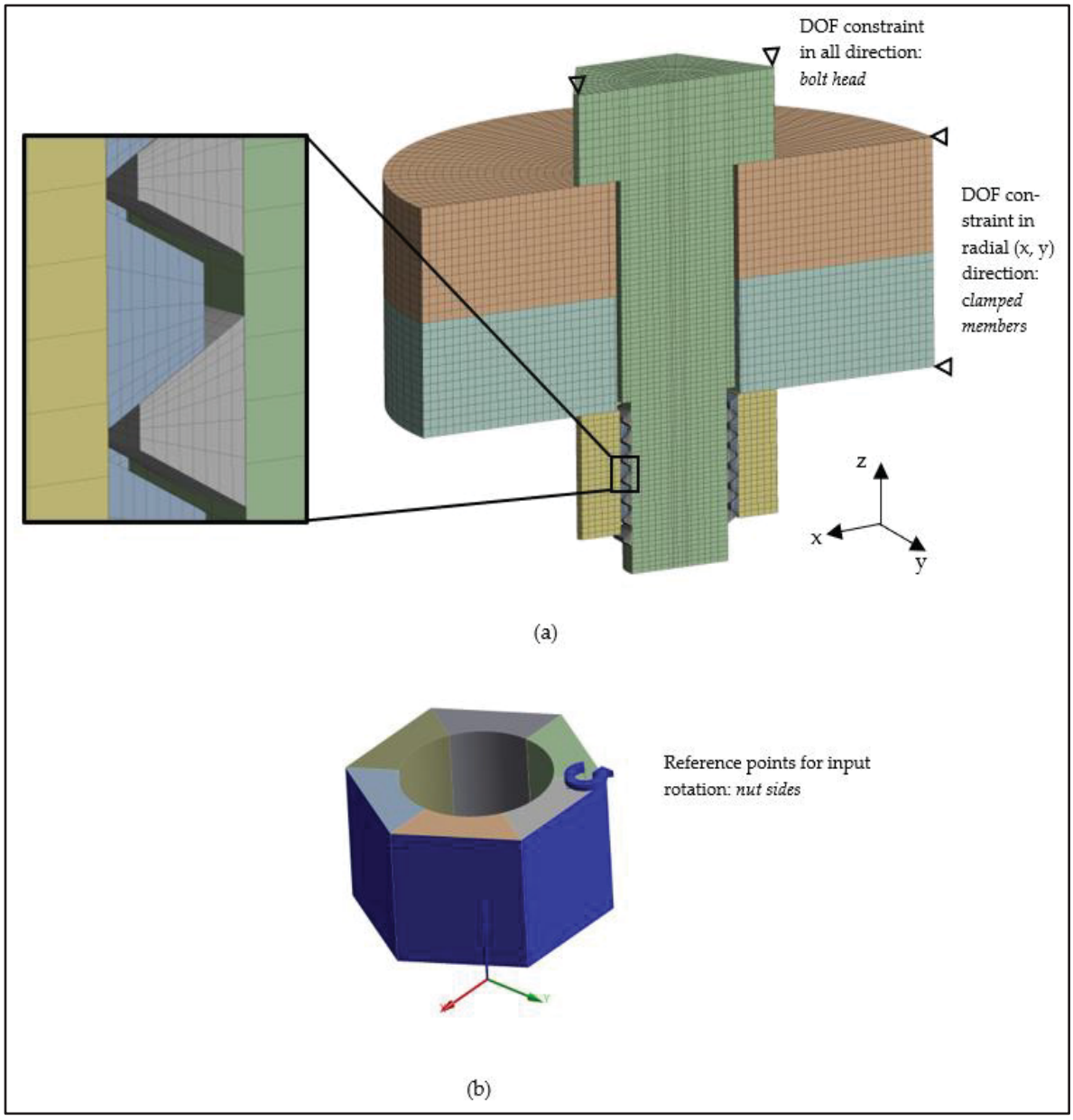

Figure 4.5 Three-dimensional FE model of bolted joint showing engaged thread elements: (a) complete model with constraints and thread mesh details; (b) nut rotation

Table 4.1 Mechanical properties of SA-193 B7 bolt and nut, and SA-285 Gr C clamped members
Taken from ASME Boiler and Pressure Vessel Code (2024; 2017)

Material Properties	Bolt and Nut (SA-193 B7)	Clamped Member (SA-285 Gr C)
Ultimate tensile strength [MPa]	860	450
Yield strength [MPa]	720	205
Young's Modulus [GPa]	206.8	206.8
Poisson's ratio	0.3	0.3

4.5 Results and discussion

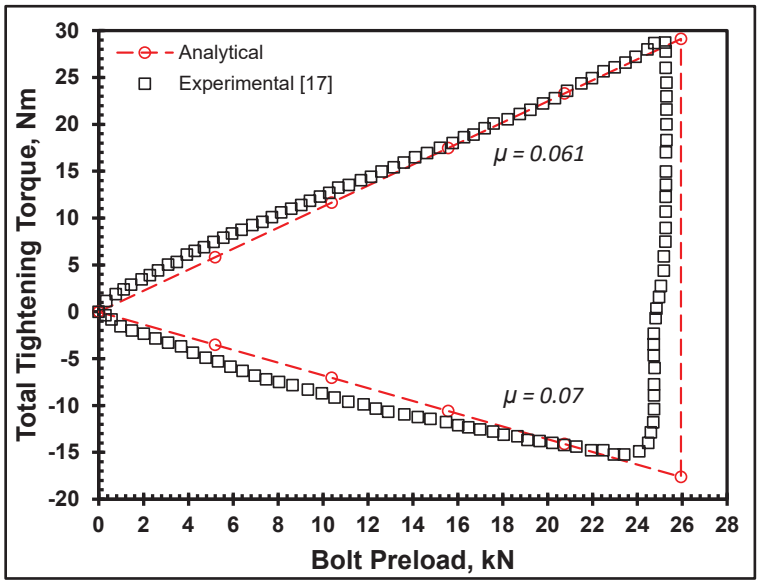

Figure 4.6 Comparison of analytical and experimental results of Eccles (2014) showing tightening and untightening stages

Figure 4.6 shows the comparison between the result from the analytical model described earlier and the experimental result of Eccles (2014) from the tests conducted on M12 standard hex bolts and nuts with low coefficients of friction of 0.061 and 0.07, respectively, during tightening and untightening. The analytical model curves for the tightening and untightening of the joint match well the experimental data. It is to be noted that the un-tightening of the joint

requires a lesser amount of torque compared to that of the tightening. According to the result, the developed analytical model can replicate accurately the actual cycle of the tightening and untightening of any size bolt used with any lubricant.

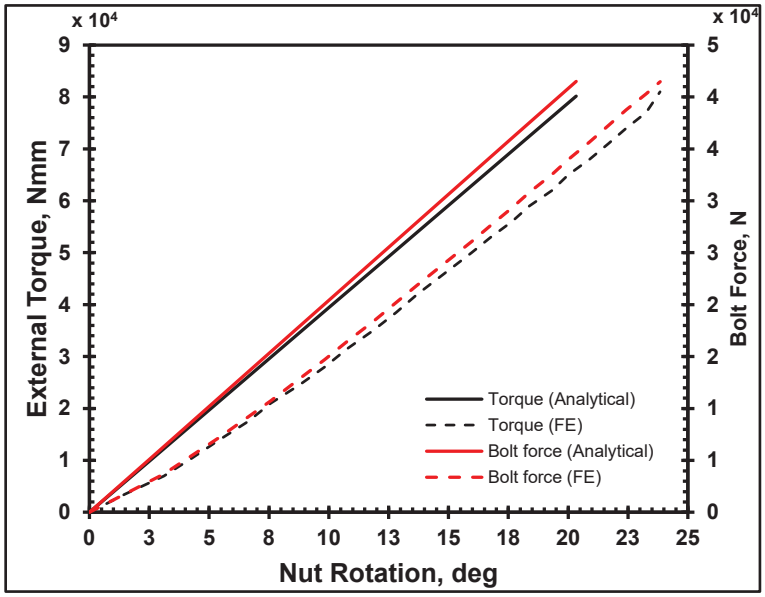

Figure 4.7 Torque and bolt force with respect to nut rotation for analytical and FE tightening cycles

A correlation between the torque and the required angle of rotation of the nut to achieve the bolt force is presented in Figure 4.7, where both the analytical and FE model results are compared with the same coefficient of friction for the bolt and threads, $\mu = \mu_b = \mu_t = 0.12$. The external torques required in both models are in close agreement with each other.

A slight nonlinearity is observed with the FE results of external torque as a function of nut rotation in the beginning because initially the contact surface of the threads under the nut and head is partial; thus, the load is not evenly distributed, making the joint less rigid. The remaining matting surfaces get in contact with further nut rotation. When the settlement of the bearing surfaces is completed, after around 3°, the curve becomes linear. As a result, a slightly higher nut rotation is observed with FEM in the beginning of the tightening as compared to the analytical results to achieve the desired amount of torque and bolt force.

Since both the analytical and FE models show reasonable agreement in reproducing the tightening and untightening processes for a particular friction coefficient so far, it is better to investigate other friction conditions, including no friction as well. Figure 4.8 gives an overall picture of both the tightening and untightening torques for different friction coefficients for the M12 hex bolt. A comparison among the results of FE, the analytical model, and the Motosh model (equation (4.1)) shows perfect agreement for all friction conditions. Since the Motosh equation is a simplified version for torque evaluation and is limited to only tightening loads and single bolted joints concentric with the bolt axis (Bickford, 1995), the current model can be considered an improvement without such limitations.

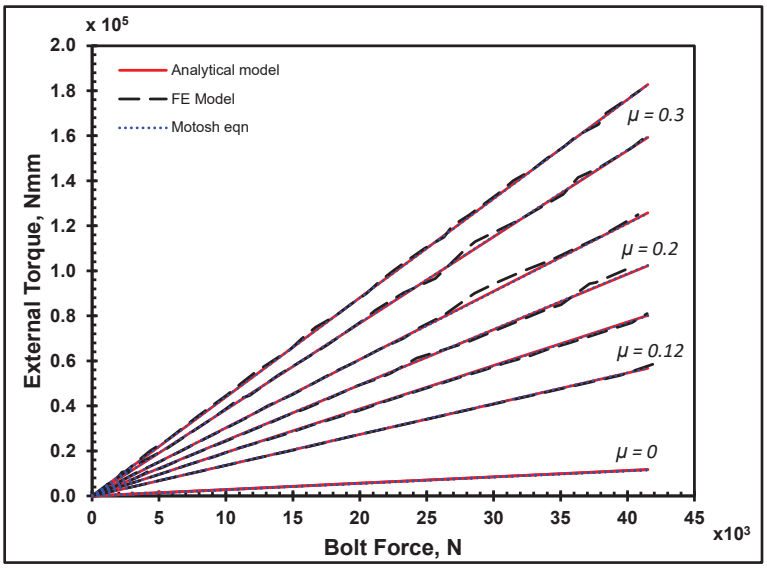

Figure 4.8 Torque and bolt force in M12 × 1.75 bolt for different friction coefficients

As the analytical model shows good agreement with FE results and the Motosh model for the M12 bolt so far, a bigger-sized bolt such as the M36 × 4 hex bolt is also tested and compared between the analytical and Motosh models. Figure 4.9 shows that the current analytical model is diverse enough to encompass wide ranges of bolt sizes and coefficients of friction.

Figure 4.10 presents the relationship between the coefficient of friction and the corresponding nut factor with different methods and bolt sizes. According to Bickford, the nut factor K is approximately 0.04 greater than the corresponding coefficient of friction. As can be seen in the

figure, the curves of the analytical and Motosh models are superimposed to fit in a line and agree well with Bickford's assumption, the expression of which is as follows:

$$K = 1.16\mu + 0.02 \tag{4.23}$$

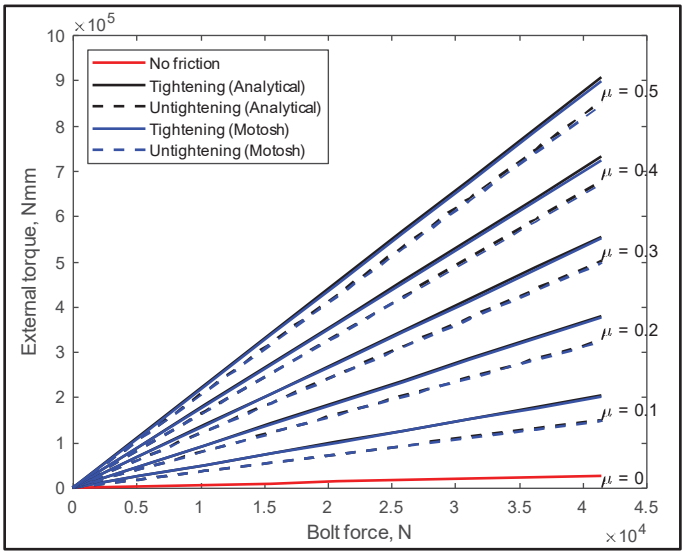

Figure 4.9 Comparison of analytical and Motosh models with torque and bolt force in M36 × 4 bolt for different friction coefficients

To find the amounts of various torque components (T_b, T_t, and T_p) during both the tightening and subsequent untightening sequences resulting from the external torques (T_e), a detailed comparison of the analytical and FE model results for a particular coefficient of friction is presented in Figure 4.11. The results are quite satisfactory, as both agree very well. In particular, the amounts of torque components when the joint is at rest can be known when the input tightening torque is removed after achieving the desired bolt force. Table 4.2 shows the percentage difference of the different torque components between the analytical and FE models.

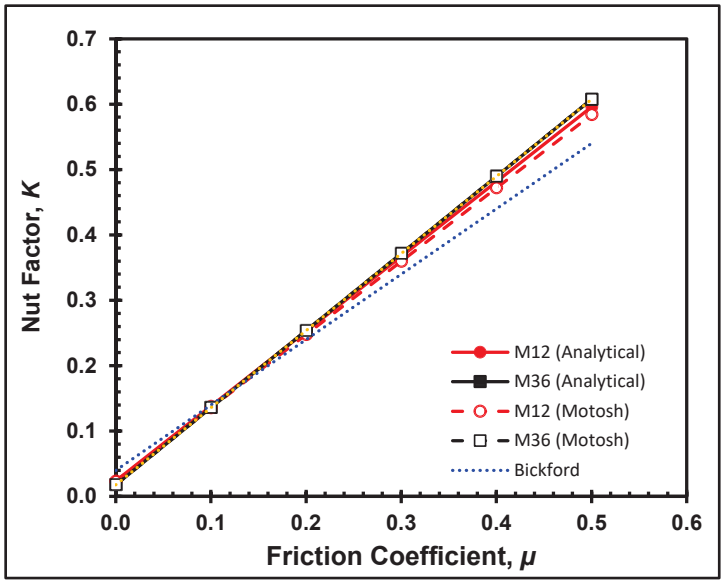

Figure 4.10 Comparison of nut factor as a function of friction coefficient

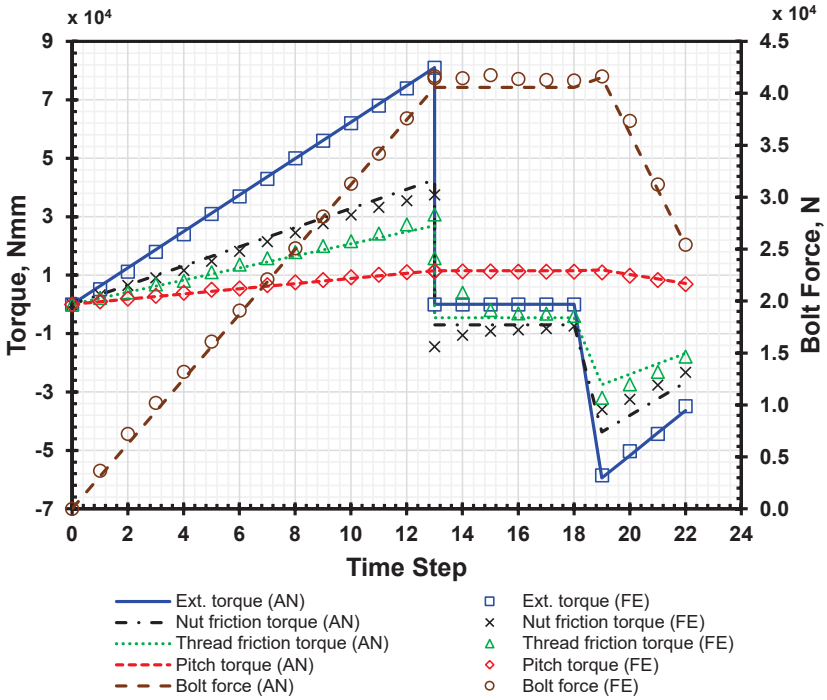

Figure 4.11 Analytical and FE results of torque components during tightening and untightening

Table 4.2 Comparison of various torque components after tightening and untightening

	Tightening			Untightening		
Torques	Analytical	FE	Percentage Difference (%)	Analytical	FE	Percentage Difference (%)
T_e	81,083	81,000		59,474	58,487	
T_b	42,702	37,476	12.2	43,705	36,009	17.6
T_t	26,894	30,813	-12.7	27,526	31,968	-13.8
T_p	11,487	11,344	1.2	11,757	10,902	7.2

4.6 Conclusions

The phenomenon of loosening of a bolted joint is complex in nature, especially when it comes to investigating critical parameters like individual torque components between the tightening and untightening sequences. This study introduces a comprehensive FE method to quantitatively assess the individual contribution and impact of the bearing friction, thread friction, and pitch torque components in a bolted joint. Also, it shows their fluctuations during the tightening and untightening sequences under static conditions. An analytical model is developed for the evaluation of the three torque components and compared with experimental data obtained from the literature (Eccles, 2014), which was conducted on the M12 bolted joint during the tightening and untightening sequences. The validated analytical model is also tested against the FE modeling, and the results are compared well. A direct correlation between the angle of nut rotation to achieve the desired clamping force and the resultant input tightening torque shows logical agreement between them, which has a major role in the joint stiffness. Both models agree very well with the change in the coefficient of friction during the tightening and untightening of the bolted joint. Finally, the torque components are quantitatively measured and compared during tightening and untightening, including at the condition of rest. Given the versatility of the current approach, this study can serve as a valuable reference for future studies that examine the variations in torque components of joints subjected to repeated

tightening and untightening over time, considering factors such as adhesion due to material corrosion and thread plastic deformations, relaxation, vibration, and self-loosening.

CHAPTER 5

EFFECT OF CLAMPED MEMBER MATERIAL AND THICKNESS ON SELF-LOOSENING OF BOLTED JOINTS

Rashique Iftekhar Rousseau [a] and Abdel-Hakim Bouzid [b]

[a] Department of Mechanical Engineering, École de technologie supérieure,
1100 Notre-Dame St. West, Montreal, Quebec, H3C 1K3
[b] ASME Fellow, Department of Mechanical Engineering, École de technologie supérieure,
1100 Notre-Dame St. West, Montreal, Quebec, H3C 1K3

Paper submitted for publication, November 2024

5.1 Abstract

Bolted joints, prevalent in industrial applications for component fastening, are susceptible to self-loosening - a critical issue resulting in a gradual reduction of clamping force. This research investigates how the stiffness of components influences self-loosening in bolted joints subjected to transverse loading. By altering the material and thickness of the clamped members, this study examines stiffness effect on self-loosening. An experimental setup emulating real-world conditions is devised to simulate loosening due to cyclic lateral displacement. Testing involves steel and High-Density Polyethylene (HDPE) clamped members of different grip lengths to assess the impact of stiffness on the self-loosening of the bolted joint. Parameters for measurement and analysis include bolt axial load, transverse force on clamped members, relative displacement, and rotation between the bolt and nut. Self-loosening manifests in two distinct stages: stage-I involves early loosening due to material plastic deformation at the asperities level, while stage-II results from relative rotation between the bolt and nut. This investigation offers valuable insights into self-loosening by testing diverse clamped member materials and grip length combinations, enabling comparison of material and stiffness effects. Furthermore, it facilitates a comprehensive understanding of

stage-II loosening, as each test concludes with complete preload drop, revealing diverse patterns of loosening phenomena for comparative analysis.

5.2 Introduction

Despite being widely popular for the use of fastening in most industries due to their ease of installation and removal techniques, bolted joints are likely to be subjected to self-loosening, a major problem that is defined as a gradual decrease of their clamping force. Self-loosening occurs in a clamped joint under various types of loadings, and in particular transverse, vibration, and shock loadings. A tiny imbalance in rotating machines or the influence of dynamic forces in static structures can cause vibrations, by which the contact stress in the engaged threads and in other contact surfaces of the joint components are unbalanced creating a misalignment between the bolt and nut causing untightening during sliding of the latter with the adjacent clamped member. Consequently, rotational self-loosening occurs due this mechanism causing the joint to loosen. Therefore, the joint must have a minimum amount of preload to ensure enough clamping force and structural integrity (Bickford, 1995). However, excess amount of preload can cause plastic deformation and hence notable reduction in joint integrity (Jiang et al., 2004). There are methods proposed as solutions to prevent the occurrence of self-loosening, such as adding nylock nut, aerotight nut, chemical lock, cheveloc nut or flash washer etc. (Bhattacharya, Sen & Das, 2010). Nonetheless, no conclusive and reliable solution has been brought into being due to the lack of control over loosening phenomenon and the intricate nature of the behavior of bolted joint when subjected to transverse loadings. There are basically two separate stages of loosening. The first one refers to early-stage loosening (stage-I) due to cyclic plastic material deformation happening at the contact surface of the engaged threads and other contact interfaces, which results in the reduction of the clamping force because of stress redistribution as the cycle advances (Jiang, Zhang & Lee, 2003). No relative rotation between the bolt and nut happens in this stage. The subsequent stage of loosening (stage-II), namely self-loosening, is due to the gradual rotation of the bolt relative to the nut, although the background mechanism is still unclear as various effects can contribute to its occurrence (Finkelston, 1972). For example, the loss of initial

preload reduces the friction forces in the contact surfaces to a critical level under which the backing-off of the nut becomes obvious. The duration of the external forces also matters as short intervals intensify the frequency of the excitation force. Even, tiny change in the lead angle of threads can enhance quick loosening, which makes coarse-pitch threaded joints more prone to loosening due to the higher internal loosening torque compared to fine-pitch threaded joints. Higher preload in the joint results in greater friction forces in the contact surfaces that increases the corresponding normal forces, thus governs the amount of maximum friction forces. Overall, the factors controlling the backing-off of the nut during the self-loosening stage remain ambiguous. During the transition from stage-I to stage-II, a combination of material plastic deformation and backing-off of the nut may be involved in the loosening process. Jiang et al., (2004) experimentally showed the demarcation between these two stages by defining a rotation of 0.5 degree between bolt and nut, although this precise distinction between both stages is difficult to identify in practical applications.

Daadbin & Chow (1972) demonstrate the effects of the parameters mentioned above, namely initial preload, applied load duration, contact surface frictions and thread lead angles on self-loosening of a joint subjected to impact loadings and their combinations that define the loosening intensity. Junker (1969) first discovered by experiment that self-loosening is more obvious when a joint experiences vibration loading perpendicular to the bolt axis namely transverse loading, compared to axial loading. This brought the idea of transverse slip on the bolt head bearing contact surface to be the initiation of loosening. On the contrary, the idea of the occurrence of localized thread slip to initiate slight loosening before the bolt head slip came up by Pai & Hess (2002; 2002) with their experimental and three-dimensional finite element (FE) analysis. A study close to the earlier ones mentioned was carried out by Izumi et al. (2005) where theoretical and numerical aspects were explored to investigate both tightening and loosening processes of threaded joints. Their investigation included three-dimensional FE modeling and classical theory of solid mechanics. The self-loosening phenomenon in an actual bolted joint and the application of preload considering the interactions of joint components are investigated by Dinger & Friedrich (2011), which pointed out the system parameters and the external load profile being responsible to affect localized contact state.

A lot of experimental and analytical studies have been conducted on self-loosening investigating different joint parameters and their effects. For example, Nassar & Housari (2007) investigated the effect of joint hole clearance and fits between bolt-nut engaged threads on loosening of a joint subjected to cyclic lateral loading. Zaki, Nassar & Yang (2010a; 2010b) performed a couple of experimental studies to demonstrate how the friction coefficients on the bolt bearing and thread contact surfaces, and the conical angle and thread pitch (Zaki, Nassar & Yang, 2012) affect the loosening of a preload countersunk bolt when subjected to similar cyclic lateral loading. Later, they developed an analytical model and compared the results with that of earlier experiment results from the same test setup (Zaki, Nassar & Yang, 2011). Yang, Nassar & Wu (2010) showed analytically and experimentally the effect of increased Young's modulus and decreased grip length which increase self-loosening and both situations need greater amount of preload. In another analytical study, they showed the importance of decreasing the hole clearance and increasing thread fits to reduce the transverse amplitude, thus preventing loosening (Yang & Nassar, 2011b).

Research also showed noticeable impact of the materials of joint component on loosening. Shahin, Barsoum & Korkees (2021) studied the impact of temperature on the performance of High-Density Polyethylene (HDPE) flanged joint supported by steel backing rings using FE analysis and discovered noticeable stress relaxation of the material. Much of the bolt stress relaxation takes place within the first 1200 hours, which is also observed earlier both numerically and experimentally by Jacobsson, Andersson & Vennetti (2011a; 2011b). By experimentally determining the time-and-temperature dependent mechanical properties of HDPE under isothermal conditions over a one-year service period, they found significant dependence of flanged joints on temperature as leakage takes place initially with the temperature increase and thus recommended at least one re-torquing of bolts within the service period. A thermo-mechanical nonlinear FE analysis including heat transfer and structural modeling is performed by Barsoum, Barsoum & Islam (2019) to investigate the integrity and performance of a manhole structure of 78-inch HDPE stub-end, steel ring and blind flange used with a CNAF (Compressed Non-Asbestos Fibre) gasket. They found that factors like stud-bolt pretorque level, internal pressure and outer temperature strongly influence the manhole

integrity and performance.

In this study, the self-loosening of a bolted joint subjected to transverse loading is observed by analyzing the impact of components stiffness. Investigated parameters are the material and thickness of the clamped members, which affects the stiffness of the individual joint components as well as that of the overall joint, and thus impacts the loosening behavior. An experimental setup is designed to replicate the loosening phenomenon due to cyclic transverse loading. The test program includes an investigation of the material effects of the clamped members namely steel and HDPE, and different grip lengths. The idea is to provide an enhanced understanding of stage-II loosening by measuring parameters such as transverse load and displacement amplitude, nut rotation, bolt force and number of cycles, which helps demonstrate the diverse pattern of the self-loosening and understand its mechanism.

5.3 Experimental setup

Figure 5.1a shows the experimental text rig with its major components developed in the Static and Dynamic Sealing Laboratory that can replicate the self-loosening phenomenon of a bolted joint under cyclic transverse loading. It consists of two clamped members of equal thickness with two different materials HDPE and steel (see Figure 5.2b) tightened with a bolt, a nut and two washers.

The instrumented joint system is mounted on an existing fatigue test machine that consists of a holding structure, electrical motor, adjustable crank system, basic control panel, grips and universal joint, actuator lever and an adjustable frame. The clamped members having three different thicknesses of 10, 12 and 14 mm are considered in this study, which have holes of 13.6 mm diameter to accommodate and fasten an M12×1.75 mm hex bolt and a nut. Therefore, the setup can accommodate bolted joints with different effective lengths of 25, 29 and 33 mm including two washers of 2.4 mm thickness each on both sides of the clamped members. To measure the bolt preload, a 1.5 mm diameter strain gauge of bolt type is installed permanently inside the bolt to avoid adding a load cell that can alter the grip length and joint stiffness. Since

the relative rotation between the bolt and the nut is important for the evaluation of stage-II loosening, a rotary variable differential transformer (RVDT) is installed on the nut with three M3 screws and attached to the bolt end through a tongue and groove system.

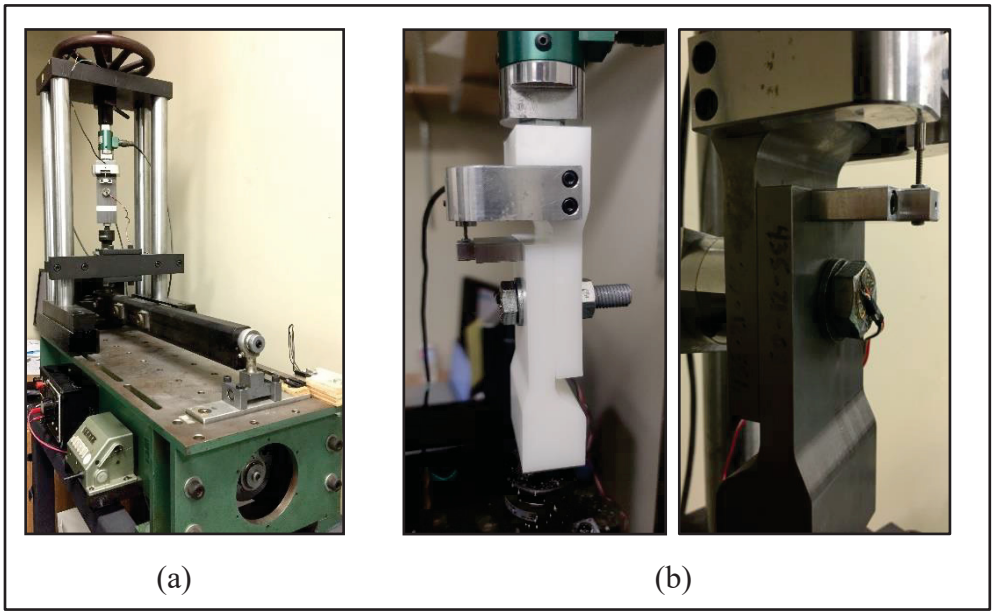

Figure 5.1 (a) Experimental test rig; (b) bolted joint with M12 hex bolt, nut, washers, and a pair of HDPE (left) and steel (right) clamped members of equal thickness

A force transducer (GSE load cell 5410-8k) is connected to one of the clamped members to measure the lateral force while a displacement transducer is used to measure the amplitude of the transverse movement. The moving clamped member is connected to an actuator by means of a universal ball joint, which is operated by a crank drive mechanism. Therefore, the actuator converts the rotational movement of the motor shaft to a reciprocal lateral movement, giving the desired transverse displacement. A spring-loaded flexible plate system installed between the joint specimen and actuator lever helps controlling the loading. The displacement provided to the actuator through the crack drive mechanism is not entirely reflected on the clamped member end and a measurement of the relative displacement between the members is required. Therefore, a linear variable differential transformer (LVDT) is installed on the moving member close to the bolt to precisely measure the relative displacement. To count the number of loading cycles of the transverse displacement as well as to stop the test automatically, a magnetic pulse count sensor is installed at the junction of the actuator lever and connecting crank rod. A data

acquisition and control system unit from National Instrument is connected to the test bench by means of a computer and programmed with the LabView software to directly monitor and record the data.

The mechanical properties of the bolt and clamped members made from steel and HDPE are given in Table 5.1. Table 5.2 provides some experimental test data conducted on both steel and HDPE joints with different preloads and amplitudes of lateral displacements.

Table 5.1 Mechanical properties of bolt (SA-193 B7) and clamped members of steel (SA-285 Gr C) and HDPE

	Bolt	Clamped member	
		Steel	HDPE
Ultimate tensile strength (MPa)	860	450	30
Yield strength (MPa)	720	165	21.9
Young's modulus (GPa)	206.8	206.8	0.995
Poisson's ratio	0.3	0.3	0.45

Table 5.2 Experimental test data for HDPE and steel joints with different preloads and initial amplitudes of lateral displacement

Material	Thickness (mm)	Preload (kN)	Amplitude (mm)
Steel	10	10	0.05
	12	10	0.05
	14	10	0.04
HDPE	10	4	0.5
	12	4	0.49
	14	4	0.38

5.4 Results and discussion

5.4.1 Effect of joint stiffness

To observe the influence of stiffness, both joints with HDPE and steel clamped members of different thickness are subjected to tests under transverse loading cycles. For steel clamped members, two single row flat roller bearings (INA-HYDREL Flat Cage Assemblies FE series) are added between the clamped members to reduce friction between the contact faces in case of higher amount of initial preload (see Figure 5.2a). A 3D printed hard plastic housing is used to properly accommodate the bearings by which the rollers can be placed between the members without titling when the components are clamped and tightened together (see Figure 5.2b). Therefore, higher preload of 10 kN and over can be applied for tests with different thickness.

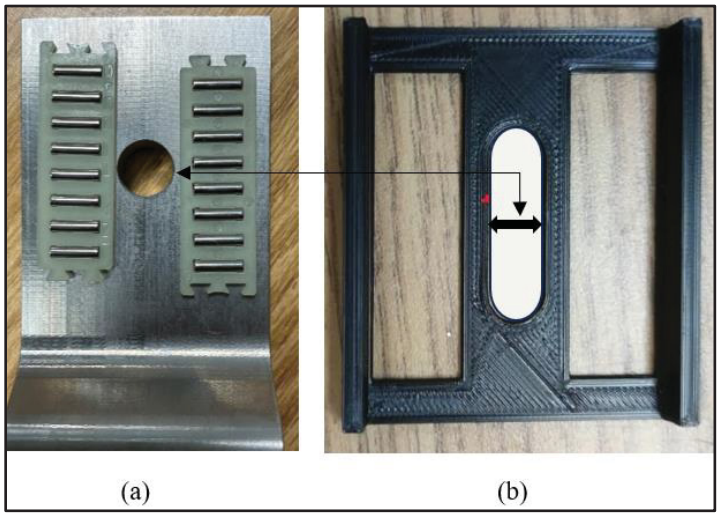

Figure 5.2 (a) Two roller bearings on the clamped member; (b) 3D printed hard plastic housing to accommodate the bearings and the bolt through the hole

5.4.1.1 Effect of the thickness of the clamped members

A series of experiments are conducted to examine how the thickness of the clamped members influences the self-loosening behavior of bolted joints. Figure 5.3 illustrates the loosening behavior by displaying the change in preload drop and relative rotation between the bolt and nut for the HDPE clamped members with thicknesses of 10, 12, and 14 mm as loading cycles

progress. In this case, the joint is tightened with a lower initial preload of 4 kN due to the use of HDPE clamped members. Stage-II self-loosening is more prominent in joints with thinner clamped members, showing a quicker preload drop as the number of load cycles increases. A similar pattern of stage-II loosening is evident, with an increased rate of rotation between the bolt and nut in joints with thinner clamped members. Both plots clearly show that stiffer joints, specifically those with thinner clamped members, tend to loosen more quickly. Thus, the thickness of the clamped member plays a crucial role in the loosening behavior of the joint, directly affecting its stability. The stiffness of bolted joints is a key design factor that must be considered to enhance their performance, reliability, and longevity.

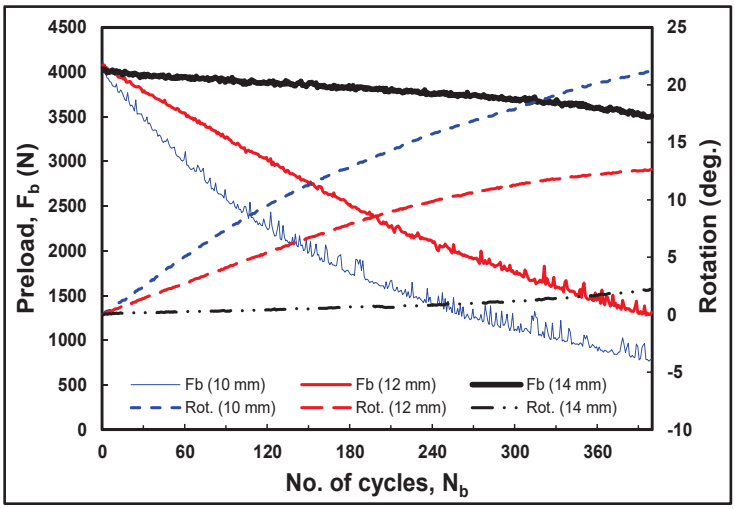

Figure 5.3 Loosening by preload drop and bolt-nut relative rotation for HDPE clamped members of different thickness

Figure 5.4 depicts the loosening behavior by showing the loss of preload when the joint is tightened with a higher preload of 10 kN for the same thickness range of the steel clamped members as in the case of HDPE. As previously observed, joints with thicker clamped members retain preload more effectively than those with thinner members. The relative rotation between the bolt and nut is greater in joints with thin clamped members, due to their higher stiffness.

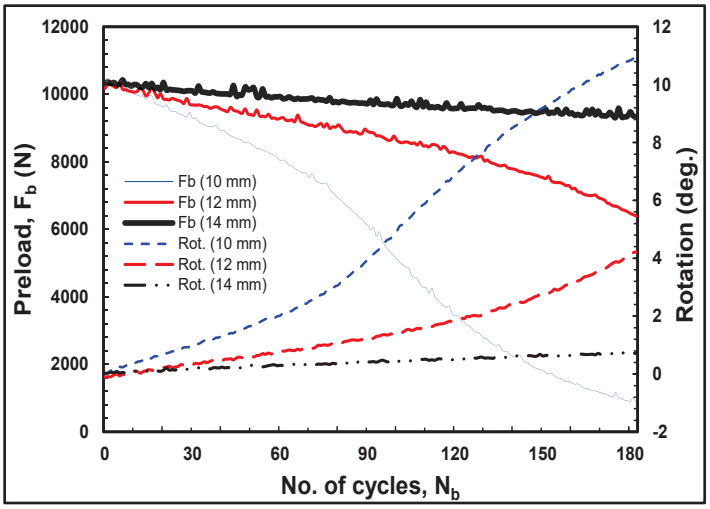

Figure 5.4 Loosening by preload drop and bolt-nut relative rotation for steel clamped members of different thickness

5.4.1.2 Effect of the material of clamped members

Self-loosening of bolted joints is highly dependent on the materials selected for the clamped members. A few identical sets of steel and HDPE clamped members are chosen for this analysis. To maintain the test conditions similar, the joints with steel clamped members do not include flat roller bearing as in earlier tests. Therefore, a lower preload of 3.5 kN is chosen to tighten both joints for the tests. Figure 5.5 shows the results of two tests conducted on bolted joints with clamped members of 10 mm thickness for both materials. Both bolted joints underwent 100 transverse displacement cycles with an amplitude of 0.2 mm. As shown in the figure, joint with steel members loses preload quickly, thus showing less capability of retaining preload leading to gradual loosening with the number of cycles. However, bolted joints with HDPE clamped members exhibit greater resistance to self-loosening by maintaining the initial tension more effectively throughout the entire test. The relative rotation between the bolt and the nut is higher for steel joints as compared to HDPE joints, allowing a faster occurrence of stage-II loosening comparatively. The results of Figure 5.5 clearly indicate that the joints with stiffer clamped members are more likely to undergo rapid loosening. This gives an insight as to the selection of the material when designing bolted joints for practical applications.

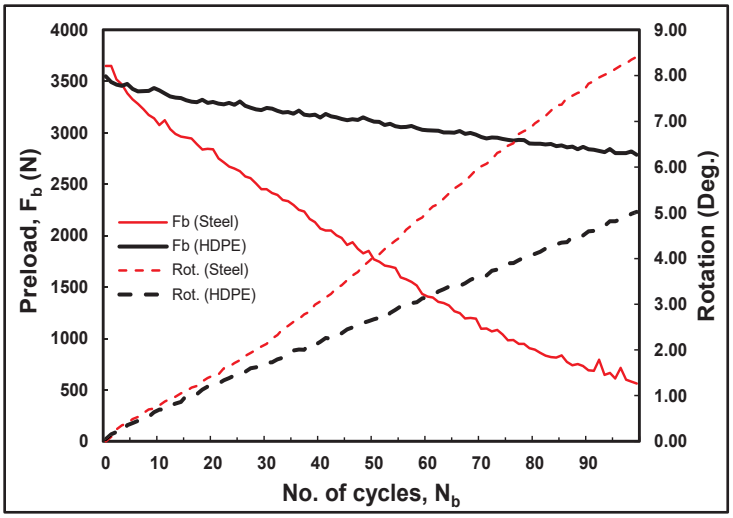

Figure 5.5 Preload drop and bolt-nut relative rotation with 10 mm HDPE and steel clamped members

Figure 5.6 shows self-loosening by the loss of initial preload of 4 kN at different stiffness points for joints with HDPE clamped members at 100th and 182nd loading cycle. The amplitudes of lateral displacement at the two selected cycles remain constant for each grip length. The consistent displacement levels indicate that HDPE joints have a stronger resistance to self-loosening.

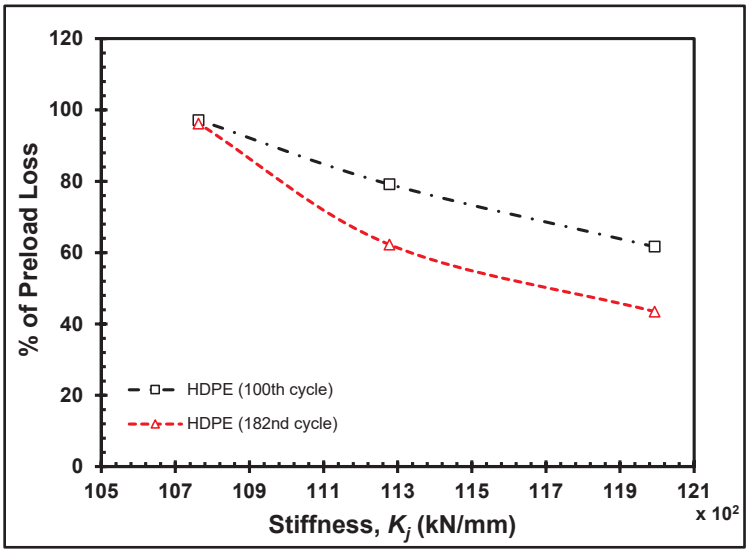

Figure 5.6 Self-loosening by preload loss at different stiffness points for HDPE joints

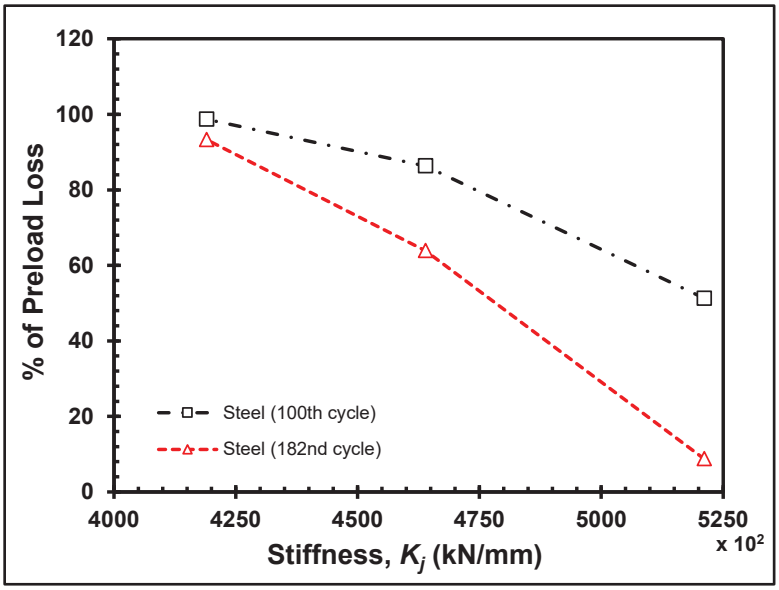

Figure 5.7 Self-loosening by preload loss at different stiffness points for steel joints

For steel joints with an initial preload of 10 kN, loss of preload is bigger with increased stiffness, i.e., decreased grip length at selected loading cycles, as shown in Figure 5.7.

Overall, both materials maintain better bolt preload at lower stiffness values, while loosening becomes more pronounced as stiffness increases. The self-loosening behavior of joints with HDPE and steel clamped members is challenging to compare directly due to differing lateral movement amplitudes at the beginning and throughout loading cycles. However, joints with steel clamped members are noticeably more rigid and experience preload loss more frequently than HDPE joints. Although preload drop occurs in both joints, steel joints exhibit a slightly higher rate of preload loss resulting in self-loosening, even with a lateral displacement amplitude that is ten times lower than that of HDPE, as shown in Table 5.2.

5.4.2 Effect of cycles on transverse force

Figure 5.8 illustrates the behavior over several loading cycles, highlighting the influence of transverse force on the joint as it undergoes self-loosening until the complete loss of preload. A similar pattern is observed across all loop shape curves within the selected ranges of loading cycles, each characterized by two oblique lines and two almost horizontal lines. The oblique

lines are increase of the lateral force from negative to positive with the displacement and represent the bending of the bolt due to transverse force of the clamped member, with no sliding between the contact surfaces. The horizontal part of the curve begins when the transverse force reaches a threshold equating the friction force during the loading cycle, allowing sliding at the contact surfaces between the bolt head or nut bearing surfaces and clamped members, thereby causing relative rotation between the bolt and nut.

Figure 5.9 shows a similar behavior trend of the transverse force with a bolted joint having 12 mm HDPE clamped members. Since the transverse force depends on the friction at all interacting contact surfaces, this force is to decrease with the cycles because the bolt force also decreases with the cycles. Nevertheless, the transverse force is shown greater for the 12 mm clamped members when compared to that for 10 mm because the load is relatively higher at the given cycles shown in Figures 5.8 and 5.9, for the same initial preload of 4 kN, and coefficient of friction (μ = 0.22) and a lateral displacement of 0.5 mm.

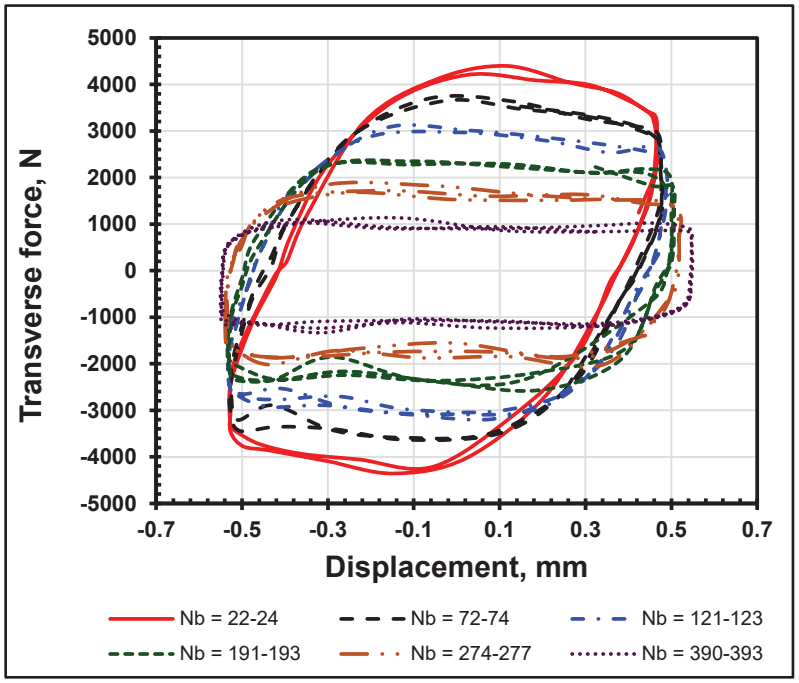

Figure 5.8 Effect of transverse force on 10 mm HDPE joint at different cycle range

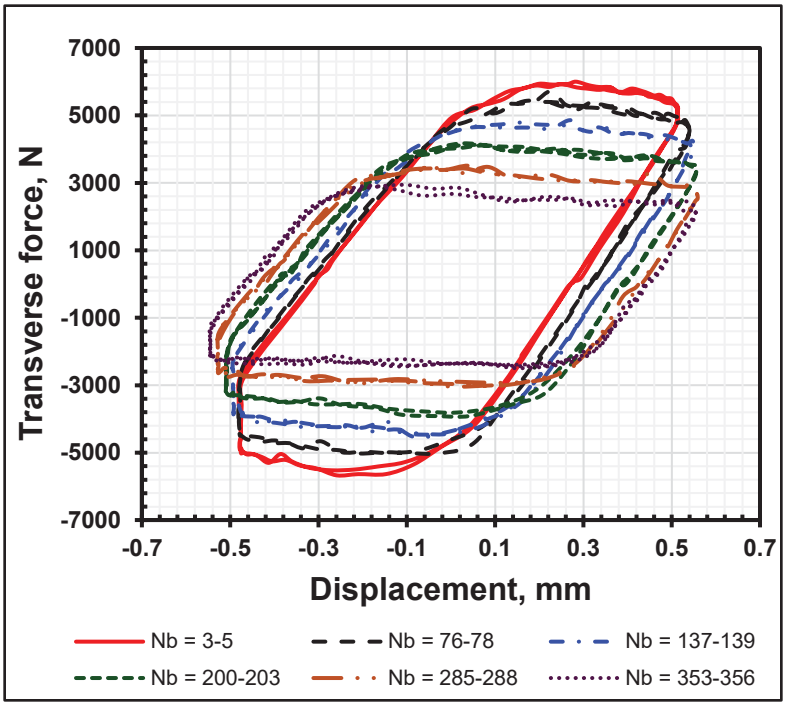

Figure 5.9 Transverse force on 12 mm HDPE joint at different cycle range

5.4.3 Effect of the amplitude of lateral displacement

Figure 5.10 illustrates the effect of varying the amplitude of lateral displacement on a joint of steel clamped members with the roller bearings. The initial preload is set at 10 kN. As in the previous section, the two distinct oblique lines are still present during the loading cycles. The slope of these lines represents bolt bending stiffness. However, the slope of the second part of the curve is small and is related to the sliding between the engaged thread contact surfaces causing the self-loosening by bolt-to-nut relative rotation.

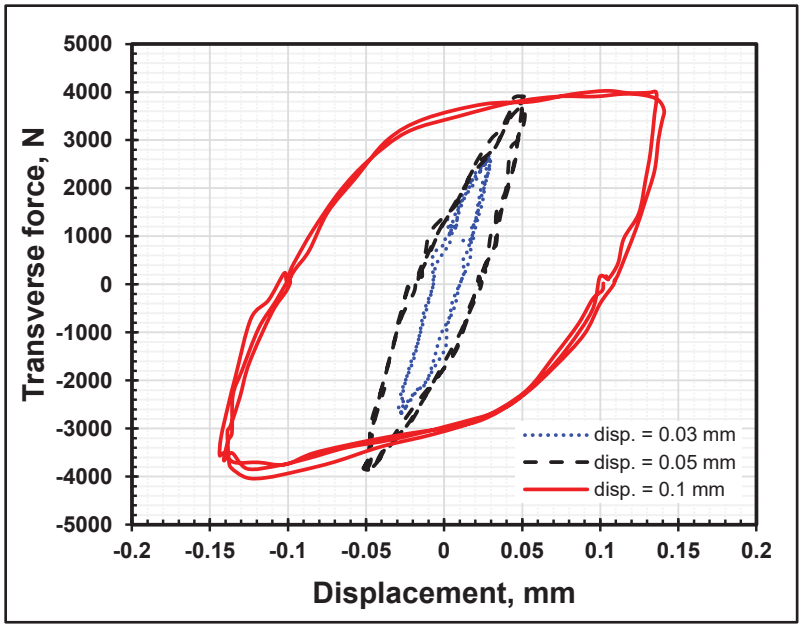

Figure 5.10 Effect of amplitude of lateral displacement on joints with steel clamped members

5.5 Conclusion

An experimental study is performed to show the influence of joint stiffness on the self-loosening of a bolted joint subjected to transverse loading. Effects of different parameters on loosening, such as the thickness and material of the clamped members, are studied. The impact of the amplitude of the lateral displacement and the transverse force are shown to have a big influence. Joints with thicker clamped members demonstrate better resistance to self-loosening because of their lower stiffness. The rotation of the nut relative to the bolt increases with the number of load cycles and amplitude. Also, HPDE joints retain better preload compared to steel joints. Transverse loading causes bending of the bolt until sliding at the bolt or nut bearing surfaces occur, after which self-loosening takes place by relative rotation.

CONCLUSION

Bolted joints are inherently complex, yet they are widely employed in most engineering and industrial applications. Self-loosening, particularly in joints subjected to vibration, shock, and dynamic loading, is a common issue. Despite the availability of various countermeasures and ongoing efforts, this problem remains a persistent challenge till today due to the complex forces acting on bolted joints, design trade-offs, and environmental variability. This study uncovers the key mechanisms responsible for self-loosening in bolted joints and investigates the role of various contributing factors. By identifying the underlying causes of self-loosening, the study provides valuable insights into how loading, friction, geometry, material properties, and environmental conditions interact to jeopardize the integrity of bolted joints. Understanding these dynamics enables engineers to make informed decisions when designing joints for critical applications. The project objectives are achieved through the following approaches:

- Developing an effective methodology to accurately evaluate the stiffness of bolted joints, with a focus on measuring the stiffness of the clamped members.
- Accurately analyzing the contributions of various torque components, such as bearing friction, thread friction, and pitch torque, in response to the applied external torque on the bolted joint.
- Investigating the occurrence of self-loosening in bolted joints under cyclic transverse loading by examining the effects of material, grip lengths, lateral displacement, and applied transverse force.

The first objective is the subject of the first paper that introduces a numerical finite element (FE) technique for accurately evaluating the stiffness of clamped members in bolted joints with different bearing bolt surfaces and grip lengths, addressing the overestimation issue present in previous methods. While most studies have relied on numerical approaches to estimate the member stiffness considering the same contact region between the bolt head and the clamped members, the selection of the contact nodes undergoing axial deformation has been arbitrary, ranging from the joint hole radius to either half of the bolt bearing contact width or beyond incorporating additional nodes. As a result, the stiffness of clamped members has largely been

estimated based on assumptions. This new method accurately evaluates member stiffness by focusing on the axial displacement of nodes that belong to the bolt mid length section using an axisymmetric FE model to obtain joint stiffness and then calculate back the member stiffness knowing the bolt stiffness. The method was applied to a wide range of bolt sizes (M6 to M36) and varying grip lengths. After validating the model with two different types of loading, the study proposes a unique relationship for calculating member stiffness, based on the bolt or nut bearing width in contact with the corresponding clamped member. All in all, the study clearly highlights the flaws in existing techniques that overestimate the stiffness of clamped members.

The second objective achieved in the paper presents an effective method to quantify the various torque components involved in a bolted joint. The developed model is used in conjunction with an external input torque to be tested for the two cases of tightening and untightening processes. Past studies assumed the consumption of applied input torque by the friction torques at various contact surfaces of a joint. Though the distributions of friction torque components between a loading cycle that involves tightening and untightening, and the contribution of pitch torque to enhance loosening have not been quantified. This study thoroughly examines the friction torques at the bearing and thread contact surfaces, as well as the pitch torque, throughout the full tightening and untightening cycle. The contributions are analyzed using a three-dimensional FE model of a threaded bolted joint and compared with an analytical model. The results, validated against a previous experimental study, show strong agreement. Also, a clear correlation between nut rotation angle and input tightening torque within a range of coefficients of friction demonstrates their consistent relationship to achieve required clamping force, which are significantly impacted by joint stiffness. This study can help engineers evaluate the right amount of tightening torque in bolted joints without compromising the efficiency, reliability and safety of bolted joint assemblies while providing optimal joint clamping force, improving load distribution, reducing fatigue and extending the lifespan of components.

The results related to the third objective are summarized in a third paper that examines the joint stiffness on self-loosening of a bolted joint subjected to repeated transverse loading. The influence of stiffness of joint components is investigated by analyzing the effects of different

parameters, such as material type (steel and High-Density Polyethylene-HDPE) and joint grip length (10, 12 and 14 mm). Additionally, the impact of lateral displacement on steel clamped joints and the effect of transverse force on HDPE joints of varying lengths are observed. A greater resistance to self-loosening is observed when the joints have thicker clamped members as they have lower stiffness. HDPE clamped members being lower in stiffness retain better initial preload in a joint compared to steel counterparts. Two distinct self-loosening phases are observed in clamped joints during selected loading cycles: first, initial bolt bending after sliding between clamped members but before sliding at the bolt and nut bearing contact surfaces until a critical transverse displacement is reached, followed by sliding at the thread contact surfaces. Self-loosening in HDPE joints of different thicknesses is also observed by analyzing the transverse force required for the same lateral movement.

RECOMMENDATIONS

In summary, the project effectively explores self-loosening in bolted joints by addressing key gaps from previous studies and investigating these issues using relevant, impactful methodologies through numerical, analytical, and experimental approaches. The following recommendations may guide future work in this field:

- This study can serve as a more reliable reference for measuring the stiffness of joint components by separately considering the stiffness of the threaded section of the bolt, especially in cases involving complex threaded fasteners, to enable more precise measurements.
- This study can be a useful reference for future investigations on torque variations in joints undergoing repeated tightening and untightening, accounting for factors like corrosion, thread deformation, relaxation, cyclic vibration, and self-loosening.
- The study provides valuable insights into the self-loosening behavior of bolted joints under repeated transverse loading for different clamped member materials (HDPE and steel) and various grip lengths, highlighting the influence of joint stiffness. Therefore, testing and analyzing additional industry-standard materials relevant to the application could further broaden the understanding of self-loosening and improve knowledge of the input conditions required for loosening resistance.
- The amplitude of transverse vibration is a key factor to the prediction of self-loosening. However, one should associate to this effect of amplitude, thread gap, bolt bending stiffness, thread stress redistribution and clamped member rotational bearing stiffness.
- Effect of creep on the relaxation of the clamping load in high temperature applications.

APPENDIX I

Strain gage (KYOWA)

Strain Gages for Measuring Axial Tension of Bolts

Patterns Gage Resistance, Gage Factors	Models	Dimensions (mm) Grid Length	Grid Width	Base Length	Base Width	Remarks

●KFG Series Foil Strain Gages for Measuring Axial Tension of Bolts

CE

Uniaxial
Resistance: 120 Ω
Gage factor: Approx. 1.9

If it is difficult to bond a strain gage to the surface of a bolt for measuring the tightening stress, these gages enable measurement by embedding them into a hole, 2 mm diameter, bored from the top head of the bolt. They are applicable to materials having a linear expansion coefficient of 11 ×10⁻⁶/ °C.
ϕ0.14 Polyester-coated copper cable 5 cm long

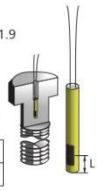

Length from the tip of base to the center of grid

L	KFG-3: 2.7 mm
	KFG-1.5: 1.75 mm

Applicable Adhesives

	Operating Temp. after Curing the Adhesive
EP-370	Normal Temp. to 50°C

5 gages/pkg

Optional Accessories: Dedicated gage terminal

Model	Dimensions	Base material	Conductor material	Remarks
T-F29	Outer: ϕ6 Inner: ϕ2.5	Glass epoxy	Copper foil	For bolt gages

T-F29

KFG-3-120-C20-11	3	Approx. 6	11.5	ϕ1.9	Bore diameter 2
KFG-1.5-120-C20-11	1.5	Approx. 6	5	ϕ1.9	Bore diameter 2

General-purpose Foil Strain Gages (KFGT)

Patterns Gage Resistance, Gage Factors	Models	Dimensions (mm) Grid Length	Grid Width	Base Length	Base Width	Remarks

●KFGT Series Foil Strain Gages with a Temperature Sensor

CE

Uniaxial 3-wire system
Polyester-coated copper lead wire
1 m long each
Resistance: 120 Ω
Gage factor: Approx. 2.1
Temperature sensor: T-type thermocouple
Accuracy: Within ±1.5 °C

The KFGT gages are foil strain gages incorporating a T-type thermocouple for simultaneous measurement of strain and temperature. They ensure efficient strain measurement under environments where temperature change or temperature gradient requires simultaneous measurement of strain and temperature. They also provide highly precise compensation of thermally-induced apparent strain. It is recommended to use Kyowa data logger UCAM-60B as a measuring instrument.

Applicable Adhesives

	Operating temp. after Curing the Adhesive
CC-33A	−10 to 120°C
CC-36	−10 to 100°C
CC-35	−10 to 120°C
EP-340	−10 to 120°C

KFGT-5-120-C1-11 N1M3	5	2.1	10	4.5	Standard accessories: Lead-wire stopper to prevent damage to the gage
KFGT-5-120-C1-16 N1M3					
KFGT-5-120-C1-23 N1M3					
KFGT-5-120-C1-27 N1M3					
KFGT-2-120-C1-11 N1M3	2	1.8	7	4.5	Pre-attached lead wire 1-m long
KFGT-2-120-C1-16 N1M3					
KFGT-2-120-C1-23 N1M3					
KFGT-2-120-C1-27 N1M3					5 gages/ pkg

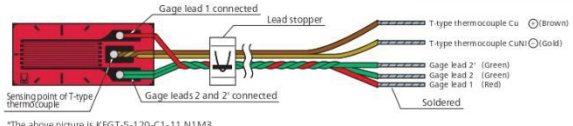

*The above picture is KFGT-5-120-C1-11 N1M3.

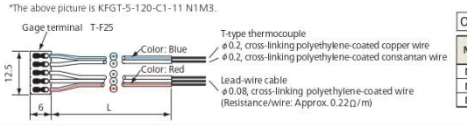

Optional Accessories: Extension lead-wire cables

Models	Dimensions (mm) Length	Operating Temperature Ranges	Remarks
NT-1M	1000	-10 to 120°C	5 gages/pkg
NT-2M	2000		
NT-4M	4000		

APPENDIX II

RVDT (CP-2UT by MIDORI PRECISIONS)

Blue Lot contactless — **Contactless Angle Sensor**

<RoHS Compliance>

CP-2UN
CP-2UTN

■FEATURES

- Substitute model of CP-2UX and CP-2UTX
- Low current consumption
- Compact & light weight
- Low torque

Electrical Angle	±45°
Output Sensitivity	2%Vin/10° MIN.
Independent Linearity	±2%FS (FS=90°)
Input Impedance	14±50% (7~21KΩ)
Input Voltage	DC 10V MAX.
Load Resistance	5MΩ MIN.

Mechanical Angle	360° Endless
Torque	0.05mN・m MAX.
Weight	Approx.10g
Shaft Radial Load	5N
Shaft Thrust Load	1N

Vibration	200m/S² 3axes 2hours each
Shock	1000m/S²3Axis 6Directions 3Times each
Operating Temp.	-40~100℃
Storage Temp.	-40~100℃

OPTIONS

・Built-in Temp Compensate Resistance

Temp. Compensting Range & Temp. Characteristics

	TCA	TCB	TCC
Temp.Range	0~60℃	-20~80℃	-30~100℃
At 0°	±0.5°	±0.5°	±0.8°
At ±45°	±3.5°	±6°	±8°

■DIMENSION

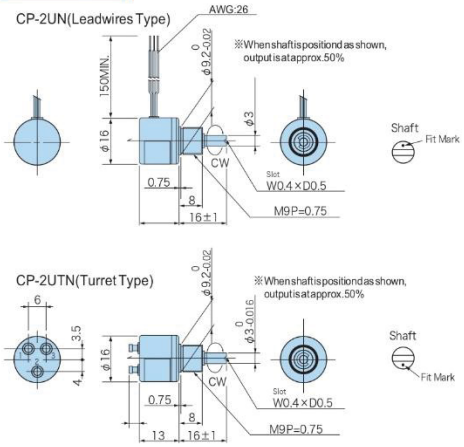

■MOUNTING

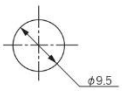

■SCHEMATIC

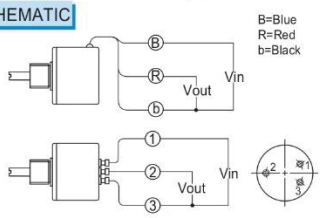

■OUTPUT CHARACTERISTICS

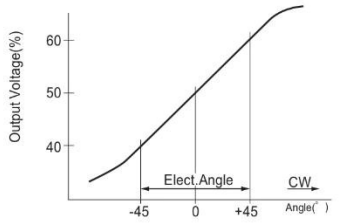

■MOUNTING HARDWARE

M9nut, Lock Washer

BIBLIOGRAPHY

Alkatan, F., Setphan, P., Daidie, A., & Guillot, J. (2007). Equivalent axial stiffness of various components in bolted joints subjected to axial loading. *Finite Elements in Analysis and Design*, *43*(8): 589–598.

ANSYS Inc. (2019), Ansys Workbench 19.1, (Version 2019 R1); [Computer program]. Canonsburg, Pennsylvania: Ansys Inc.

ASME. (1989a). *B18.2.3.5 M Metric Hex Bolts*. New York: ASME.

ASME. Boiler and Pressure Vessel Code, Section II, Part A. (2017). *Materials Specifications. ASTM A285/A285M - Standard Specification for Pressure Vessel Plates, Carbon Steel, Low- and Intermediate-Tensile Strength*. Latest ed. West Con-shohocken, PA, USA: ASTM International.

ASME. Boiler and Pressure Vessel Code, Section II, Part A. (2024). *Materials Specifications. ASTM A193/A193M - Standard Specification for Alloy-Steel and Stainless Steel Bolting for High-Temperature or High-Pressure Service and Other Special Purpose Applications*. Latest ed. West Conshohocken, PA, USA: ASTM International.

Barsoum, I., Barsoum, Z., & Islam, M. (2019). Thermomechanical evaluation of the performance and integrity of a HDPE stub-end bolted flange connection. *Journal of Pressure Vessel Technology*, *141*(5): 051206.

Basava, S., & Hess, D. P. (1998). Bolted joint clamping force variation due to axial vibration. *Journal of Sound and Vibration*, *210*(2): 255–265.

Baubles, R. C., McCormick, G. J., & Faroni, C. C. (1966). Loosening of fasteners by vibration. Union NJ: Elastic Stop Nut Corporation of America (ESNA).

Bhattacharya, A., Sen, A. & Das, S. H. (2010). An investigation on the anti-loosening characteristics of threaded fasteners under vibratory conditions. *Mechanism and Machine Theory*, *45*(8): 1215-1225.

Bickford, J. H. (1995). *An introduction to the design and behavior of bolted joints* (3rd ed.) Marcel Dekker, New York.

British Standards (2006). BS EN 10319-2 Metallic materials. Tensile stress relaxation testing - Procedure for bolted joint models.

BS 3643: Part 2. (1981). *ISO Metric Screw Threads. Limits and Tolerances for Fine Pitch Threads (Constant Pitch Series)*. BSI: Singapore.

Chen, Y., Gao, Q., & Guan, Z. Q. (2017). Self-loosening failure analysis of bolt joints under vibration considering the tightening process. *Shock and Vibration*, *2017*: 2038421.

Clark, S. K., & Cook, J. J. (1966). Vibratory loosening of bolts. *SAE Technical Paper* 660432.

Daadbin, A, & Chow, Y. M. (1992). A theoretical model to study thread loosening. *Mech Mach Theory*, *27*(1): 69–74.

Dinger, G. (2016). Design of multi-bolted joints to prevent selfloosening failure. *Proceedings of the Institution of Mechanical Engineers, Part C: Journal of Mechanical Engineering Science*, *230*(15): 2564–2578.

Dinger, G., & Friedrich, C. (2011). Avoiding self-loosening failure of bolted joints with numerical assessment of local contact state. *Engineering Failure Analysis*, *18*(8): 2188–2200.

Dong, Y., & Hess, D. P. (1999). Effect of thread dimensional conformance on vibration-induced loosening. *Journal of Vibration and Acoustics*, *Transactions of the ASME*, *121*(2): 209-213.

Dong, Y., & Hess, D. P. (2000). Shock-induced loosening of dimensionally nonconforming threaded fasteners. *Journal of Sound and Vibration*, *231*(2): 451- 459.

Eccles, W. (2014). A new approach to the checking of the tightness of bolted connections. *In Proceedings of the Lubrication, Maintenance and Tribotechnology (LUBMAT)*, Manchester, UK.

Fernando, A., Lee, J., Pokharel, T., & Gad, E. (2022). Improvements to torque versus tension relationship considering nut dilation effects. *Proceedings of the Institution of Mechanical Engineers, Part C: Journal of Mechanical Engineering Science*, *236*(7): 3578–3594.

Finkelston, R. J. (1972). How much shake can bolted joints take. *Machine Design*, *44*: 122-125.

Fort, V., Bouzid, A.-H., & Gratton, M. (2019). Analytical modeling of self-loosening of bolted joints subjected to transverse loading. *Journal of Pressure Vessel Technology*, *141*(3): 031205.

Fukuoka, T. (1992). Finite element simulation of tightening process of bolted joint with a tensioner. *Journal of Pressure Vessel Technology*, *114*(4): 433–438.

Gong, H., Liu, J., & Ding, X. (2020). Thorough understanding on the mechanism of vibration-induced loosening of threaded fasteners based on modified Iwan model. *Journal of Sound and Vibration*, *473*: 115238.

Goodier, J. N. and Sweeney, R. J. (1945). Loosening by vibration of threaded fastenings. *Mechanical Engineer*, *67*: 798-802.

Grabon, W. A., Osetek, M., & Mathia, T. G. (2018). Friction of threaded fasteners. *Tribology International*, *118*: 408–420.

Grosse, I. R., & Mitchell L. D. (1990). Nonlinear axial stiffness characteristics of axisymmetric bolted joints. *Journal of Mechanical Design*, *112*(3): 442–449.

Guillot, J. (1997). Assemblage par eléments filetés; modélisation et calculs. *Tech de l'ingénieur. Tome 1 BM5563 v1* (pp. 1–11), Paris, France.

Haviland, G. S. (1981). Unraveling the myths of the fastener world. *SAE Paper*, 810509.

Hess, D. P., & Davis K. (1996). Threaded components under axial harmonic vibration, part 1: experiments. *Journal of Vibration and Acoustics*, *118*(3): 417–422.

Hess, D. P., & Sudhirkashyap, S. V. (1996). Dynamic analysis of threaded fasteners subjected to axial vibration. *Journal of Sound and Vibration*, *193*(5): 1079–1090.

Hess, D. P., (1996). Threaded components under axial harmonic vibration, part 2: kinematic analysis. *Journal of Vibration and Acoustics*, *118*(3): 423–429.

Hongo, K. (1964) Loosening of bolt and nut fastening. *Transactions of Japan Society of Mechanical Engineers*, *30*: 934–939.

Housari, B. A., & Nassar, S. A. (2007). Effect of thread and bearing friction coefficients on the vibration-induced loosening of threaded fasteners. *Journal of Vibration and Acoustics*, *129*(4), pp. 484–494.

Huang, J., & Guo, L. S. (2011). The research on the torque-tension relationship for bolted joints. *Key Engineering Materials*, *486*: 242–245.

Izumi S, Yokoyama T, Iwasaki A & Sakai S. (2005). Three-dimensional finite element analysis of tightening and loosening mechanism of threaded fastener. *Engineering Failure Analysis*, *12*(4): 604–615.

Izumi, S., Kimura, M., & Sakai, S. (2007). Small loosening of bolt-nut fastener due to micro bearing-surface slip: A finite element method study. *Journal of Solid Mechanics and Materials Engineering*, *1*(11): 1374–1384.

Jacobsson, L., Andersson, H., & Vennetti, D. (2011a). Tightness of flange joints for large polyethylene pipes – part 1 numerical simulations. SP Technical Research Institute of Sweden, *Building Technology and Mechanics*. *49*.

Jacobsson, L., Andersson, H., & Vennetti, D. (2011b). Tightness of flange joints for large polyethylene pipes – part 2 full scale experimental investigation. SP Technical Research Institute of Sweden, *Building Technology and Mechanics*, *50*.

Jiang, Y., Zhang, M & Lee, C-H. (2003). A study of early stage self-loosening of bolted joints. *Journal of Mechanical Design*, *125*(3): 518-526.

Jiang, K., Liu, Z., Wang, Y., Tian, Y., Zhang, C., & Zhang, T. (2022). Effects of different friction coefficients on input torque distribution in the bolt tightening process based on the energy method. *Journal of Tribology*, 144(7): 1–21.

Jiang, Y., Chang, J., & Lee, C.-H. (2001). An experimental study of the torque-tension relationship for bolted joints. *International Journal of Materials and Product Technology*, *16*(4/5): 417–429.

Jiang, Y., Zhang, M., Park, T., & Lee, C. (2004). An experimental study of self-loosening of bolted joints . *ASME Journal of Mechanical Design*, *126*(5): 925-931.

Junker, G. H. (1969). New criteria for self-loosening of fasteners under vibration. SAE Trans. 78: 314-335. doi.org/10.1115/1.1767814.

Juvinall, R. C., & Marshek, K. M. (2000). *Fundamentals of machine component design* (3rd ed.). Wiley.

Kasei, S. (2007). A study of self-loosening of bolted joints due to repetition of small amount of slippage at bearing surface. *Journal of Advanced Mechanical Design, Systems, and Manufacturing*, *1*(3): 358–367.

Kasei, S., Ishimura, M., & Ohashi, N. (1988). On self-loosening of threaded joints in the case of absence of macroscopic bearing-surface sliding. Loosening mechanism under transversely repeated force. *J Jpn Soc Precis Eng*, *54*(7): 1381–1386.

Koga, K. (1970). Loosening by repeated impact of threaded fastenings. *Bull JSME*, *13*(55): 140–149.

Koga, K. (1973). The effect of thread angle on loosening by impact: 1st report, theoretical analysis. *Bull JSME*, *16*(96): 1010–1019.

Kogut, L., & Etsion, I. (2004). A static friction model for elastic-plastic contacting rough surfaces. *Journal of Tribology*, *126*(1): 34–40.

Lehnhoff, T. F., & Bunyard, B. A. (2001). Effects of bolt threads on the stiffness of bolted joints. *Journal of Pressure Vessel Technology*, *123*(2): 161–165.

Lehnhoff, T. F., Ko, K. I., & Mckay, M. L. (1994). Member stiffness and contact pressure distribution of bolted joints. *Journal of Mechanical Design*, *116*(2): 550–557.

Li, L., Yun, Q.-Q., Tian, H.-F., Cai, A.-J., & Cao, A.-Y. (2019). Investigation into the contact characteristics of rough surfaces with surface tension. *Journal of the Brazilian Society of Mechanical Sciences and Engineering*, *41*: 343.

Li, Z., Chen,Y., Sun, W., Jiang, P., Pan, J., & Guan, Z. (2021). Study on self-loosening mechanism of bolted joint under rotational vibration. *Tribology International*, *161*: 107074.

Little, R. E. (1967). Bolted joints: how much give? *Machine Design*, 173–175.

Liu, J. H., Ouyang, H. J., Feng, Z. Q., Cai, Z. B., Liu, X. T., & Zhu, M. H. (2017). Study on self-loosening of bolted joints excited by dynamic axial load. *Tribololology International*, *115*(5): 432–451.

Liu, J. H., Ouyang, H. J., Peng, J. F., Zhang, C. Q., Zhou, P. Y., Ma, L. J., & Zhu, M. H. (2016). Experimental and numerical studies of bolted joints subjected to axial excitation. *Wear*, 346–347: 66–77.

Liu, Z., Zheng, M., Yan, X., Zhao, Y., Cheng, Q., & Yang, C. (2020). Changing behavior of friction coefficient for high strength bolts during repeated tightening. *Tribology International*, *151*: 106486.

Maruyama, K., Yoshimoto, I., & Nakano, Y. (1975). On spring constant of connected parts in bolted joints. *Bulletin JSME*, *18*(126): 1472–1480.

Meyer, G. & Strelow, D. (1972). How to calculate preload loss die to permanent set in bolted joints. *Assembly Engineering*.

Meyer, G., & Strelow, D. (1972). Simple diagrams aid in analyzing forces in bolted joints. *Assembly Engineering*, *15*: 28–33.

Motosh, N. (1976). Development of design charts for bolts preloaded up to the plastic range. *Journal of Engineering for industry*, *98*(3): 849–851.

Musto, J. C., & Konkle, N. R. (2006). Computation of member stiffness in the design of bolted joints. Journal of Mechanical Design, *128*(6): 1357–1360.

Naruse, T., & Shibutani, Y. (2010). Equivalent stiffness evaluations of clamped plates in bolted joints under loading. *Journal of Solid Mechanics and Materials Engineering*, *4*(12): 1791–1805.

Naruse, T., & Shibutani, Y. (2012). Higher accurate estimation of axial and bending stiffnesses of plates clamped by bolts. *Journal of Solid Mechanics and Materials Engineering*, *6*(5), pp. 397–406.

Nassar, S. A., & Abboud, A. (2008). New formulation of bolted joint stiffness. In *ASME 2008 Pressure Vessels and Piping Conference*. p. 793–801. American Society of Mechanical Engineers.

Nassar, S. A., & Housari, B. A. (2006). Effect of thread pitch and initial tension on the self-loosening of threaded fasteners. *Journal of Pressure Vessel Technology*, *128*(4): 590–598.

Nassar, S. A., & Housari, B. A. (2006). Study of the effect of hole clearance and thread fit on the self-loosening of threaded fasteners. *Journal of Mechanical Design*, *129*(6): 586–594.

Nassar, S. A., & Yang, X. (2008). Torque-angle formulation of threaded fastener tightening. *Journal of Mechanical Design*, *130*(2): 024501.

Nassar, S. A., & Yang, X. J.. (2009). A mathematical model for vibration induced loosening of preloaded threaded fasteners. *Journal of Vibration and Acoustics*, *131*(2): 021009.

Nassar, S. A., & Zaki, A. M. (2009). Effect of coating thickness on the friction coefficients and torque-tension relationship in threaded fasteners. *Journal of Tribology*, *131*(2): 021301.

Nassar, S. A., Barber, G. C., & Dajun, Z. (2005). Bearing friction torque in bolted joints. *Tribology Transactions*, *48*(1): 69–75.

Nassar, S. A., Matin, P. H., & Barber, G. C. (2005). Thread friction torque in bolted joints. *Journal of Pressure Vessel Technology*, *127*(4): 387–393.

Nassar, S. A., Yang, X. J., Gandham, S. V. T., & Wu, Z. J. (2011). Nonlinear deformation behavior of clamped bolted joints under a separating service load. *Journal of Pressure Vessel Technology*, *133*(2): 021001.

Nassar, S.A. & Housari, B.A. (2006). Effect of thread pitch and initial tension on the self-loosening of threaded fasteners. *Journal of Pressure Vessel Technology*, *Transactions of the ASME*, *128*(4): 590-598.

Nechache, A. & Bouzid, A. H. (2006). Creep analysis of bolted flanged joints. *International Journal of Pressure Vessels and Piping*, *84*(3) : 185-194.

Nishimura, N., Hattori, T., Yamashita, M., & Hayakawa, N. (2007). Sliding and loosening behavior of thread joints under transverse loading. *Key Engineering Materials*, *353–358*: 894–897.

Nishimura, N., Murase, K., Hattori, T., & Watanabe, T. (2013). Loosening evaluation of bolt-nut fastener under transverse cyclic loading. *Engineering Transactions*, *61*(2): 151–160.

Noda, N. A., Chen, X., Sano, Y., Wahab, M. A., Maruyama, H., Fujisawa, R., & Takase, Y. (2016). Effect of pitch difference between the bolt–nut connections upon the anti-loosening performance and fatigue life. *Materials and Design*, *96*: 476–489.

Norton, R. L. (2000). *Machine design: an integrated approach* (2nd ed.). Pearson Education Inc.

Pai, N. G., & Hess, D. P. (2002). Experimental study of loosening of threaded fasteners due to dynamic shear loads. *Journal of Sound and Vibration*, *253*(3): 585–602.

Pai, N. G., & Hess, D. P. (2002). Three-dimensional finite element analysis of threaded fastener loosening due to dynamic shear load. *Engineering Failure Analysis*, *9*(4): 383–402.

Pedersen, N. L., & Pedersen, P. (2008). On prestress stiffness analysis of bolt-plate contact assemblies. *Archive of Applied Mechanics*, 78(2): 75–88.

Rotscher, F. (1927). *Die Maschinenelemente*. Springer.

Rousseau, R. I., Bouzid, A. -H. & Zhao, Z. (2021). Accurate evaluation of bolt and clamped members stiffnesses of bolted joints. In *ASME 2021 Pressure Vessels and Piping Conference (Virtual, Online),* American Society of Mechanical Engineers.

Sakai, T. (1978) Investigations of bolt loosening mechanisms: 2nd report, on the center bolts of twisted joints. *Bulletin JSME*, *22*(165): 412–419.

Sakai, T. (1978). Investigations of bolt loosening mechanisms : 1st report, on the bolts of transversely loaded joints, *Bulletin JSME*, *21*(159) : 1385–1390.

Sakai, T. (1979) Investigations of bolt loosening mechanisms: 3rd report, on the bolts tightened over their yield point. *Bulletin JSME*, *22*(165): 412–419.

Sakai, T. (2011). Mechanism for a bolt and nut self loosening under repeated bolt axial tensile load. *Journal of Solid Mechanics and Materials Engineering*, *5*(11): 627–639.

Sauer J. A., Lemmon D. C., Lynn E. K. (1950). Bolts: How to prevent their loosening. *Mach Des*, *22*: 133–139.

Sawa, T., & Maruyama, K. (1976). On the deformation of the bolt head and nut in a bolted joint. *Bulletin JSME*, *19*(128): 203–211.

Sawa, T., & Maruyama, K. (1976). On the deformation of the bolt head and nut in a bolted joint. *Bulletin JSME*, *19*(128): 203–211.

Sawa, T., Ishimura, M., & Karami, A. (2010). A bolt-nut loosening mechanism in bolted connections under repeated transverse loadings (effect of inclined bearing surfaces on the loosening). In *ASME 2010 Pressure Vessels and Piping Conference* (pp. 397-403), American Society of Mechanical Engineers.

Sawa, T., Ishimura, M., & Nagao, T. (2012). A loosening mechanism of bolted joints under repeated transverse displacements. In *ASME 2012 Pressure Vessels and Piping Conference* (pp. 333-341), American Society of Mechanical Engineers.

Sethuraman, R., & Kumar, T. S. (2009). Finite element based member stiffness evaluation of axisymmetric bolted joints. *Journal of Mechanical Design*, *131*(1): 011012:1–11.

Shahin, A., Barsoum, I., & Korkees, F. (2021). Analysis of a HDPE flanged connection with a time and temperature dependent constitutive behavior. *International Journal of Pressure Vessels and Piping*, *191*: 104375.

Shigley, J. E., & Mischke, C. R. (1989). *Mechanical engineering design* (5th ed.). McGraw-Hill.

Shigley, J. E., & Mitchell, L. D. (1983). *Mechanical engineering design* (4th ed.). McGraw-Hill.

Shoji, Y., & Sawa, T. (2008). Self-loosening mechanism of nuts due to impacts. In *ASME 2008 Pressure Vessels and Piping Conference* (pp. 219-225), American Society of Mechanical Engineers.

Shoji, Y., Sawa, T., & Yamanaka, H. (2007). Self-loosening mechanism of nuts due to lateral motion of fastened plate. In *ASME 2007 Pressure Vessels and Piping Conference* (pp. 223-230), American Society of Mechanical Engineers.

Stuck, K. (1968). Untersuchungen über die federeigenschaften der ver-spannten teile von schraubenverbindungen. *Dissertation*, Technischen Hochs- chule Aachen.

Tanaka, M., Hongo, K., & Asaba, E. (1982). Finite element analysis of the threaded connections subjected to external loads. *Bull JSME*, *25*(200): 291–298.

VDI (2003). "VDI 2230 - Systematic Calculation of High Duty Bolted Joints." *Verein Deutscher Ingenieure*.

Vinogradov, O., & Huang, X. (1989) On a high frequency mechanism of self-loosening of fasteners. In *Proceedings of 12th ASME Conference on Mechanical Vibration and Noise*, Montreal, Quebec, 1989: 131–137.

Wileman, J., Choudhury, M., & Green, I. (1991). Computation of member stiffness in bolted connection. *Journal of Mechanical Design*, *113*(4): 432–437.

Yamamoto, A, & Kasei, S. (1977). Investigations on the self-loosening of threaded fasteners under transverse vibration. *Journal of the Japan Society of Precision Engineering*, *43*(508): 470–475.

Yang, J., & DeWolf, J. (1999). Mathematical Model for Relaxation in High Strength Bolted Connections. *Journal of Structural Engineering*, *125*(8): 803-809.

Yang, X. J., Nassar, S. A., Wu, Z. J., & Meng, A. D. (2012). Nonlinear behavior of preloaded bolted joints under a cyclic separating load. *Journal of Pressure Vessel Technology*, *134*(1): 011206.

Yang, X., & Nassar, S. A. (2011a). Effect of non-parallel wedged surface contact on loosening performance of preloaded bolts under transverse excitation. In *ASME 2011 Pressure Vessels and Piping Conference* (pp. 405-415), American Society of Mechanical Engineers.

Yang, X., & Nassar, S. A. (2011b). Effect of thread profile angle and geometry clearance on the loosening performance of a preloaded bolt-nut system under harmonic transverse excitation. In *ASME 2011 Pressure Vessels and Piping Conference* (393-404), American Society of Mechanical Engineers.

Yang, X., Nassar, S. A., & Wu, Z. (2010). Formulation of a criterion for preventing self-loosening of threaded fasteners due to cyclic transverse loading. In *ASME 2010 Pressure Vessels and Piping Conference* (pp. 415-425), American Society of Mechanical Engineers.

Yang, X., Nassar, S. A., & Wu, Z. (2011). Criterion for preventing self-loosening of preloaded cap screws under transverse cyclic excitation. *Journal of Vibration and Acoustics*, *133*(4): 1–11.

Yokoyama, T., Izumi, S., & Sakai, S. (2010). Analytical modelling of the mechanical behavior of bolted joint subjected to transverse loading. *Journal of Solid Mechanics and Materials Engineering*, *4*(9): 1427–1443.

Yokoyama, T., Olsson, M., Izumi, S., & Sakai S. (2012). Investigation into the self-loosening behavior of bolted joint subjected to rotational loading. *Engineering Failure Analysis*, *23*(159): 35–43.

Zadoks, R. I., & Kokatam, D. P. R. (2001). Investigation of the axial stiffness of a bolt using a three-dimensional finite element model. *Journal of Sound and Vibration*, *246*(2): 349–373.

Zadoks, R. I., & Yu, X. (1997). An investigation of the self-loosening behavior of bolts under transverse vibration. *Journal of Sound and Vibration*, *208*(2): 189–209.

Zaki, A. M., Nassar, S. A, & Yang, X. (2011). Criterion for preventing self-loosening of preloaded countersunk head threaded fasteners. In *ASME Pressure Vessels and Piping Conference* (pp. 369-380), American Society of Mechanical Engineers.

Zaki, A. M., Nassar, S. A., & Yang, X. (2010a). Effect of thread and bearing friction coefficients on the self-loosening of preloaded countersunk-head bolts under periodic transverse excitation. *Journal of Tribology*, *132*(3): 031601.

Zaki, A. M., Nassar, S. A., & Yang, X. (2010b). Vibration loosening model for preloaded countersunk-head bolts. In *ASME Pressure Vessels and Piping Conference* (pp. 361-371), American Society of Mechanical Engineers.

Zaki, A. M., Nassar, S. A., & Yang, X. (2012). Effect of conical angle and thread pitch on the self-loosening performance of preloaded countersunk-head bolts. *Journal of Pressure Vessel Technology*, *134*(2): 1–8.

Zhang, D., Gao, S., & Xu, X. (2016). A new computational method for threaded connection stiffness. *Advances in Mechanical Engineering*, *8*(12): 1–9.

Zhang, J., Feng, J., Li, W., & Liao, R. (2024). Improving torque-tension relationship in bolted joints: Accurate threaded surface repre-sentation and pressure distribution considerations. *Mechanics Based Design of Structures and Machines*, *52*(10): 1–21.

Zhang, M., Jiang, Y. Y., & Lee, C. H. (2006). An experimental investigation of the effects of clamped length and loading direction on self-loosening of bolted joints. *Journal of Pressure Vessel Technology*, *128*(3): 388–393.

Zhang, M., Jiang, Y. Y., & Lee, C. H. (2007). Finite element modeling of self-loosening of bolted joints. *Journal of Mechanical Design*, *129*(2): 218–226.

Zou, Q., Sun, T. S., Nassar, S. A., Barber, G. C., & Gumul, A.K. (2007). Effect of lubrication on friction and torque-tension relationship in threaded fasteners. *Tribology Transactions*, *50*(1): 127–13